UNIVERSITY OF CALIFORNIA

Santa Barbara

Exposure and sensitivity of ponderosa pine to climate change in mountainous western North American landscapes

A dissertation submitted in partial satisfaction of the

requirements for the degree Doctor of Philosophy

in Environmental Science & Management

by

Ian McCullough

Committee in charge:

Professor Frank Davis, Chair

Professor James Frew

Professor Christina Tague

June 2017

The dissertation of Ian McCullough is approved.

_____

James Frew

_____

Christina Tague

_____

Frank Davis, Committee Chair

ACKNOWLEDGEMENTS

There seems to be a widely held notion that pursuing a PhD is some sort of personal, lonely intellectual journey. Although I cannot completely disagree with that statement, at least for me, it is still false. I would have had little success if it were not for the advice, inspiration and encouragement I received from people around me during my time as a PhD student. My advisor Frank Davis repeatedly shared his acumen with me and exhibited patience since day one. My committee, James Frew and Christina Tague, shared their expertise with me over the years and provided valuable advice at various critical junctures. Numerous research collaborators who shared data or advice include John Dingman, Alan Flint, Lorraine Flint, Janet Franklin, G. Andrew Fricker, Alex Hall, Lee Hannah, Max Moritz, Kelly Redmond, Helen Regan, Josep Serra-Diaz, Nicholas Synes, Alexandra Syphard and A. Park Williams. I also thank Peter Brewer, Ellis Margolis, Joel Michaelsen and Michael White for being expert consultants. I appreciate the help of Frank Davis, Elizabeth Hiroyasu, Jason McClure and Phoebe Prather for help with field work, which included trekking through rough terrain on hot summer days. I thank Sage Davis for providing tools and space for preparation of my tree-ring samples. I am grateful to the Tejon Ranch Company and Tejon Ranch Conservancy for granting access to their land and resources for my research. Others deserving appreciation for various forms of help, large or small, include Benjamin Best, William Brandt, Julien Brun, Helen Chen, Janet Choate, Ginger Gillquist, Benjamin Halpern, Randall Long, Sean McKnight, Aaron Ramirez, Ryan Salladay, Mark Schildauer, Kyongho Son, Oliver Soong, Laura Urbisci and Lorena Vieli. I also thank the Global Lake Ecological Observatory Network (GLEON) graduate fellowship

program for training in ecological modeling and interdisciplinary team science. Finally, I gratefully acknowledge the ever-ready and dedicated staff at the Bren School of Environmental Science & Management for numerous forms of support over my years as a PhD student.

Funding for my research was provided by the National Science Foundation Macrosystems Biology Program, NSF #EF-1065864, the University of California Institute for the Study of Ecological and Evolutionary Climate Impacts, the UCSB Earth Research Institute and the Bren School. Additional logistical support was provided by staff at the Earth Research Institute, the Bren School and the UCSB National Center for Ecological Analysis and Synthesis.

VITA OF IAN McCULLOUGH
June 2017

EDUCATION

Bachelor of Arts in Environmental Studies, Colby College, May 2010
Master of Science in Ecology & Environmental Science, University of Maine, May 2012
Doctor of Philosophy in Environmental Science & Management, University of California, Santa Barbara, June 2017 (expected)

PROFESSIONAL EMPLOYMENT

2008-2010: Undergraduate research assistant, Environmental Studies Program, Colby College
2010-2012: Graduate research assistant, Department of Wildlife Ecology, University of Maine
2011: Teaching assistant, Department of Wildlife Ecology, University of Maine
2012: Geographic Information Systems Specialist and Data Analyst, Maine Cooperative Fish and Wildlife Research Unit, Department of Wildlife Ecology, University of Maine
2012-2017: Graduate student researcher, Bren School of Environmental Science & Management, University of California, Santa Barbara
2015-2016: Graduate Intern, Science for Nature and People Partnership, National Center for Ecological Analysis and Synthesis, University of California, Santa Barbara
2015-2017: Teaching assistant, Bren School of Environmental Science & Management, University of California, Santa Barbara

PUBLICATIONS

Apr 2017 Dugan, H. A., Bartlett, S. L., Burke, S. M., Doubek, J. P., Krivak-Tetley, F. E., Skaff, N. K., Summers, J. C., Farrell, K. J., **McCullough, I. M.**, Morales-Williams, A. M., Roberts, D., Scordo, F., Yang, Z., Hanson, P. C. and K. C. Weathers. Salting our freshwater lakes. *Proceedings of the National Academy of Sciences* 114 (17), 4453-4458

Nov 2016 Davis, F. W., Sweet, L., Serra-Diaz, J. M., Franklin, J., **McCullough, I. M.**, Flint, A., Flint, L., Dingman, J. R., Regan, H. M., Syphard, A., Hannah, L., Redmond, K. and M. A. Moritz. Shrinking windows of opportunity for oak seedling establishment in southern California mountains. *Ecosphere* 7(11).

Jun 2016 **McCullough, I. M.**, Davis, F. W., Dingman, J. R., Flint, L. E., Flint, A. L., Serra-Diaz, J. M., Syphard, A. D., Moritz, M. A., Hannah, L. and J. Franklin. High and dry: high elevations disproportionately exposed to regional climate change in Mediterranean-climate landscapes. *Landscape Ecology* 31 (5), 1063-1075.

Oct 2015 Serra-Diaz, J. M., Franklin, J., Sweet, L, **McCullough, I. M**., Syphard, A. D., Regan, H., Flint, L., Flint, A., Dingman, J., Moritz, M. A., Redmond, K., Hannah, L. and F. W. Davis. Averaged 30 year climate change projections mask opportunities for species establishment. *Ecography.* DOI: 10.1111/ecog.02074.

May 2015 Hannah, L., Flint, L. E., Syphard, A. D., Moritz, M. A., Buckley, L. B. and **I. M. McCullough**. Place and process in conservation planning for climate change: a reply to Keppel and Wardell-Johnson. *Trends in Ecology and Evolution* 30(5): 233-234.

Feb 2015 Aceves-Bueno, E., Adeleye, A. S., Bradley, D., Brandt, W. T., Callery, P., Feraud, M., Garner, K. L., Gentry, R., Huang, Y., **McCullough, I. M**., Pearlman, I., Sutherland, S. A., Wilkinson, W., Yang, Y, Zink, T., Anderson, S. E. and C. Tague. Citizen science as a tool for overcoming insufficient monitoring and inadequate stakeholder buy-in in adaptive management: Criteria and evidence. *Ecosystems* 18(3): 493-506.

Jul 2014 Hannah, L., Flint, L., Syphard, A. D., Moritz, M. A., Buckley, L. B. and **I. M. McCullough**. Fine-grain modeling of the response of species to climate change:
holdouts, stepping-stones and microrefugia. *Trends in Ecology and Evolution* 29 (7): 390-397.

Oct 2013 Dingman, J. R., Sweet, L. C., **McCullough, I. M**., Davis, F. W., Flint, A., Franklin, J. and L. E. Flint. Cross-scale modeling of surface temperature and seedling establishment to improve projections of tree distribution shifts under climate change. *Ecological Processes* 2-30.

Sep 2013 **McCullough, I. M**., Loftin, C. S. and S. A. Sader. Landsat imagery reveals declining clarity of Maine's lakes during 1995-2010. *Freshwater Science* 32(3): 741-752.

Mar 2013 **McCullough, I. M**., Loftin, C. S. and S. A. Sader. Lakes without Landsat? An alternative approach to remote lake monitoring with MODIS 250 m imagery. *Lake and Reservoir Management* 29: 89-98.

Jan 2013 **McCullough, I. M**., Loftin, C. S. and S. A. Sader. A manual for remote sensing of Maine lake clarity. *Maine Agricultural and Forest Experimentation Station,* University of Maine. Technical Bulletin 207. ISSN: 1070-1054.

Sep 2012 **McCullough, I. M**., Loftin, C. S. and S. A. Sader. High-frequency remote monitoring of large lakes with MODIS 500 m imagery. *Remote Sensing of Environment* 124: 234-241.

Aug 2012 **McCullough, I. M**., Loftin, C. S. and S. A. Sader. Combining lake and watershed characteristics with Landsat TM data for remote estimation of regional lake clarity. *Remote Sensing of Environment* 123: 109-115.

AWARDS

2016 Audience Selected Best Oral Presentation (UCSB Bren School PhD Symposium)
2015 Graduate Student Research Fellowship, University of California Institute for the Study of the Ecological Effects of Climate Impacts
2014 Summer Research Fellowship, Earth Research Institute, University of California, Santa Barbara
2012 Horace Bond Scholarship, Penobscot County Conservation Association
2006 Ralph J. Bunche Scholarship, Colby College

SERVICE

Scientific Peer Review	Ecological Applications
	Ecography
	Remote Sensing of Environment
Society Membership	Ecological Society of America
	Global Lake Ecological Observatory Network

LEADERSHIP

Mentor, Master's Group Project Mentorship Program (2015-2017)
PhD Student Representative, Dean's Advisory Council (2016-2017)
Founder & Member, Graduate Directives Committee (2014-2016)

ABSTRACT

Exposure and sensitivity of ponderosa pine to climate change in mountainous western North American landscapes

by

Ian McCullough

Climate change has emerged as one of the most potent threats to forests across the globe. This study examined the exposure and sensitivity of ponderosa pine (*Pinus ponderosa*) to climate change from landscape to continental scales across its geographic range in western North America. We began by developing a framework for assessing climate change exposure based on climatic water deficit (CWD), a metric of unmet evaporative demand and strong predictor of plant species distributions. The framework combined change in average annual CWD and frequency of departure from the local historical range of variability in annual CWD. We applied this framework to Tejon Ranch, a mountainous landscape in the Tehachapi Mountains of Southern California. We found disproportionate climate change exposure at high elevations due to projected losses in snowpack associated with warmer winters. Next, we assessed long-term relationships between climate and ponderosa pine growth at Tejon Ranch. Interannual variability in tree growth was explained by a combination of climatic water deficit over the current and preceding water-year (Oct 1 – Sep 30), March precipitation, July maximum and January minimum air temperatures

(adjusted R^2 = 0.55-0.57). In general, growth is expected to decline under future climate change in current stands, but heterogeneous topography offered potential favorable growing habitat under all climate projections, particularly on north-facing slopes at higher elevations. Under warmer and drier projections, overall habitat availability decreased in terms of distance to the nearest suitable patch from current stands for both mid- (2040-2069) and end-of-century (2070-2099) periods. Spatiotemporal climate variability, however, created suitable patches within average seed dispersal distance of current stands, potentially offering ephemeral windows of opportunity for local range shifts without long-distance dispersal. Finally, we examined the sensitivity of ponderosa pine to climate variability across its range in western North America by combining the Tejon Ranch tree rings and 159 published chronologies from the International Tree Ring Data Bank. We encountered heterogeneous climate sensitivities across the species range to a suite of limiting climate variables. Our results indicated that position along environmental gradients interacts with genetically based local adaptation to determine climate sensitivity of individual ponderosa pine populations. Although all ponderosa pine populations will likely be exposed to locally novel climate regimes in the 21st Century, the species' overall wide variability in climate sensitivity will likely buffer some populations from negative effects of climate change. Future conservation efforts for ponderosa pine and other wide-ranging species should consider the mediating role of geographic patterns of genetic structure in within-species climate sensitivities.

CHAPTER 1

HIGH AND DRY: HIGH ELEVATIONS DISPROPORTIONATELY EXPOSED TO REGIONAL CLIMATE CHANGE IN MEDITERRANEAN-CLIMATE LANDSCAPES

Ian M. McCullough[1], Frank W. Davis[1], John R. Dingman[2], Lorraine E. Flint[3], Alan L. Flint[3], Josep M. Serra-Diaz[4], Alexandra D. Syphard[5], Max A. Moritz[6], Lee Hannah[7], Janet Franklin[8]

[1]Bren School of Environmental Science and Management, 2400 Bren Hall, University of California, Santa Barbara, CA 93106, USA

[2]Air Resources Board, California Environmental Protection Agency, 10001 I St., P.O. Box 2815, Sacramento, CA 95812, USA

[3]U.S. Geological Survey, California Water Science Center, Placer Hall, 6000 J. St., Sacramento, CA 95189, USA

[4]Harvard Forest, Harvard University, Petersham, MA 01366, USA

[5]Conservation Biology Institute, 10423 Sierra Vista Ave, La Mesa, CA 91941, USA

[6]Department of Environmental Science, Policy and Management, 130 Mulford Hall, University of California, Berkeley, CA 94720, USA

[7]Betty and Gordon Moore Center for Science and Oceans, Conservation International, 2011 Crystal Drive Suite 500, Arlington, VA 22202, USA

[8]School of Geographical Sciences and Urban Planning, Arizona State University, P.O. Box 875302, Tempe, AZ 85287-5302, USA

Abstract

Predicting climate-driven species' range shifts depends substantially on species' exposure to climate change. Mountain landscapes contain a wide range of topoclimates and soil characteristics that are thought to mediate range shifts and buffer species' exposure. Quantifying fine-scale patterns of exposure across mountainous terrain is a key step in understanding vulnerability of species to regional climate change. We demonstrated a transferable, flexible approach for mapping climate change exposure in a moisture-limited, mountainous California landscape across 4 climate change projections under phase 5 of the Coupled Model Intercomparison Project (CMIP5) for mid-(2040–2069) and end-of-century (2070–2099). We produced a 149-year dataset (1951–2099) of modeled climatic water deficit (CWD), which is strongly associated with plant distributions, at 30-m resolution to map climate change exposure in the Tehachapi Mountains, California, USA. We defined climate change exposure in terms of departure from the 1951–1980 mean and historical range of variability in CWD in individual years and 3-year moving windows. Climate change exposure was generally greatest at high elevations across all future projections, though we encountered moderate topographic buffering on poleward-facing slopes. Historically dry lowlands demonstrated the least exposure to climate change. In moisture-limited, Mediterranean-climate landscapes, high elevations may experience the greatest exposure to climate change in the 21st Century. High elevation species may thus be especially vulnerable to continued climate change as habitats shrink and historically energy-limited locations become increasingly moisture-limited in the future.

Introduction

Biogeographers and landscape ecologists are increasingly focusing attention on the role of local topoclimates and microclimates (hereafter referred to as "microenvironments") in mediating species' extinction risks and range shifts in response to climate change (Potter et al 2013; Hannah et al 2014). Mountainous topography encompasses a wide variety of microenvironments that may buffer species' exposure to climate change, allowing local retention or redistribution of species by reducing climate change velocities and providing stepping-stone habitat connectivity (Loarie et al. 2009; Ackerly et al. 2010; Scherrer and Korner 2011; De Frenne et al. 2013; Lenoir et al. 2013; Hannah et al. 2014); both of these factors may be particularly important for slowly dispersing species (Schloss et al. 2012; Zhu et al. 2012; Corlett and Westcott 2013). Methods are being developed to identify and map the distribution of microenvironments across landscapes (Ashcroft et al. 2012; Dingman et al. 2013), with the goal of using this fine-scale information to improve species distribution models (SDMs) (Franklin et al. 2013) and conservation planning under climate change (Anderson et al. 2014, Keppel et al. 2015).

The vulnerability of species to climate change is a product of their exposure and sensitivity (Williams et al. 2008). Although sensitivity is species-specific, climate exposure (hereafter, "exposure") is largely a function of local climate and can thus be projected into the future using downscaled outputs from general circulation models (GCMs). Spatial variation in the magnitude and pace of exposure can be attributed to fine-scale variation in surface energy balance, hydrology, soil characteristics and vegetation structure, all of which are thought to produce *microrefugia*, which are often defined as regionally unique microenvironments that support isolated populations of species outside their main

distributions (Rull 2009; Dobrowski 2011). Microrefugia is a term taken from paleoecology, where it is primarily used to describe survival of species through glacial cycles (Bennett et al. 1991; Tzedakis et al. 2002; McLachlan et al. 2005; Stewart et al. 2010; Gavin et al. 2014; Patsiou et al. 2014). Whether the concept is useful in the context of species vulnerability to modern climate change is a topic of ongoing research and discussion (Hannah et al. 2014). For isolated populations to persist through periods of rapid climate change, the microenvironments they inhabit must be somewhat climatically decoupled from regional climate for those climate factors that limit the species' distribution (Dobrowski 2011; Hylander et al. 2015).

Conceptually, climate change at a given site constitutes a change in the probability distributions of climate variables with associated changes in descriptors of those distributions (e.g., the mean and standard deviation of the normal distribution) (Katz and Brown 1992). Changes in extremes can be particularly influential in natural systems (Easterling et al. 2000) and may be masked by analyses focused on changes in long-term means (Polade et al. 2014). Here we present an approach for quantifying the magnitude of exposure at a given site along two main axes representing change in mean annual climate and in frequency of climate extremes relative to the historical range of variability (HRV, Landres et al. 1999; Maher et al. 2017) in a historical reference period (Fig. 1). Exposure has been broadly defined as encompassing both the rate and magnitude of climate change (Dawson et al. 2011) and combined changes in both mean climate and frequency of extreme events have been previously used to assess exposure (Williams et al. 2007; Beaumont et al. 2011; Benito-Garzon et al. 2014). In mountainous regions we would expect sites to vary considerably in the rate of change in both means and extremes relative to the regional trend. Ignoring

dispersal limitations, microrefugia would arguably be associated with those sites that show the least change from historical conditions (i.e., fall as near to the origin of these two axes as possible) and are thus least coupled to regional climate trends. Vulnerability of individual species will ultimately depend on their sensitivity to changes in mean and/or extreme conditions.

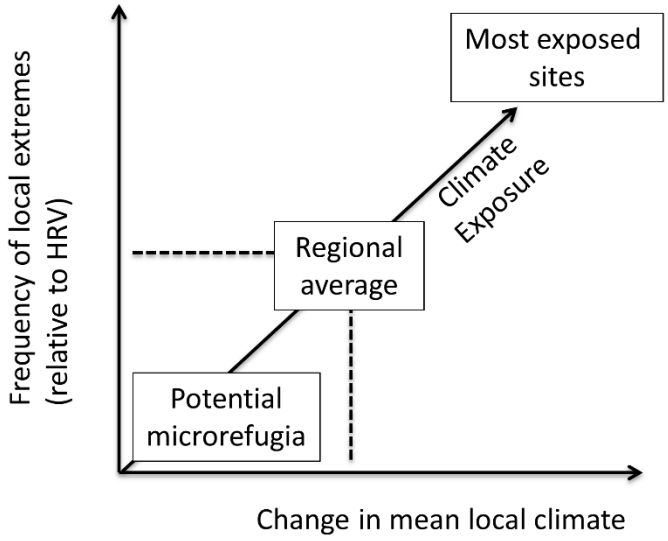

Fig. 1. Conceptual diagram of potential microrefugia in terms of climate change exposure, which is a function of both changes in mean climate and frequency of extremes relative to historical climate. The exposure of a given site is determined by its position along these two main axes.

We applied our approach and concept of exposure to a biologically diverse mountainous study region in Southern California. Because we were especially interested in plant distributions, we modeled and analyzed fine-scale changes in climatic water deficit (CWD), a bioclimatic variable that exerts strong, topographically-driven controls on plant

distributions in Mediterranean-climate landscapes of California and elsewhere (Stephenson 1998; Lutz et al. 2010). We focused solely on CWD because it integrates interactions among temperature, precipitation and soil properties, all of which play a strong role in determining species distributions. Our research questions were: 1) How is CWD projected to change across a rugged landscape under mid-century and end-of-century climate projections in comparison to historical conditions? 2) How will rates of climate change exposure vary across the landscape as a function of local microenvironments?

Methods

Study area

Our study area was located in the western Tehachapi Mountains, California, USA (34°58´N, 118°35´W). This area, which is the site of ongoing research to measure and model microclimates and plant establishment (Davis and Sweet 2012), is characterized by rugged topography and steep climate gradients, providing a suitable case study of local variation in climate and projected climate change exposure. The area is mostly private land owned and managed by the Tejon Ranch Company for cattle ranching, hunting, agriculture and rare species conservation. Our climate grids and study area covered a rectangular subregion of Tejon Ranch and some adjacent areas to the northeast, spanning approximately 33,000 ha and steep elevational gradients (370-2,364 m) (Fig. 2). The climate is Mediterranean, with hot, dry summers and cool, wet winters. Mean annual precipitation for the period 1896-2010 varied from around 250 mm in the driest, low elevation portions of the area to over 500 mm at the highest elevations. At elevations above roughly 1500-1600 m, precipitation regimes are historically snow-dominated (Western Regional Climate Center 2015). Our focal climate

indicator (CWD) varies widely across the landscape, mainly as a result of topographically controlled variation in solar radiation, temperature and precipitation but also due to differences in soil water holding capacity (Fig. 3). At low elevations, soils are granite-derived, coarse-loamy thermic typic Haploxerolls with maximum depths of approximately 61-122 cm (USDA 2015). High elevation sites include coarse-sandy loams derived from schist and classified as mesic Pachic Haploxerolls, as well as granite-derived medium- and coarse-sandy loams classified as mesic Haploxerolls. Maximum soil depths at high elevations are approximately 127-229 cm (USDA 2015). The topographically varied landscape supports diverse vegetation cover ranging from arid grasslands and shrublands to deciduous and evergreen oak woodlands and montane conifer forests.

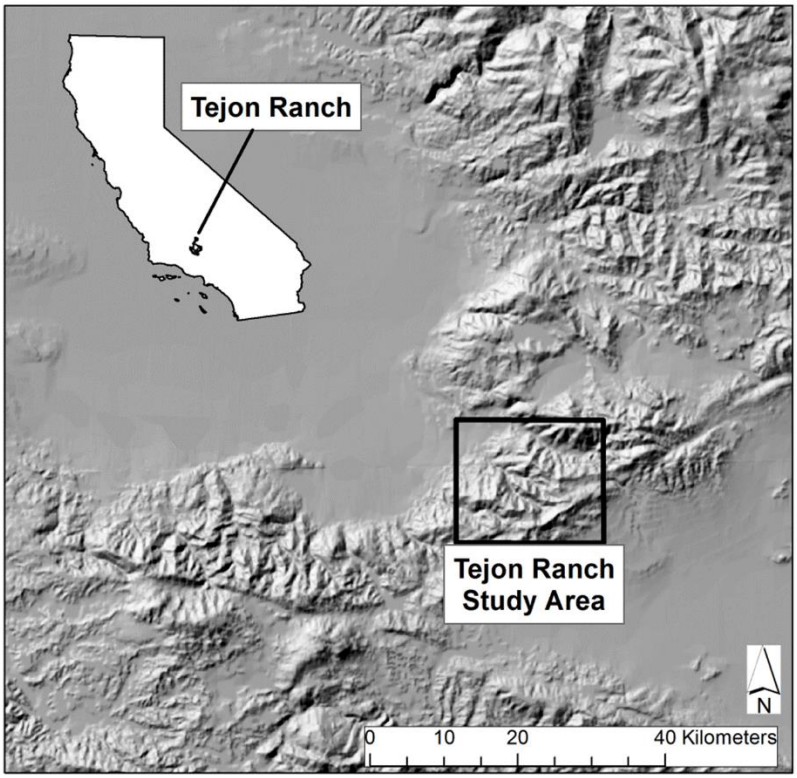

Fig. 2. Study site. Tejon Ranch is located in the Tehachapi Mountains, California, USA, near the southern edge of the San Joaquin Valley and the Sierra Nevada. Our model domain (inset box) covers 33,000 ha and an elevational gradient of 370-2364 m.

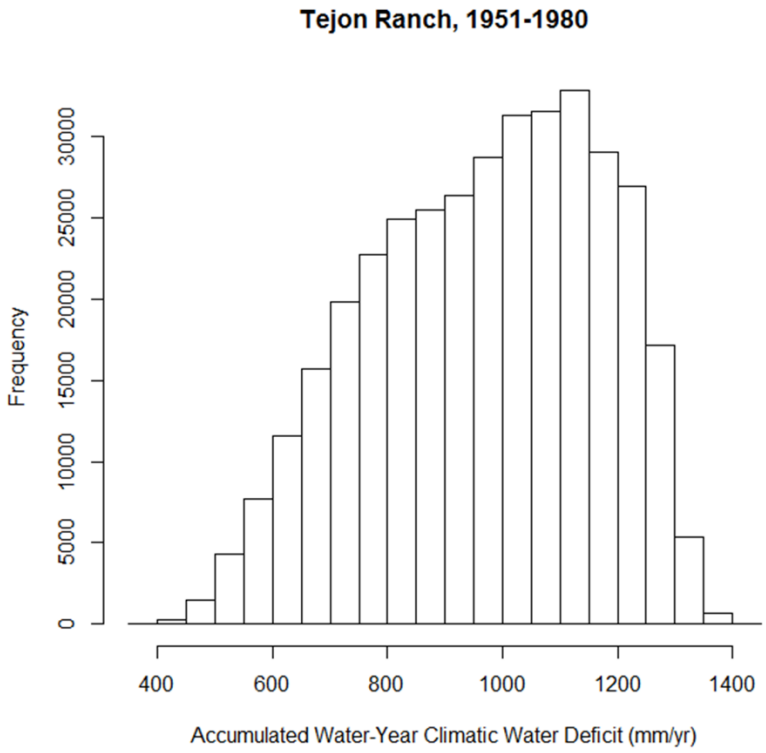

Fig. 3. Frequency distribution of accumulated water-year climatic water deficit (CWD) for Tejon Ranch expressed as cell means for 1951-1980.

Table 1. CMIP5 models used for analysis and projected climate change between baseline (1951-1980) and end-of-century (2070-2099) at Tejon Ranch.

GCM	RCP	July tmax (°C)	Jan tmin (°C)	WY precip (mm)	WY cwd (mm)
Max Planck Institute Earth System Model (MPI)	4.5	1.94	1.98	24.38	92.58
Model for Interdisciplinary Research on Climate (MIROC)	4.5	2.6	1.94	-67.64	156.54
Community Climate System Model (CCSM4)	8.5	4.07	4.02	14.87	148.82
Model for Interdisciplinary Research on Climate	8.5	4.63	4.61	-111.2	244.79

WY = water-year (Oct 1-Sep 30), cwd = climatic water deficit.

Mapping historical and projected future climates

To represent historical climate conditions, PRISM (Parameter-elevation Relationships on Independent Slopes Model) (Daly et al 2008) temperature and precipitation data were spatially downscaled from 800 to 30 m using Gradient-Inverse-Distance-Squared (GIDS) downscaling (Flint and Flint 2012). This method basically drapes the downscaled climate data over the landscape and has been shown either to match the coarser resolution gridded climate or improve the match to measured station data for both precipitation and air temperature by incorporating local topography, adiabatic lapse rates and climatic gradients (Flint and Flint 2012). A validation exercise was performed to provide evidence of the local skill in the downscaling for our site by comparing downscaled climate to weather station data collected at our study sites for 2012-2013 that were not used in downscaling. Correlation (r) of observed with modeled monthly averages of daily maximum air temperatures in 2013 was 0.99 (Mean Absolute Error (MAE) = 1.73 °C) for foothill stations and 0.95 (MAE = 1.66°C for montane stations. Correlation for minimum air temperatures was 0.97 (MAE = 1.51 °C) and 0.97 (MAE = 1.97 °C) for foothill and montane stations (3 of each), respectively, in 2013. Very similar results were obtained for 2012. Interpolated precipitation values were not as reliable. At foothill stations, correlation with monthly precipitation was 0.85 (MAE = 16 mm) in 2012 and 0.77 (MAE = 14.4 mm) in 2013. At montane stations, correlation was 0.94 (MAE = 6 mm) in 2012 and 0.84 (MAE = 6 mm) in 2013.

We analyzed 4 future projections that bracketed a reasonable range of climate futures for the Tehachapi landscape (Table 1). Due to computational constraints, we downscaled a strategic subset of Coupled Model Intercomparison Project Phase 5 (CMIP5) climate projections as part of our larger study (Davis and Sweet 2012). We chose projections

using a clustering analysis that plotted future projections along two axes and directions of climate change (temperature and precipitation), placing projections in one of four quadrants (hot-dry, cool-dry, hot-wet and cool-wet) for our study area (Weiss et al. in review). We then reduced this set to nine projections that bracketed the range of climate projections across the four quadrants, which included three RCP 8.5, one RCP 6.0, two RCP 4.5 and three RCP 2.6 projections. For our study, we only considered RCP 8.5 (business-as-usual emissions for the 21st Century) and 4.5 (stabilizing emissions by mid-21st Century) because 1) RCP 6.0 futures are bracketed by RCP 8.5 and 4.5 projections and 2) RCP 2.6 projections are overly optimistic relative to current emissions trajectories in their requirement for declining rather than stabilizing radiative forcing by 2100 (Van Vuuren et al 2007). The RCP 4.5 subset included the Model for Interdisciplinary Research on Climate (MIROC) and the Max Planck Institute Earth System Model (MPI). We reduced the three RCP 8.5 model subset to the Community Climate System Model v4 (CCSM4) and MIROC, excluding the intermediate model, the Flexible Global Ocean-Atmosphere-Land System Model (FGOALS), in order to use an equal number of RCP 8.5 and 4.5 projections in this study. We did not consider projections of negative temperature change due to their unrealistic nature, so we instead selected projections that were relatively cooler than the RCP 8.5 projections. We calculated the average changes projected for our study area using each model (Table 1) to verify that local projections for Tejon Ranch covered our four target climate scenarios (hot-dry, cool-dry, hot-wet and cool-wet).

Future projections were downscaled using the method of constructed analogues with bias correction and GIDS interpolation (Flint and Flint 2012). In our study area, downscaled CCSM4 and MPI models project relatively small increases in precipitation when comparing

1951-1980 to end-of-21st-Century (2070-2099) levels, whereas MIROC predicts considerable decreases over the same time frame (Flint and Flint 2014). Air temperatures are projected to increase ~1.9 to 4.6°C across the four models (Table 1). We acknowledge, however, that these 30-year mean climate descriptions potentially mask changes in temporal frequency of weather events, particularly prolonged droughts and large storms (Polade et al. 2014, Berg and Hall 2015).

Modeling CWD

Mapping exposure requires accurate representation of microenvironments at biologically appropriate scales (Franklin et al. 2013; Potter et al. 2013). We produced a 149-year (1951-2099), 30-m spatial resolution dataset of annual water-year (Oct 1-Sep 30) accumulated climatic water deficit (CWD) using the Basin Characterization Model (BCM). The BCM is a distributed-parameter, deterministic water balance model used to estimate potential recharge on a monthly time step (Flint et al. 2004, 2013). The model accounted for variation in climatic and edaphic conditions, integrating spatial data on precipitation amount, timing and storage, minimum and maximum air temperature, relative humidity, radiation (net short and longwave), soil-water holding capacity and vegetative cover. The BCM was calibrated and validated with 68 and 91 California watersheds, respectively, to ensure the model was regionally robust (Flint et al. 2013). Soil information was obtained from SSURGO soil databases (NRCS 2006). These climate grids were spatially downscaled using GIDS methodology applied to local elevational gradients in a multi-step process from 12 to 4 km to 30 m (Flint and Flint 2012). Potential and actual evapotranspiration were calculated using the Priestley and Taylor (1972) equation and the National Weather Service Snow-17

model (Anderson 1976). Amounts of available water below field capacity were considered as actual evapotranspiration (Flint et al. 2013). CWD was calculated as the difference between potential and actual evapotranspiration. CWD integrates precipitation, energy loading, soil water storage, and evapotranspiration and corresponds to water that would be used by plants if it were available, and relates well to the distribution of dominant plant species (Stephenson 1998). Because CWD relies heavily on temperature-induced increases in PET, CWD increases in nearly all future climate projections (Fig. A1).

Analyzing projected changes in CWD and mapping climate change exposure

To characterize the historical reference climate, we calculated mean annual accumulated water-year CWD (CWD_{WY}) for the period 1951-1980 for each 30-m grid cell (Fig. 3). We use the period of 1951-1980 as our historical baseline due to relatively stationary temperatures prior to rapid global warming in the 1980s (Fig.1 in Hansen et al. 2006). CWD_{WY} showed no significant directional trend in our study area during this period. Prior to 1951 we lacked sufficient station data for reliable modeling of CWD across the region.

We analyze departure from historical mean conditions (ΔCWD_{WY}) and frequency of extreme years (ΔHRV) for each 30-m cell (368,520 cells) at mid-(2040-2069) and end-of-century (2070-2099) for each CMIP5 projection. Mean CWD_{WY} increased everywhere in the landscape over the course of the 21st Century, so departure from baseline mean CWD_{WY} measures the relative shift towards drier conditions of each cell. Our approach to identifying changes in extreme years was somewhat similar to that of Klausmeyer et al. (2011), who analyzed HRV in climate variables to define a "coping range" vs. stressful climate conditions

for landscapes in California. We used the frequency distribution of annual CWD values within the historical reference period to define climatic extremes for each grid cell in the landscape. We expressed the departure as a percentage rather than absolute change given the more than 3-fold range in average CWD_{WY} across the region. We defined departure from the historical range of variability (HRV) in drought years as the number of years in each 30-year period in which CWD_{WY} exceeded approximately the 93rd percentile of the HRV (i.e., drier than all but the 2 driest years in the reference period) for each cell. We did not consider variation in extremely wet years relative to historical conditions. Because the 93% threshold is somewhat arbitrary, we tested the sensitivity of results to cutoffs at approximately the 90th and 87th percentiles. To evaluate changes in the likelihood of multi-year droughts, which may be especially stressful to long-lived plants (Bigler et al. 2007; Vicente-Serrano et al. 2013), we also analyzed historical departure in three-year moving windows (ΔHRV3) for the same set of GCMs, time periods and HRV thresholds. Analyses were performed using the R package "raster" (Hijmans 2015).

Arguably, sites with minimal divergence from historical climate in terms of changes in mean climate and frequency of extreme years (years outside the HRV) offer the greatest potential as microrefugia (Fig. 1). As shown in Fig. 1, the distance of a site from the origin in this two-dimensional space represents climate exposure, which we labeled an exposure score. To facilitate comparison to percent change from mean historical climate, we re-scaled the frequency of extreme years from 0-30 to 0-100. Although previous studies used combinations of both mean climate change and frequency of extreme events to assess climate change exposure, methods varied somewhat in terms of temporal scaling and relative contributions of means vs. extremes. As such, we calculated climate change exposure as

$(\Delta CWD_{WY}^2 + \Delta HRV^2)^{0.5}$, providing equal weight to changes in mean vs. extreme climate. We mapped exposure scores across the landscape for each future projection, focusing on end-of-century projections to emphasize the requisite long-term climatic decoupling of microrefugia.

Results

Climatic water deficit

Spatial patterns of ΔHRV were similar across climate projections and time periods, but varied in magnitude (Figs. 4 and 5, Table 2). Projected ΔCWD_{WY} changes in both means (Figs. A2-A3) and ΔHRV increased with elevation and were highest on equator-facing slopes. Under the warmest and driest projection (MIROC RCP 8.5), ΔHRV ranged from 11 to 30 out of 30 years (Fig. 4) and ΔCWD_{WY} increased 13-67% by end-of-century (Fig. A2). Mitigated emissions projections (RCP 4.5) showed less divergence from the HRV and historical mean climate, particularly under the wetter MPI model (Fig. A3). Lowering the HRV thresholds slightly increased ΔHRV, particularly maximum values in RCP 4.5 projections (Table 2). Cells with the lowest ΔHRV departure rates were less sensitive to changes in thresholds across all projections (Table 2).

Values of ΔHRV3 were generally similar to ΔHRV, but with lower maxima (Table 3). Spatial patterns across the landscape were also similar, with the greatest departure rates at high elevations and lower rates on poleward (north)-facing slopes than equator-facing slopes at the same elevations. Contrary to the single-year analysis, however, rates of three-year departures from historical climate were insensitive to more restrictive definition of the HRV (Table 3).

Table 2. Number of years (out of 30) with accumulated water-year climatic water deficit (CWD) outside the historical range of variability (presented as landscape minimum and maximum values)

	93%		90%		87%	
GCM	**Mid**	**End**	**Mid**	**End**	**Mid**	**End**
CCSM4 RCP 8.5	2, 24	5, 29	2, 28	5, 30	2, 28	8, 30
MIROC RCP 8.5	2, 27	11, 30	2, 30	11, 30	2, 30	16, 30
MIROC RCP 4.5	2, 22	6, 27	2, 29	6, 30	2, 29	7, 30
MPI RCP 4.5	1, 19	2, 20	2, 27	2, 24	4, 28	4, 25

Table 3. Number of years (out of 30) with accumulated water-year climatic water deficit (CWD) outside the historical range of variability (presented as landscape minimum and maximum values) using moving 3-year averages

	93%		90%		87%	
GCM	**Mid**	**End**	**Mid**	**End**	**Mid**	**End**
CCSM4 RCP 8.5	1, 23	5, 27	1, 23	5, 27	1, 23	5, 27
MIROC RCP 8.5	2, 28	9, 28	2, 28	9, 28	2, 28	9, 28
MIROC RCP 4.5	2, 22	6, 26	2, 22	6, 26	2, 22	6, 26
MPI RCP 4.5	2, 20	2, 20	2, 20	2, 20	2, 20	2, 20

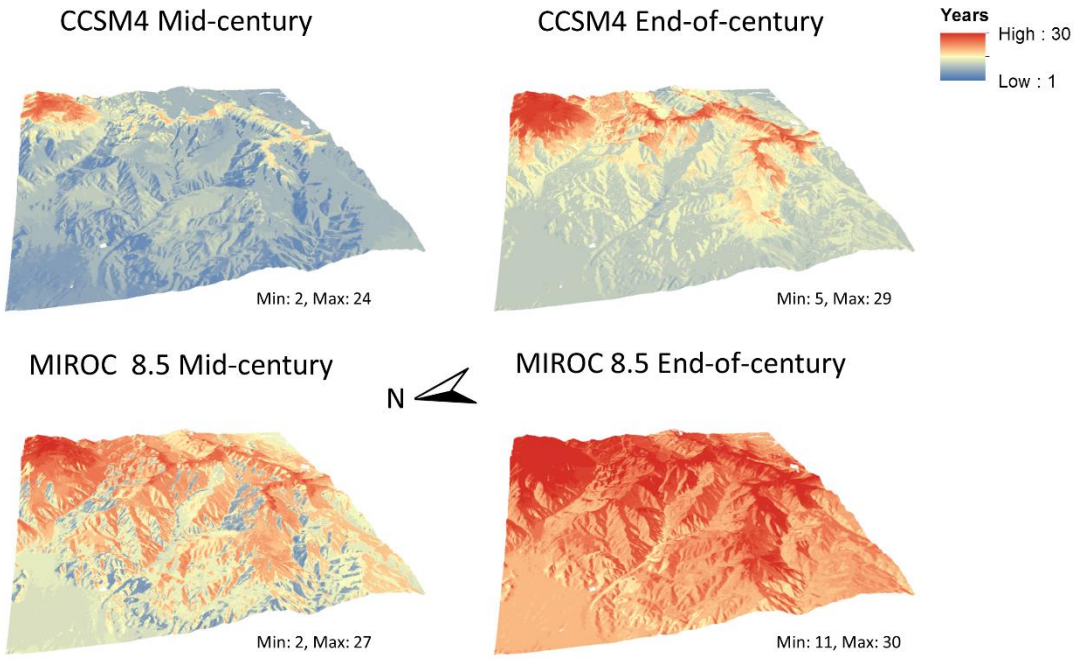

Fig. 4. Number of years of departure from the historical range of variability in terms of accumulated water-year climatic water deficit (mm/yr) during mid- (2040-2069) and end-of-century (2070-2099) periods for two general circulation models (GCMs) at representative concentration pathways of 8.5: the Community Climate System Model v4 (CCSM4) and the Model for Interdisciplinary Research on Climate (MIROC).

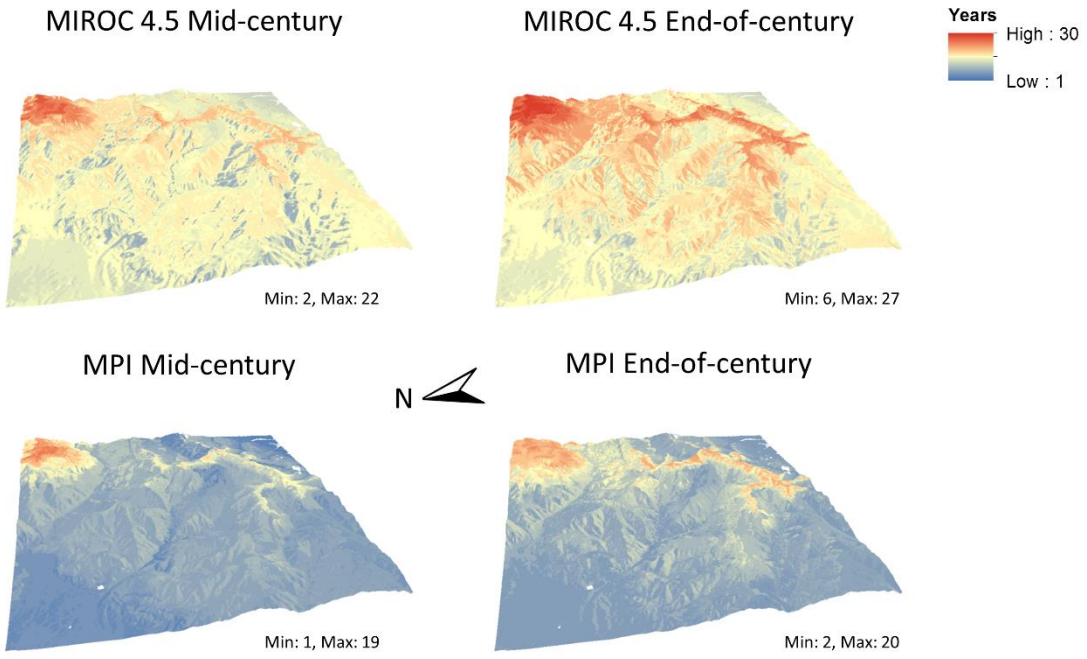

Fig. 5. Number of years of departure from the historical range of variability in terms of accumulated water-year climatic water deficit (mm/yr) during mid- (2040-2069) and end-of-century (2070-2099) periods across two general circulation models (GCMs) at representative concentration pathways of 4.5: the Model for Interdisciplinary Research on Climate (MIROC) and the Max Planck Institute Earth System Model (MPI).

Mapping climate change exposure

Across all projections, exposure scores generally increased with elevation (Fig. 6, A4). However, exposure scores varied widely across the landscape and across projections, ranging from 17 for some locations under MPI to a maximum of 119 under MIROC RCP 8.5. Scatterplots of ΔCWD_{WY} versus ΔHRV (cf. Fig 1) for each projection at end-of-century indicated that high exposure scores mainly result from high ΔHRV (Fig. 6). Topographic buffering of climate exposure occurs on poleward-facing slopes, but these areas still received relatively high exposure scores compared to flat lowlands, particularly those below 500 m

(Fig. 6). Because complex topography somewhat obscures the buffering effects of poleward-facing slopes, we performed a post hoc regression tree analysis (RTA) using the R package "tree" (Ripley 2015) to explore relationships among exposure, elevation and northness (calculated as sin(slope) * cos(aspect)). The RTA revealed that although elevation was the primary control on exposure, northness reduced exposure at moderate and low elevations (Fig. A5).

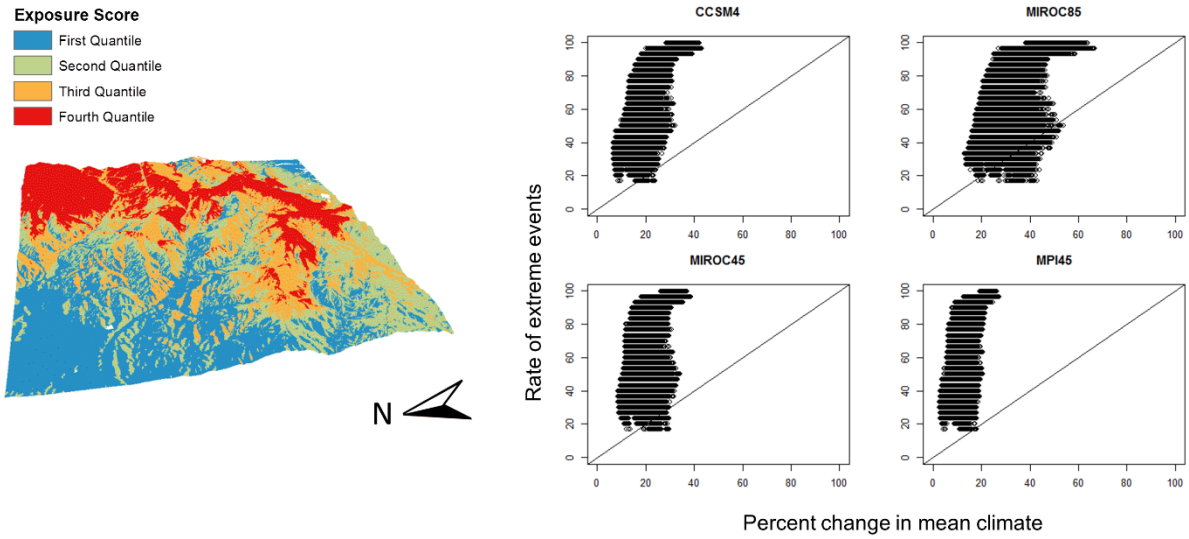

Fig. 6. Relative climate change exposure across all four climate change projections at end-of-century (2070–2099). Exposure scores were calculated for each future projection as the product of the percent change in mean climate and the rate of extreme years (departures from the HRV). Presented here are mean exposure scores across all four projections.

Discussion

Spatial patterns of climate change exposure

Large variation in CWD-based climate exposure scores suggests considerable decoupling of local sites from regional climate trends in mountain landscapes. Whether this decoupling is adequate to support microrefugia ultimately depends on widely varying species' sensitivity to changes in either or both ΔCWD_{WY} and ΔHRV. The lowest exposure scores in our landscape occurred at low elevations in sites that currently experience high CWD_{WY} and will continue to do so throughout the 21st Century. Plant species currently occupying these sites (mainly annual grasses and forbs) tolerate dry conditions, though this is not to say these species are not vulnerable to other dimensions of climate change. For example, grasslands are sensitive to the timing as well as the amount of soil moisture (Hobbs et al 2007).

We might expect microrefugia to occur in the highest (cooler and moister) portions of mountain landscapes. Our analysis suggests the opposite could be true. Those sites with historically low CWD_{WY} levels have the potential for relatively larger increases in ΔCWD_{WY} associated with warming that can affect actual evapotranspiration (AET) (Stephenson 1998). This will be especially true for historically snow-dominated sites that will receive an increasing fraction of precipitation as rain as well as shorter snowpack duration with associated increases in runoff, AET and soil evaporation (Rangwala and Miller 2012; Rangwala et al. 2013). Depending on water availability, AET will increase initially in response to warming temperatures, but will eventually level off and decline when available water is exhausted (Rosenberg et al. 1983). Exhaustion of water supplies can lead to plant mortality and vegetation type conversions (Breshears et al. 2005). Consequently, plant communities currently found at the highest elevations in moisture-limited landscapes may

face shrinking habitat and limited opportunities for long-term survival under accelerated climate exposure (Gottfried et al. 2012).

Changes in water availability coincident with increasing temperatures at high elevations are consistent with projections for our study area. In our study region, departure from historical CWD regimes was particularly dramatic at elevations above approximately 1700 m (Figs 4-5). This elevation currently marked a shift from snow-dominated to rain-dominated precipitation. By end-of-century, winter temperatures are projected to raise the rain-snow transition zone above approximately 1700 m in the RCP 4.5 scenarios and above 2000 m in CCSM4 RCP 8.5, and convert the entire landscape to rain-dominated under MIROC RCP 8.5. At lower elevations, snow was historically less important or absent entirely, so changes in moisture availability in these locations are projected to be a function of changes in total precipitation. Therefore, we suspect that sites historically within the rain-snow transition zone in moisture-limited landscapes may be most exposed to climate change. Although absent from our landscape, locations that are strongly temperature-limited and that are currently far from the rain-snow transition zone (e.g., alpine or subalpine habitats) are unlikely to experience departures from historical climate as dramatic as those projected at Tejon Ranch. More generally, we would expect that both changes in overall precipitation and the position of the rain-snow transition zone will combine to influence the exposure of any given site (Tague and Peng 2013, Thorne et al. 2015).

Although high elevation areas within the changing rain-snow transition zone are likely to become increasingly “high and dry”, we observed some buffering of these effects on poleward-facing slopes, which may be less exposed to climate change than other aspects and ridgetops. Systematically lower solar irradiance, lower potential evapotranspiration and

longer snowpack duration compared to the rest of the landscape combined to reduce the local rate of departure from historical climate. Buffering of losses in snowpack on poleward-facing slopes may be particularly important for snow-dependent species (Curtis et al. 2014). The RTA revealed that exposure was primarily controlled by elevation in our study landscape, but with secondary, interactive effects of northness (Fig. A5). On the highest poleward-facing slopes (Fig. 6), exposure was particularly great due to warming-induced loss of historically important snow. Snow reduction accelerated increases in CWD and negated topographic buffering of northerly aspects. At lower elevations, where snow was historically uncommon or absent, poleward-facing slopes exhibited some buffering of exposure. Conversely, vegetation density and local land management history may combine to increase AET in some cases and negate the additional moisture availability on poleward-facing slopes (Guarin and Taylor 2005). Finally, absent from our discussion have been riparian areas, which were not directly defined by the BCM because, although this model calculated recharge, it did not incorporate lateral flow. Riparian areas may also reduce climate change exposure due to accumulation of moisture, cool air and shade-providing vegetation. These topographically derived distinctions in climatic conditions represent a form of decoupling from regional climate and may produce potential microrefugia.

On the transferability of our approach

The approach we described here using departure from historical climate as a method of examining climate change exposure across landscapes is widely transferrable to other landscapes, useful for conservation planning and not subject to arbitrary decisions on the spatial extent of analysis. Although transferability will be ultimately limited by spatial (and possibly temporal) resolution of climate grids, fine spatial resolution is essential for

identifying microenvironments and potential microrefugia. Increasingly fine spatial resolution has been shown to reduce rates of range shifts owing to better detection of microenvironments (Serra-Diaz et al. 2014). We recognize that downscaling from coarse GCM grids to local topoclimates introduces additional uncertainty into climate projections that remains poorly quantified (Hall 2014), but nevertheless downscaled climate projections are useful for the purpose of ecological vulnerability assessment (Franklin et al. 2013). Use of varying time windows (e.g., ΔHRV vs. ΔHRV3) provides additional flexibility in terms of temporal scaling of the interactions among climate change and species' tolerance limits. Definitions of the HRV may also be manipulated depending on the nature of the distribution of focal climate variables across years. Because our method is not tied to specific biological targets, it allows local managers to decide how local changes in climate variables interact with biological sensitivity and translate into changes in species distributions. Managers could group cells of similar rates of historical departure (e.g., 0-5 of 30 years) to analyze patch structure and configuration, if desired. In these more specific contexts, it may make sense to view landscapes through the lens of individual species (e.g., commercially valuable or keystone species); however, we believe that the generic nature of our approach boosts its transferability.

Conclusions

Considering that a common, stated objective in conservation is to protect species in the places they currently inhabit, in regions undergoing rapid climate change, microrefugia should be sites that protect the same species both now and in the future. In this vein, the allure of microrefugia is understandable. If we could only identify parts of landscapes

somehow immune or resistant to climate change, we could protect and/or actively manage these sites to prevent extinctions (Keppel et al. 2012). Our analyses, however, suggest that such sites may be limited to rare localities in future landscapes. Nonetheless, we illustrate how the magnitude of climate change exposure can vary widely over short distances in heterogeneous topography and provide a means for locating areas that could experience less climate change and lower change velocities relative to regional trends. These areas may be especially valuable conservation and management targets and may play important roles in mediating range shifts and/or local persistence of species (Hannah et al. 2014, Serra-Diaz et al. 2015).

References

Ackerly DD, Loarie SR, Cornwell WK *et al*. (2010) The geography of climate change: implications for conservation biogeography. *Diversity and Distributions*, **16**, 476-487

Anderson EA (1976) A point energy and mass balance model of a snow cover. Technical report NWS 19, 150 p. U.S National Oceanographic and Atmospheric Administration (NOAA). Silver Spring, MD.

Anderson MG, Clark M, Sheldon AO (2014) Estimating Climate Resilience for Conservation across Geophysical Settings. *Conservation Biology*, **28**, 959-970.

Ashcroft MB, Gollan JR, Warton DI, Ramp D (2012) A novel approach to quantify and locate potential microrefugia using topoclimate, climate stability, and isolation from the matrix. *Global Change Biology*, **18**, 1866-1879.

Beaumont LJ, Pitman A, Perkins S (2011) Impacts of climate change on the world's most exceptional ecoregions. *Proceedings of the National Academy of Sciences*, **108**, 2306-2311.

Benito-Garzon M, Leadley PW, Fernandez-Manjarres JF (2014) Assessing global biome exposure to climate change through the Holocene-Anthropocene transition. *Global Ecology and Biogeography*, **23**, 235-244.

Bennett KD, Tzedakis PC, Willis KJ (1991) Quaternary refugia of north European trees. *Journal of Biogeography*, **18**, 103-115.

Berg N, Hall, A (2015) Increased interannual precipitation extremes over California under climate Change. *Journal of Climate*, **28**, 6324-6334.

Bigler C, Gavin DG, Gunning C, Veblen TT (2007) Drought induces lagged tree mortality in a subalpine forest in the Rocky Mountains. *Oikos* **116**, 1983-1994.

Breshears DD, Cobb NS, Rich PM et al (2005) Regional vegetation die-off in response to global-change-type drought. *Proceedings of the National Academy of Sciences*, **102**, 15144-15148.

Corlett RT, Westcott DA (2013) Will plant movements keep up with climate change? *Trends in Ecology and Evolution*, **28**, 482-488.

Curtis JA, Flint LE, Flint AL *et al*. (2014) Incorporating Cold-air pooling into downscaled climate models increases potential refugia for snow-dependent species within the Sierra Nevada Ecoregion, CA. *PLoS One*. doi: 10.1371/journal.pone.0106984.

Daly C, Halbleib M, Smith JI *et al*. (2008) Physiographically sensitive mapping of climatological temperature and precipitation across the conterminous United States. *International Journal of Climatology*, **28**, doi: 10.1002/joc.

Davis FW, Sweet LC. From mountain microclimates to the macroecology of tree species distributions in California. *Mountain Views*, **6**, 2-5.

Dawson TP, Jackson ST, House JI, Prentice IC, Mace GM (2011) Beyond predictions: biodiversity conservation in a changing climate. *Science*, **332**, 53-58.

De Frenne P, Rodríguez-Sánchez F, Coomes DA *et al*. (2013) Microclimate moderates plant responses to macroclimate warming. *Proceedings of the National Academy of Sciences*, **110**, 18561-18565

Dingman JR, Sweet LC, McCullough I *et al*. (2013) Cross-scale modeling of surface temperature and tree seedling establishment in mountain landscapes. *Ecological Processes*, **2**, 1-15.

Dobrowski SZ (2011) A climatic basis for microrefugia: the influence of terrain on climate. *Global Change Biology*, **17**, 1022-1035.

Easterling DR, Meehl GA, Parmesan C, Changnon SA, Karl TR, Mearns LO (2000) Climate Extremes: Observations, Modeling, and Impacts. *Science*, **289**, 2068–2074.

Flint LE, Flint AL (2014) California Basin Characteristic Model: a dataset of historical and future hydrologic response to climate change: U.S. Geological Survey data release. doi:10.5066/F76T0JPB.

Flint LE, Flint AL (2012) Downscaling future climate scenarios to fine scales for hydrologic and ecological modeling and analysis. *Ecological Processes*, **2**, 1-15.

Flint LE, Flint AL, Thorne JH, Boynton R (2013) Fine-scale hydrologic modeling for regional landscape applications: the California Basin Characterization Model development and performance. *Ecological Processes*, **2**, 1-21.

Flint AL, Flint LE, Hevesi JA, Blainey JB (2004) Fundamental Concepts of Recharge in the Desert Southwest: A Regional Modeling Perspective, in Groundwater Recharge in a Desert Environment: The Southwestern United States (eds J. F. Hogan, F. M. Phillips and B. R. Scanlon), American Geophysical Union, Washington, D. C.. doi: 10.1029/009WSA10.

Franklin J, Davis FW, Ikegami M *et al*. (2013) Modeling plant species distributions under future climates: how fine scale do climate projections need to be? *Global Change Biology*, **19**, 473-483.

Gavin DG, Fitzpatrick MC, Gugger PF *et al*. (2014) Climate refugia: joint inference from fossil records, species distribution models and phylogeography. *New Phytologist*, **204**, 37-54.

Gottfried M, Pauli H, Futschik A *et al*. (2012) Continent-wide response of mountain vegetation to climate change. *Nature Climate Change*, **2**, 111-115.

Guarín A, Taylor AH (2005) Drought triggered tree mortality in mixed conifer forests in Yosemite National Park, California, USA. *Forest Ecology and Management*, **218**, 229-244.

Hannah L, Flint L, Syphard AD, Moritz MA, Buckley LB, McCullough IM (2014) Fine-grain modeling of species' response to climate change: holdouts, stepping-stones, and microrefugia. *Trends in Ecology and Evolution*, **29**, 390-397.

Hansen J, Sato M, Ruedy R, Lo K, Lea DW, Medina-Elizade M (2006) Global temperature change. *Proceedings of the National Academy of Sciences*, **103**, 14288-14293.

Hijmans RJ (2015) raster: Geographic data analysis and modeling. R package version 2.3-33. http://CRAN.R-project/org/package=raster.

Hobbs RJ, Yates S, Mooney HA (2007) Long-term data reveal complex dynamics in grassland in relation to climate and disturbance. *Ecological Monographs*, **77**, 545-568.

Hylander K, Ehrlén J, Luoto M, Meineri E (2015) Microrefugia: Not for everyone. *Ambio*, **44**, 60-68.

Katz R, Brown B (1992) Extreme events in a changing climate: Variability is more important than averages. *Climatic Change*, **21**, 289–302.

Keppel G, Mokany K, Wardell-Johnson GW, Phillips BL, Welbergen J, Reside AE (2015) The capacity of refugia for conservation planning under climate change. *Frontier in Ecology and the Environment*, **13**, 106-112.

Keppel G, Van Niel KP, Wardell-Johnson GW *et al*. (2012) Refugia: identifying and understanding safe havens for biodiversity under climate change. *Global Ecology and Biogeography*, **21**, 393-404.

Klausmeyer KR, Shaw MR, MacKenzie JB, Cameron DR (2011) Landscape-scale indicators of biodiversity's vulnerability to climate change. *Ecosphere*, **2**, 1-18.

Landres PB, Morgan P, Swanson FJ (1999) Overview of the use of natural variability concepts in managing ecological systems *Ecological Applications*, **9**, 1179-1188.

Lenoir J, Graae BJ, Aarrestad PA *et al*. (2013) Local temperatures inferred from plant communities suggest strong spatial buffering of climate warming across Northern Europe. *Global Change Biology*, **19**, 1470-1481.

Loarie SR, Duffy PB, Hamilton H, Asner GP, Field CB, Ackerly DD (2009) The velocity of climate change. *Nature*, **462**, 1052-1055.

Lutz JA, van Wagtendonk JW, Franklin JF (2010) Climatic water deficit, tree species ranges, and climate change in Yosemite National Park. *Journal of Biogeography*, **37**, 936-950.

Maher SP, Morelli TL, Hershey M *et al*. (2017) Erosion of refugia in the Sierra Nevada meadows network with climate change. *Ecosphere*, **8**, DOI: 10.1002/ecs2.1673.

McLachlan JS, Clark JS, Manos PS (2005) Molecular indicators of tree migration capacity under rapid climate change. *Ecology*, **86**, 2088-2098.

Moritz MA, Parisien MA, Batllori E, Krawchuk MA, Van Dorn J, Ganz DJ, Hayhoe K (2012) Climate change and disruptions to global fire activity. *Ecosphere*, **3**, 1-22.

NRCS (2006) Natural Resources Conservation Service: U.S. General Soil Map (SSURGO/STATSGO2). http://www.ftw.nrcs.usda.gov/stat_data.html, http://soils.usda.gov/survey/geography/statsgo/description.html.

Patsiou TS, Conti E, Zimmermann NE, Theodoridis S, Randin CF (2014) Topo-climatic microrefugia explain the persistence of a rare endemic plant in the Alps during the last 21 millennia. *Global Change Biology*, **20**, 2286-2300.

Polade SD, Pierce DW, Cayan DR, Gershunov A, Dettinger MD (2014) The key role of dry days in changing regional climate and precipitation regimes. *Scientific Reports*, **4**, 4364.

Potter KA, Arthur Woods H, Pincebourde S (2013) Microclimatic challenges in global change biology. *Global Change Biology*, **19**, 2932-2939.

Priestley CHB, Taylor RJ (1972) On the assessment of surface heat flux and evaporation using large-scale parameters. *Monthly Weather Review*, **100**, 81–92.

Rangwala I, Miller JR (2012) Climate change in mountains: a review of elevation-dependent warming and its possible causes. *Climatic Change*, **114**, 527-547.

Rangwala I, Sinsky E, Miller JR (2013) Amplified warming projections for high altitude regions of the northern hemisphere mid-latitudes from CMIP5 models. *Environmental Research Letters*, **8**, 024040.

Ripley B (2015) tree: Classification and regression trees. R package version 1.0-36. http://CRAN.R-project.org/package=tree.

Rosenberg NJ, Blad BL, Verma SB (1983) Microclimate: The biological environment, Wiley.

Rull V (2009) Microrefugia. *Journal of Biogeography*, **36**, 481-484.

Scherrer D, Körner C (2011) Topographically controlled thermal-habitat differentiation buffers alpine plant diversity against climate warming. *Journal of Biogeography*, **38**, 406-416.

Schloss CA, Nuñez TA, Lawler JJ (2012) Dispersal will limit ability of mammals to track climate change in the Western Hemisphere. *Proceedings of the National Academy of Sciences*, **109**, 8606-8611.

Serra-Diaz JM, Franklin J, Ninyerola M *et al*. (2014) Bioclimatic velocity: the pace of species exposure to climate change. *Diversity and Distributions*, **20**, 169-180.

Serra-Diaz JM, Scheller RM, Syphard AD, Franklin J (2015) Disturbance and climate microrefugia mediate tree range shifts during climate change. *Landscape Ecology*, **30**, 1039–1053.

Stephenson N (1998) Actual evapotranspiration and deficit: biologically meaningful correlates of vegetation distribution across spatial scales. *Journal of Biogeography*, **25**, 855-870.

Stewart JR, Lister AM, Barnes I, Dalén L (2010) Refugia revisited: individualistic responses of species in space and time. *Proceedings of the Royal Society of London B-Biological Sciences*, **277**, 661-671.

Tague C, Peng H (2013) The sensitivity of forest water use to the timing of precipitation and snowmelt recharge in the California Sierra: Implications for a warming climate. *Journal Geophysical Research-Biogeosciences*, **118**, 875-887.

Thorne JH, Boynton RM, Flint LE, Flint AL (2015) The magnitude and spatial patterns of future hydrologic change in California's watersheds. *Ecosphere*, **6**, 1:30.

Tzedakis PC, Lawson IT, Frogley MR, Hewitt GM, Preece RC (2002) Buffered tree population changes in a Quaternary refugium: evolutionary implications. *Science*, **297**, 2044-2047.

USDA (2015) U.S. Department of Agriculture. https://soilseries.sc.egov.usda.gov/. Accessed 24 Mar 2015.

Van Vuuren DP, Den Elzen MGJ, Lucas PL *et al*. (2007) Stabilizing greenhouse gas concentrations at low levels: an assessment of reduction strategies and costs. *Climatic Change*, **81**, 119-159.

Vicente-Serrano SM, Gouveia C, Camarero JJ *et al*. (2013) Response of vegetation to drought time-scales across global land biomes. *Proceedings of the National Academy of Sciences*, **110**, 52-57.

Western Regional Climate Center (2015) Desert Research Institute. http://www.wrcc.dri.edu/. Accessed 21 Jan 2015.

Weiss SB, Flint L, Flint A, Micheli L (in review) Choosing your futures: high resolution climate-hydrology scenarios for San Francisco Bay Area, California.

Williams JW, Jackson ST, Kutzbach JE (2007) Projected distributions of novel and disappearing climates by 2100 AD. *Proceedings of the National Academy of Sciences*, **104**, 5738-5742.

Williams SE, Shoo LP, Isaac JL, Hoffmann AA, Langham G (2008) Towards an integrated framework for assessing the vulnerability of species to climate change *PLoS Biol*, **6**, e325.

Zhu K, Woodall CW, Clark JS (2012) Failure to migrate: lack of tree range expansion in response to climate change. *Global Change Biology*, **18**, 1042-1052.

Appendix

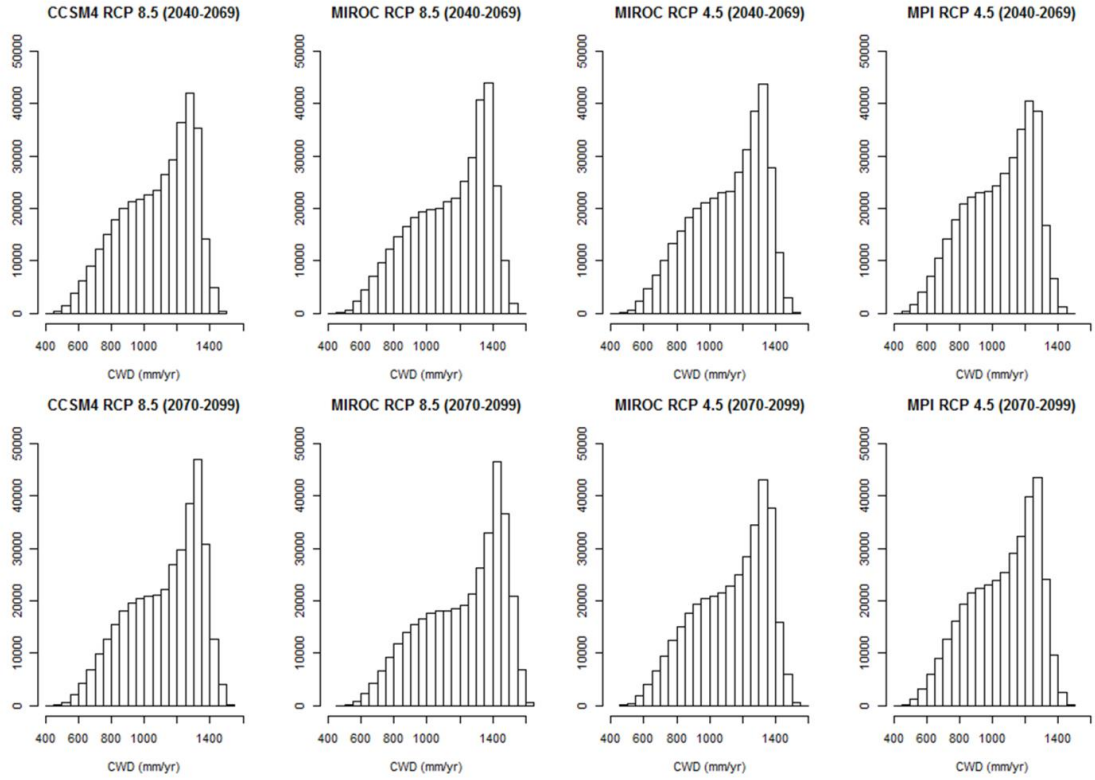

Fig. A1. Landscape distribution of accumulated water-year climatic water deficit (CWD) for Tejon Ranch expressed as cell means for mid- (2040-2069) and end-century periods (2070-2099) for CMIP5 projections. CCSM4 = Community Climate System Model version 4. MIROC = Model for Interdisciplinary Research on Climate. MPI = Max Planck Institute Earth System Model.

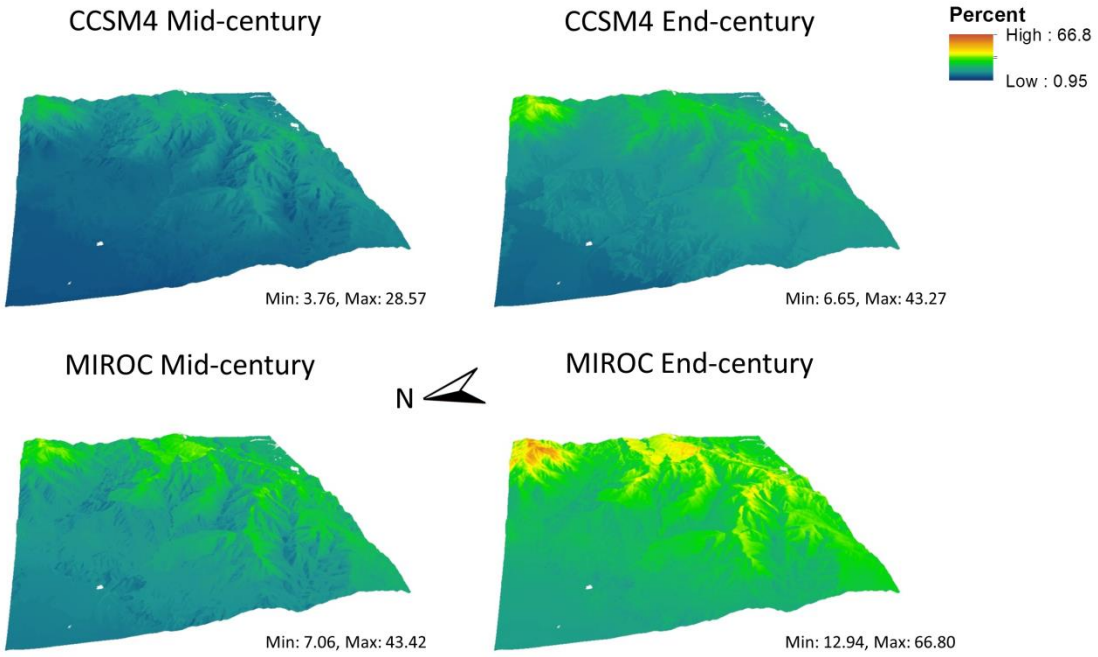

Fig. A2. Percent change in accumulated water-year climatic water deficit (mm/yr) from historical climate (1951-1980 cell means) during mid- (2040-2069) and End-of-century (2070-2099) periods across two GCMs at representative concentration pathways of 8.5. CCSM4 = Community Climate System Model version 4. MIROC = Model for Interdisciplinary Research on Climate.

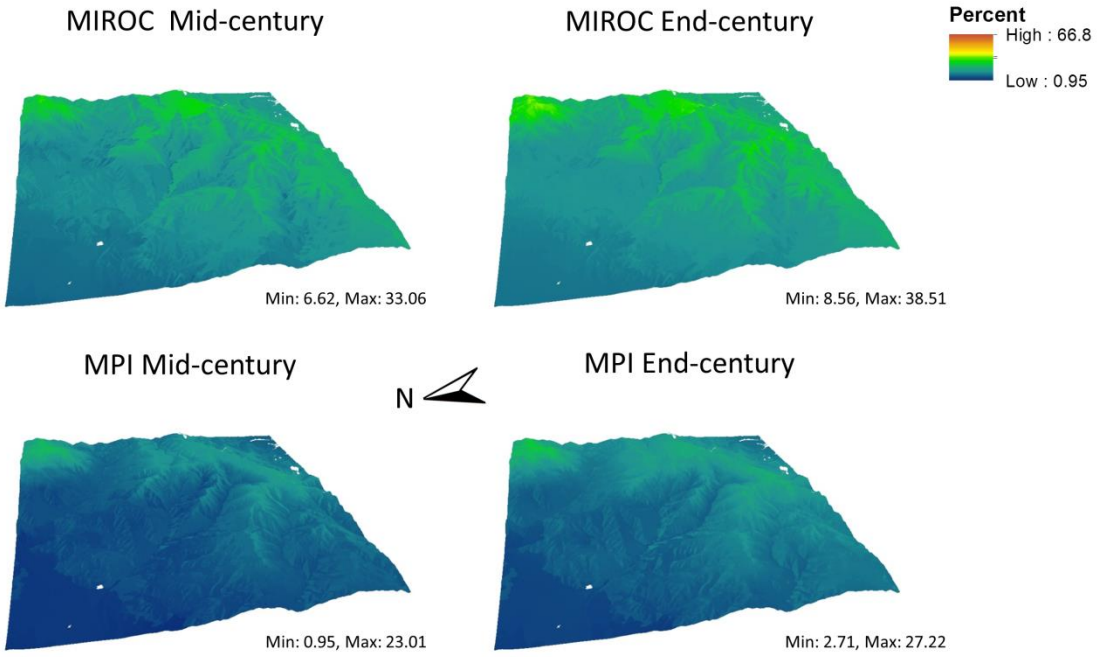

Fig. A3. Percent change in accumulated water-year climatic water deficit (mm/yr) from historical climate (1951-1980 cell means) during mid- (2040-2069) and end-of-century (2070-2099) periods across two GCMs at representative concentration pathways of 4.5. MIROC = Model for Interdisciplinary Research on Climate. MPI = Max Planck Institute Earth System Model.

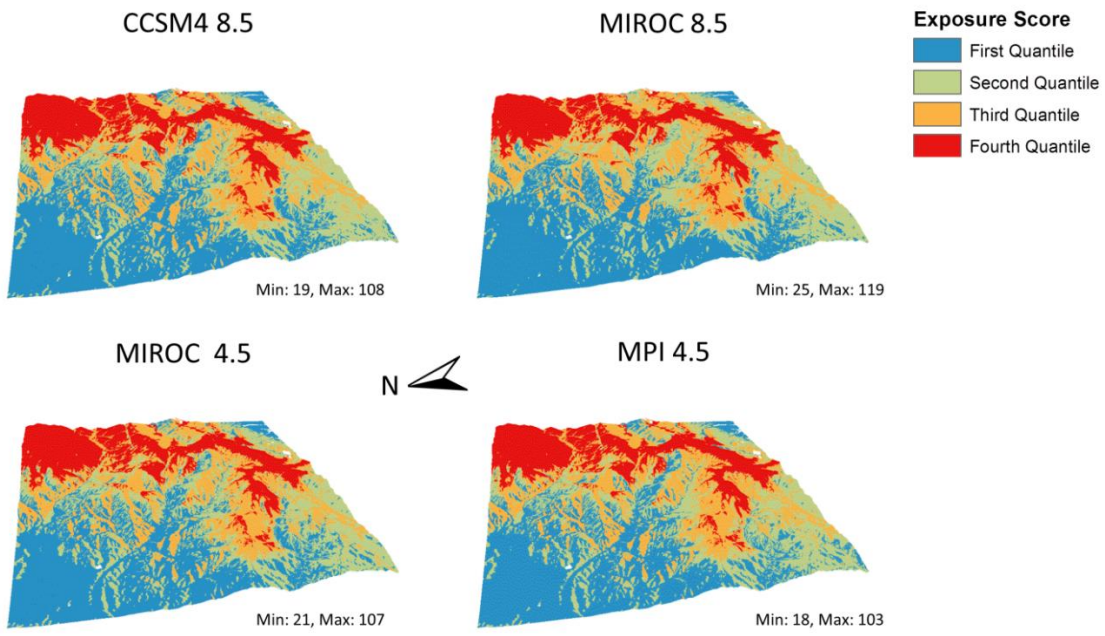

Fig. A4. Exposure scores for end-of-century (2070-2099). Exposure scores were calculated for each future scenario as the product of the percent change in mean climate and the rate of extreme events (departures from the HRV). Presented here are exposure scores across all four scenarios. Change was based on differences from the historical baseline period (1951-1980). Color gradients were calculated separately for each scenario.

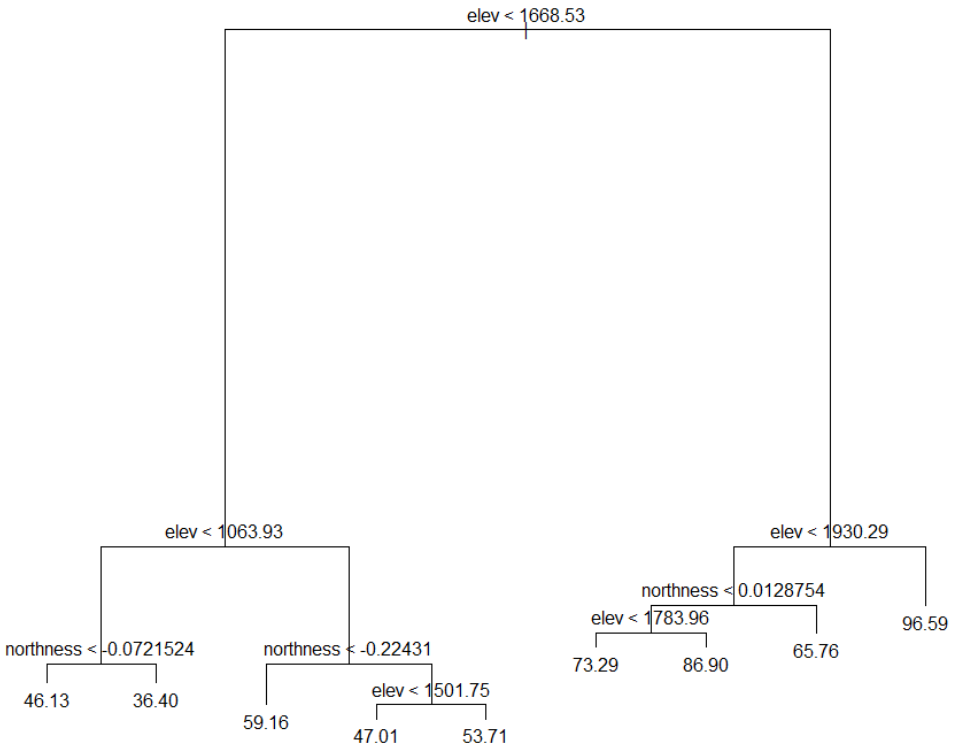

Fig. A5. Regression tree analysis (RTA) for relationships among exposure scores, elevation (m) and northness (radians). RTA is a statistical technique for exploring non-linear and non-additive relationships among variables (summarized for terrain analysis by Michaelsen et al 1994). Northness alone is weakly correlated with exposure (r=0.32) based on a 5% random sampling of the landscape, but Fig. 6 suggests a possible non-linear relationship as a function of elevation. The tree attributes 61% of deviance in exposure to elevation, but shows clear differences in exposure attributable to northness as a function of elevation. Northness was calculated as sin(slope) * cos(aspect). RTA was performed in the R package "tree" (Ripley 2015).

References

Michaelsen J, Schimel DS, Friedl MA, Davis FW, Dubayah RC (1994) Regression tree analysis of satellite and terrain data to guide vegetation sampling and surveys. *Journal of Vegetation Science*, **5**, 673-686.

Ripley R (2015) tree: Classification and Regression Trees. R package version 1.0-35. https://CRAN.R-project.org/package=tree.

CHAPTER 2

APPLICATION OF TREE RINGS AND DOWNSCALED CLIMATE GRIDS TO MAP POTENTIAL GROWTH AND DISTRIBUTION OF PONDEROSA PINE IN A MOUNTAINOUS SOUTHERN CALIFORNIA LANDSCAPE

Ian M. McCullough[1], Frank W. Davis[1], John R. Dingman[2], Lorraine E. Flint[3], Alan L. Flint[3],

[1]Bren School of Environmental Science and Management, 2400 Bren Hall, University of California, Santa Barbara, CA 93106, USA

[2]Air Resources Board, California Environmental Protection Agency, 10001 I St., P.O. Box 2815, Sacramento, CA 95812, USA

[3]U.S. Geological Survey, California Water Science Center, Placer Hall, 6000 J. St., Sacramento, CA 95189, USA

Abstract

Climate change is expected to induce range shifts in tree species, but dispersal capacities may limit the ability of trees to keep pace with the velocity of modern climate change. We used tree rings and spatially downscaled climate grids to assess long-term climate-growth relationships for ponderosa pine (*Pinus ponderosa*) and the potential for local redistribution based on climate-growth relationships in a mountainous Southern California landscape (Tejon Ranch). We fit climate response functions for ponderosa pine and applied them across the landscape for a range of climate change projections (Coupled Model Intercomparison Project; CMIP5) to identify favorable growing habitat. Interannual variability in tree growth was explained by a combination of climatic water deficit over the current and preceding water-year (Oct 1 – Sep 30), March precipitation, July maximum and January minimum air temperatures (adjusted R^2 = 0.55-0.57). In general, growth is expected to decline under future climate change in current stands, but heterogeneous topography offered potential habitat under all climate projections, particularly on north-facing slopes at higher elevations. Under warmer and drier projections, habitat availability decreased in terms of increasing distance to the nearest suitable patch and decreasing suitable habitat within average dispersal distance buffers (30 m) of current stands for both mid- (2040-2069) and end-of-century (2070-2099) periods. Spatiotemporal climate variability, however, created suitable patches within 30 m of current stands, potentially offering ephemeral windows of opportunity for local range shifts without long-distance dispersal. Successful establishment in new areas will be mediated by a combination of spatiotemporal variability in climate, seed supply and dispersal, competition and disturbances. In summary, this case study demonstrates a novel approach for projecting potential tree range shifts in response to climate

changes and highlights the importance of spatiotemporal climate variability in patch dynamics.

Introduction

A threat to forests associated with climate change is the incompatibility of typical dispersal rates with the rapid 21st Century climate change (Zhu et al. 2012, Kroiss and HilleRisLambers 2015). Mountainous terrain, however, offers potential local redistribution over relatively short distances that may reduce local extinctions and facilitate gradual range shifts (Hannah et al. 2014). Range shift projections are commonly made using relatively coarse climate grids (i.e., resolution in kilometers) that do not account for topographically controlled variability in climate across landscapes, particularly in mountainous terrain. As such, projected range contractions generally diminish as climate data resolution increases (Franklin et al. 2013). Reductions in species' exposure to climate change ("bioclimatic velocity"; Serra-Diaz et al. 2014) have been commonly attributed to "microrefugia", which are purported, relatively stable microenvironments that allow species to persist outside their main distributions and that are difficult to map using conventional gridded climate datasets (Rull 2009, Dobrowski 2011). These sites can have disproportionate influences on range shifts and/or local persistence for tree species (Serra-Diaz et al. 2015).

Although climate change exposure may be highly spatially variable across mountainous landscapes (McCullough et al. 2016), temporal variability in climatic conditions increases the dynamic structure of landscapes. For example, relatively wet years in Mediterranean landscapes create ephemeral "windows of opportunity" for seedling establishment despite generally declining or unfavorable climate across landscapes (Davis et

al. 2016). In these wet years, total suitable habitat area may triple or more with respect to median conditions (Davis et al. 2016). It is therefore likely that habitat connectivity increases or decreases through time as a function of spatiotemporal climate variability and that successful dispersal of seeds from parent trees to other suitable sites is mediated by this variability. In addition, spatiotemporal climate variability interacts with disturbance events and legacies to produce dynamic, non-equilibrium landscape structure (Hessburg et al. 2007).

In this study, we offer a novel, multi-method approach for assessing potential effects of climate change on tree species distributions at a landscape scale. We employed tree rings to examine long-term relationships between climate and growth of ponderosa pine (*Pinus ponderosa*) in a mountainous Southern California landscape (Tejon Ranch, CA). Although tree rings are typically compared to weather station data (Fritts 1976), we instead used fine (30 m) downscaled climate grids to enable mapping of potential growing habitat across the broader landscape. Use of spatial climate data therefore allowed us to analyze future suitable patch structure based on the distribution of potential growing habitat under a range of climate change projections. This analysis enabled us to estimate necessary dispersal distances for ponderosa pine to track favorable growing habitat in the future with respect to mean dispersal distances. We asked the following questions:

1. What is the historical relationship between ponderosa pine growth and climate at Tejon Ranch?
2. How will future climate change and mountainous terrain influence the potential distribution of favorable growing habitat?
3. What is the accessibility of future habitat with respect to known dispersal capacity?

Methods

Study area

Tejon Ranch is located in the western Tehachapi Mountains, CA (34°58'N, 118° 35'W). The site is characterized by rugged topography and steep climate gradients, providing a valuable case study of local variation in climate and projected climate change exposure. The area is mostly private land owned and managed by the Tejon Ranch Company for cattle ranching, hunting, agriculture and rare species conservation. Our downscaled climate grids covered a rectangular subsection of Tejon Ranch and some adjacent areas to the northeast (Cummings Peak), spanning approximately 33000 ha and steep elevational gradients (370-2364 m). The climate is Mediterranean, with hot, dry summers and cool, wet winters. Mean annual precipitation for the period 1896-2010 varied from approximately 250 mm in the driest, low elevation portions of the area to over 500 mm at the highest elevations. At elevations above roughly 1500-1600 m, a significant portion of precipitation falls as snow. See Davis et al. (2016) for additional details on vegetation and soils across the landscape.

Although ponderosa pine is one of the most widespread tree species in western North America, the species is largely restricted to high elevations and/or north-facing slopes in the southern parts of its range (Little 1971). Ponderosa pine occurs in two main stands on Tejon Ranch, both on north-facing slopes at approximately 1453 and 1676 m elevation. We refer to these stands as the lower and upper stands, respectively (Fig. 1). At the time of sampling, the upper and lower ponderosa pine stands were dominated by ponderosa pine, but contained intermixed *Quercus* spp., including predominantly California black oak (*Q. kelloggii*), and a few canyon live oak (*Q. chrysolepis*) and interior live oak (*Q. wizlizeni*) (Table 1). Over 90% of adult trees died during a recent warm drought (2012-2016), likely due to a combination of

drought exposure and pine beetle (*Dendroctonus* spp.) infestation. Several saplings survived in the upper stand, but none was observed in the lower stand. We observed evidence of beetles and associated blue stain fungus (*Grosmannia clavigera*), a phloem disrupter, in both the upper and lower stands. This mortality event was consistent with broader scale tree mortality across California (Moore and Heath 2015, Young et al. 2017).

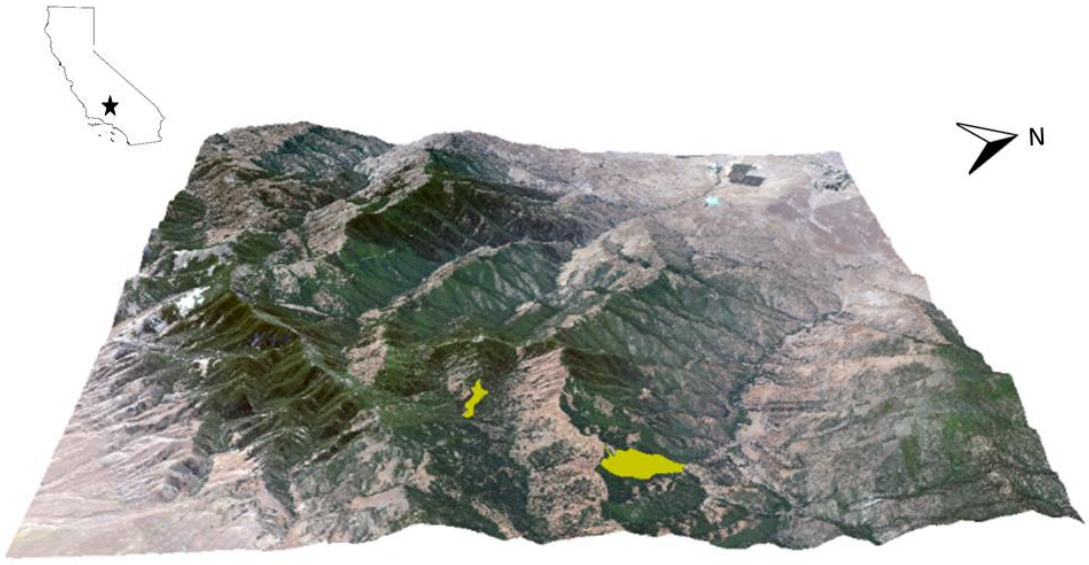

Fig. 1. Overview of Tejon Ranch study area, covering 33000 ha (approximately 20 km east-west and 17 km north-south) and an elevational gradient of 370-2364 m. The upper (left) and lower (right) ponderosa pine stands are shown in yellow.

Table 1. Ponderosa pine stand characteristics at Tejon Ranch

Stand	Area (ha)	Elevation (m)	*Pinus* BA (m^2/ha)	*Quercus** BA (m^2/ha)
Upper	19	1676	18.2	7.2
Lower	62	1453	24.3	20.2

*Q. kelloggii, Q. chrysolepis, Q. wizlizeni. BA = basal area

Tree ring sampling and preparation

We sampled tree rings from the upper stand in August 2013 and from the lower stand in August and September 2014. We sampled two cores per tree from mature trees at approximately breast height (1.3 m). To ensure we used only mature trees, which are more reliable integrators of climate (Fritts 1976, Carnwath et al. 2012), we discarded samples with no rings prior to 1925. We also discarded samples with noticeable growth releases (i.e., growth increases inconsistent with a standard growth trajectory) that may have been caused by release from competition due to mortality of neighboring trees. We only sampled live trees in the upper stand (at the time of sampling, adult mortality was minimal), but approximately two-thirds of sampled trees in the lower stand had recently died. We found no evidence of fire (fire scars on rings or visual signs on standing trees).

Tree cores were handled using standard procedures in dendrochronology (Speer 2010). We used COFECHA version 6.06P (Holmes 1983, Grissino-Mayer 2001) to validate cross-dating of samples. Reliable ring series were obtained from 28 trees from the lower stand and 22 trees from the upper stand. To remove size-related growth trends and maximize climatic signal, we standardized ring widths into a unitless ring width index (RWI; where 1 = average growth across sampled years) using a negative exponential function (R v. 3.3.3, package dplR; Bunn et al. 2008, 2016). Further details on processing and measurement of tree rings were included in the appendix (A1).

Downscaled climate grids

To represent historical climate conditions, parameter-elevation relationships on Independent Slopes Model (PRISM) (Daly et al. 2008) average monthly air temperature and

precipitation data were spatially downscaled from 800 to 30 m using Gradient-Inverse-Distance-Squared (GIDS) downscaling (Flint and Flint 2012). This method has been shown either to match the coarser resolution gridded climate or improve the match to measured station data for both precipitation and air temperature by incorporating local topography, adiabatic lapse rates and climatic gradients (Flint and Flint 2012). A validation performed using independent weather station data for 2012-2013 showed correlations between observed and modeled maximum and minimum air temperature were 0.95-0.99. Interpolated precipitation values were less reliable; correlations between observed and modeled precipitation were 0.77-0.94 (McCullough et al. 2016).

In addition to precipitation and air temperature, we included climatic water deficit (CWD) from the Basin Characterization Model (BCM). The BCM is a distributed-parameter, deterministic water balance model used to estimate potential recharge on a monthly time step (Flint et al. 2004, 2013). The model accounted for variation in climatic and edaphic conditions, integrating spatial data on precipitation amount, timing and storage, minimum and maximum air temperature, relative humidity, radiation (net short and longwave), soil-water holding capacity and vegetative cover. The BCM was calibrated and validated with 68 and 91 California watersheds, respectively, to ensure the model was regionally robust (Flint et al. 2013). Soil information was obtained from SSURGO soil databases (NRCS 2006). These climate grids were spatially downscaled using GIDS methodology applied to local elevational gradients in a multi-step process from 12 to 4 km to 30 m (Flint and Flint 2012). Potential and actual evapotranspiration were calculated using the Priestley and Taylor (1972) equation and the National Weather Service Snow-17 model (Anderson 1976). CWD was calculated as the difference between potential and actual

evapotranspiration. CWD is a predictor of Douglas-fir (*Pseudotsuga menziesii*) growth across western North America (Restiano et al. 2016), but to our knowledge has not been compared to ponderosa pine.

Climate response functions and mapping potential habitat

A climate response function is a statistical relationship between tree ring widths and climate variables (Fritts 1976). Although response functions are usually fitted using weather station data, we used downscaled climate grids to map potential growth across the broader landscape based on the climate response functions. We used the period 1950-2013 due to improved confidence in downscaled climate grids after 1950 and our desire to focus on mature trees. We used an ecologically informed forward stepwise approach for developing response functions. We initially assessed univariate relationships between RWI and climate variables to identify the variables most correlated with RWI. We found that CWD (mm) over the "current" (year of ring) and preceding water-year (wy2CWD) was the strongest RWI predictor, so we began with that variable. We iteratively added March precipitation (mm; marppt), July maximum air temperature (°C; jultmx) and January minimum air temperature (°C; jantmn). Regression model assumptions were validated using the Shapiro-Wilk test for normal residuals and the Breusch-Pagan test for heteroscedasticity. Variance inflation factors did not exceed 1.26, indicating minimal multicollinearity.

We averaged coefficients from the upper and lower stands and applied them to four climate change projections that bracketed a range of potential futures (i.e., hot-dry, hot-wet, warm-dry, warm-wet) (Ackerly et al. 2015, McCullough et al. 2016). We used two representative concentration pathway (RCP) emission scenarios (RCP 8.5: business-as-usual

trajectory and RCP 4.5: emissions peak and stabilize around 2050) under the Coupled Model Intercomparison Project (CMIP5). The RCP 4.5 models included the Model for Interdisciplinary Research on Climate (MIROC) and the Max Planck Institute Earth System Model (MPI). The RCP 8.5 models included the Community Climate System Model v4 (CCSM4) and MIROC.

Future patch dynamics

We mapped potential future ponderosa pine patches based on mapped future RWI. Patches were defined based on projected RWI. We assumed projected RWI ≥ 1, which constituted average or greater growth, represented favorable growing habitat, but we tested RWI values of 0.7-1.2 in increments of 0.1 to test the influence of this threshold on patch availability. We used two patch isolation metrics (distance to nearest patch and number of suitable cells within buffers around current stands; Bender et al. 2003) to examine the potential for local redistribution of ponderosa pine under the four future climate projections. We defined the minimum patch size as 1 cell (900 m^2), which is approximately the minimum stand size (1000 m^2) reported in other studies (Sánchez Meador et al. 2009, 2010). We tested the influence of minimum patch size on patch availability by performing all analyses on contiguous groups of 1-4 cells (four-neighbor rule). For the habitat buffers, we buffered the current stands in increments of cell widths (i.e., 30-150 m in 30 m increments). We based this decision on the known dispersal capacity of ponderosa pine. Like many tree species, ponderosa pine seeds follow a typical dispersal kernel by which most seeds fall near the parent tree and long-distance dispersal is relatively rare (Clark et al. 1999); mean dispersal distance is approximately 15-35 m and rarely exceeds 50 m (Vander Wall 2002). A

study from Oregon found just 8% of seeds dispersed 120 m or more from the parent tree (Barrett 1979). In our study, we considered 30 m as average dispersal distance due to the resolution of the climate grids. Seeds are dispersed by a combination of wind, rodents and birds (Vander Wall 2003, 2008) and recruitment often occurs in episodic pulses (White 1985, Savage et al. 1996, Brown and Wu 2005, League and Veblen 2006). We used the R raster package (Hijmans 2016) for all processing of spatial data.

Results

Climate response functions and mapped ponderosa growth

The climate response functions explained 55 and 57% of variation (adjusted R^2) in annual growth (RWI) over 1950-2013 for the upper (Fig. 2a) and lower stands (Fig. 2b), respectively (Table 2). wy2CWD (r = -0.58, -0.56) and jultmx (r = -0.34, -0.41) were negatively correlated with RWI, whereas jantmn (r = 0.41, 0.43) and marppt (r = 0.52, 0.52) were positively correlated with RWI in the upper and lower stands, respectively. Response function coefficients were greater (absolute values) in the lower stand for all variables except marppt, for which upper and lower stand coefficients were similar (0.003 and 0.002, respectively) (Table 2).

Projected ponderosa pine RWI was generally greatest on high elevation (particularly above 1800 m), north-facing slopes at both mid- and end-of-century periods (Figs. 3-4) across all climate change projections. Conversely, locations available for relatively marginal growth persisted on lower north-facing slopes, including the current upper and lower stands. Average RWI was approximately 0.96 from 1951-1980 in both stands, indicating that projected RWI represented a decline from historical conditions. The greatest and smallest

projected RWI declines were under the harshest (MIROC RCP 8.5) and mildest (MPI RCP 4.5) climate projections, respectively. For example, projected average RWI declined for the upper stand to 0.69 and 0.58 for mid- and end-of-century periods, whereas RWI declined to 0.89 and 0.78 under MPI RCP 4.5 for these same periods. Additionally, mapped RWI indicated that ponderosa pine does not currently occupy locations most favorable for growth.

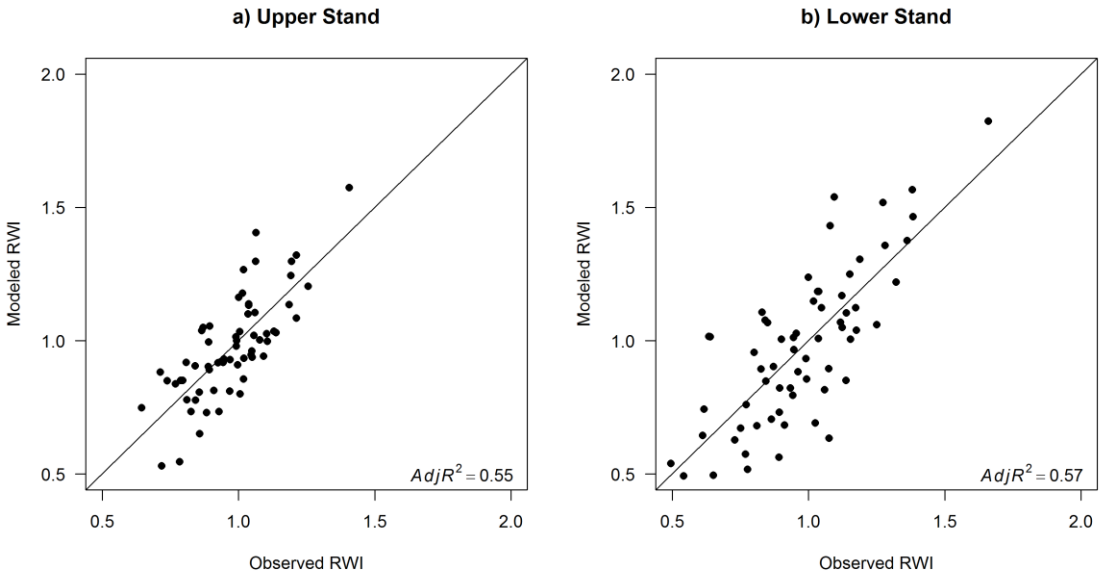

Fig. 2. Climate response functions for a) upper and b) lower ponderosa pine stands at Tejon Ranch for 1950-2013. RWI = ring width index.

Table 2. Climate response functions for ponderosa pine upper and lower stands at Tejon Ranch for 1950-2013.

Stand	Intercept	wy2CWD (mm)	jantmn (°C)	jultmx (°C)	marppt (mm)
Upper					
Coefficient	3.014	-6.645E-04	0.037	-0.034	0.003
SE	0.464	1.608E-04	0.010	0.015	3.588E-04
p-value	< 0.001	< 0.001	< 0.001	0.033	0.003
Model Adjusted R^2 = 0.55, p-value < 0.001					
Lower					
Coefficient	4.385	-7.839E-04	0.062	-0.074	0.002
SE	0.697	2.441E-04	0.015	0.023	5.470E-04
p-value	< 0.001	< 0.001	< 0.001	0.033	0.003
Model Adjusted R^2 = 0.57, p-value < 0.001					

SE = standard error, wy2CWD = cumulative climatic water deficit (mm) over current and previous water-years, jantmn = January average minimum air temperature (°C), jultmx = July average maximum air temperature (°C), marppt = March precipitation (mm).

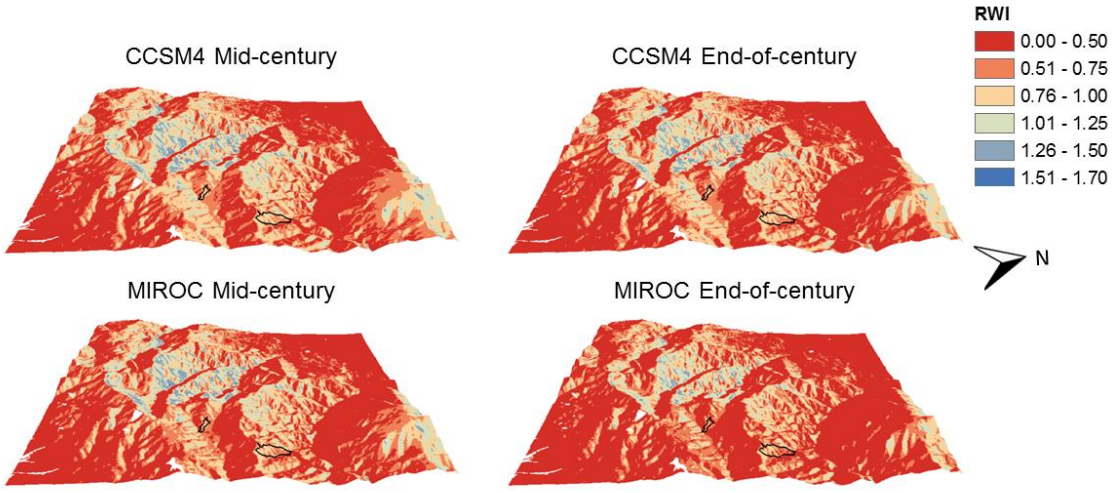

Fig. 3. Projected ponderosa pine growth (unitless ring width index; RWI) for mid- (2040-2069) and end-of-century (2070-2099) representative concentration pathway (RCP) 8.5 climate projections, overlaid on a 30-m digital elevation model. A RWI value of 1 is average. CCSM4 = Community Climate System Model v4 and MIROC = the Model for Interdisciplinary Research on Climate.

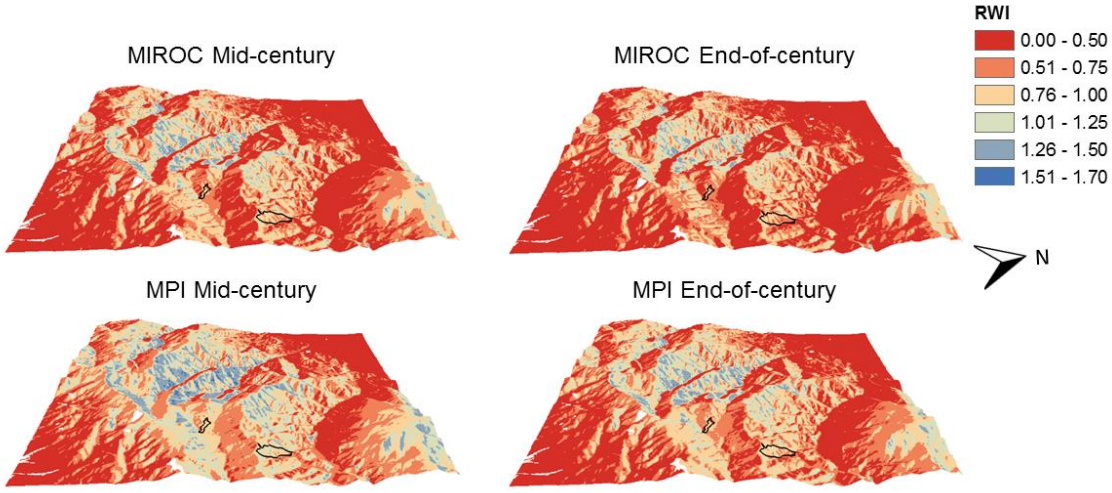

Fig. 4. Projected ponderosa pine growth (unitless ring width index; RWI) for mid- (2040-2069) and end-of-century (2070-2099) representative concentration pathway (RCP) 4.5 climate projections, overlaid on a 30-m digital elevation model. A RWI value of 1 is average. MIROC = the Model for Interdisciplinary Research on Climate and MPI = Max Planck Institute Earth System Model.

Future patch dynamics.

Distance (m) to nearest patch (minimum of 1 cell with RWI ≥ 1) generally increased throughout the 21st Century across all climate projections, but occasionally dropped to near or below average ponderosa pine dispersal distance (30 m) through approximately 2075 under the harshest projection (MIROC RCP 8.5). Distance to nearest patch approached 30 m through 2095 in the mildest projection (MPI RCP 4.5) (Fig. 5, A1). Conversely, interannual climate variability commonly drove nearest patch distance above 500 m, a distance that rarely appeared under historical climate. Nearest patch distance more commonly approached average dispersal distance during the historical period compared to all future projections (Fig. 4). On average, nearest patch distance was greater for the upper stand than for the lower stand and during the end-of-century period across all climate projections (Table 3). Average distance was greatest under MIROC RCP 8.5, smallest under MPI 4.5 and intermediate under CCSM4 RCP 8.5 and MIROC RCP 4.5. Nearest patch distance was more sensitive to the RWI threshold than minimum patch size. For example, distance from the upper stand increased from 176 to 197 m at minimum patch sizes of 1 vs. 4 cells under MIROC RCP 8.5 at mid-century (Table A1). Conversely, nearest patch distance from the upper stand was 712 m at RWI ≥ 1.2 and 23 m at RWI ≥ 0.7 at mid-century under MIROC RCP 8.5 (Table A2), which were both considerably different than nearest patch distance at RWI ≥ 1 (429 m; Table 3).

The number of suitable habitat cells within buffered areas (30 m) around the current stands mirrored trends observed from the nearest patch distance analysis. In general, the number of suitable cells within the buffers decreased consistently under all future projections, with MIROC RCP 8.5 and MPI RCP 4.5 representing the steepest and most

gradual declines, respectively (Fig. 6, A2). Historically, the number of suitable cells fluctuated between 0 and 300 cells (270000 m^2), which is approximately the area of the buffered stand. This range of values persisted under MPI RCP 4.5, but numbers increasingly approached 0 across all climate change projections through time. Similar to nearest patch distance, the number of suitable cells was more sensitive to the RWI threshold than buffer width. In general, suitable cells increased as buffer width increased (Table 4). For all projections by MPI RCP 4.5, buffers of 60 m or narrower contained no suitable cells at end-of-century. Conversely, at RWI $\geq$ 0.7, 68 suitable cells were contained within a 30 m buffer of the upper stand under MIROC RCP 8.5 at end-of-century, whereas 0 suitable cells were found at RWI $\geq$ 0.8 (Table S3).

Both path metrics indicated that landscape connectivity of favorable growing habitat varied widely through space in time and occasionally deviated considerably from connectivity under average climate conditions. For example, nearest patch distance was 517 m from the upper stand under MIROC RCP 8.5 for end-of-century average climate, but ranged from 23 to 2242 m in 2073 and 2099, respectively, corresponding to anomalously wet and dry years (Fig. 7). As such, dispersal from the upper stand to favorable growing habitat is within average dispersal distance during relatively wet years. Over 2017-2099, nearest suitable patches were within 30 m of the upper stand in 10 years, but only once (2073) in the end-of-century period (2070-2099). Conversely, nearest suitable patches were within 30 m of the upper stand in 24 years, including 6 in the end-of-century period.

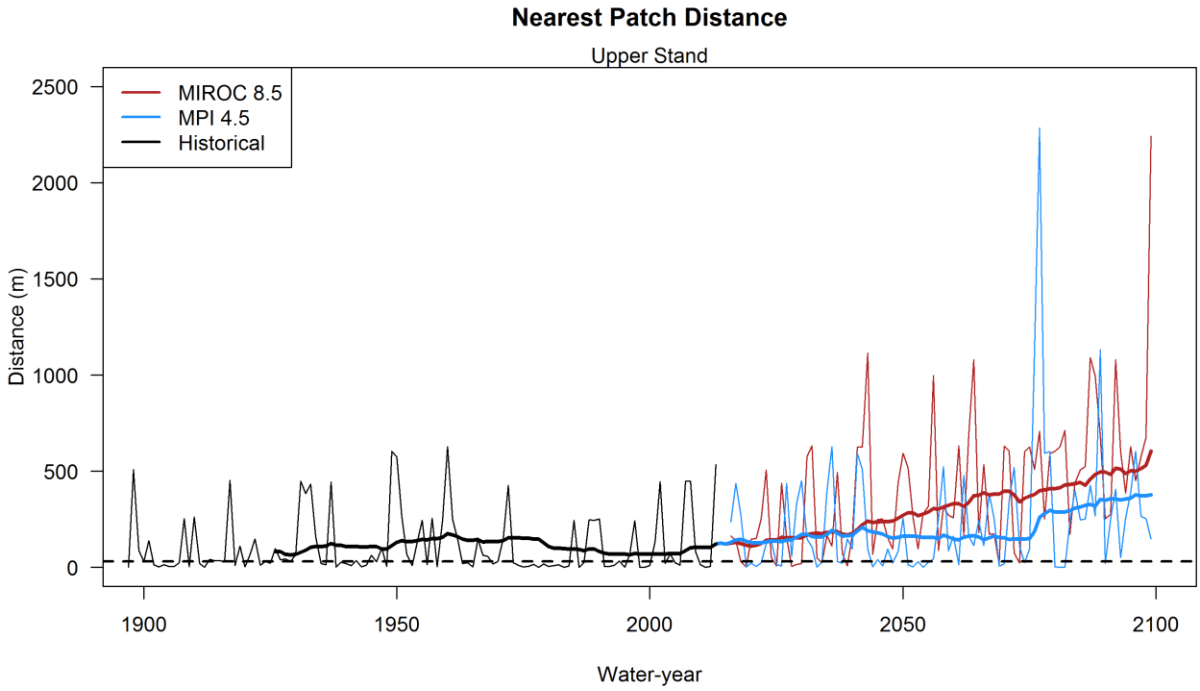

Fig. 5. Time series of distance to nearest suitable patch for the upper ponderosa pine stand for the harshest (MIROC RCP 8.5) and mildest (MPI RCP 4.5) climate change projections. Patches were defined as a minimum of 1 cell with RWI ≥ 1. Thick lines represent right-aligned 30-year moving averages. Dashed line represents average dispersal distance (30 m).

Table 3. Average distance (m) to nearest suitable patch for the lower and upper ponderosa pine stands for mid- (2040-2069; first number) and end-of-century (2070-2099; second number) average climate across CMIP5 projections. Patches were defined as a minimum of 1 cell with RWI ≥ 1.

GCM	Upper	Lower
CCSM4 RCP 8.5	397, 405	159, 173
MIROC RCP 8.5	429, 517	176, 277
MIROC RCP 4.5	254, 449	151, 241
MPI RCP 4.5	75, 247	76, 127

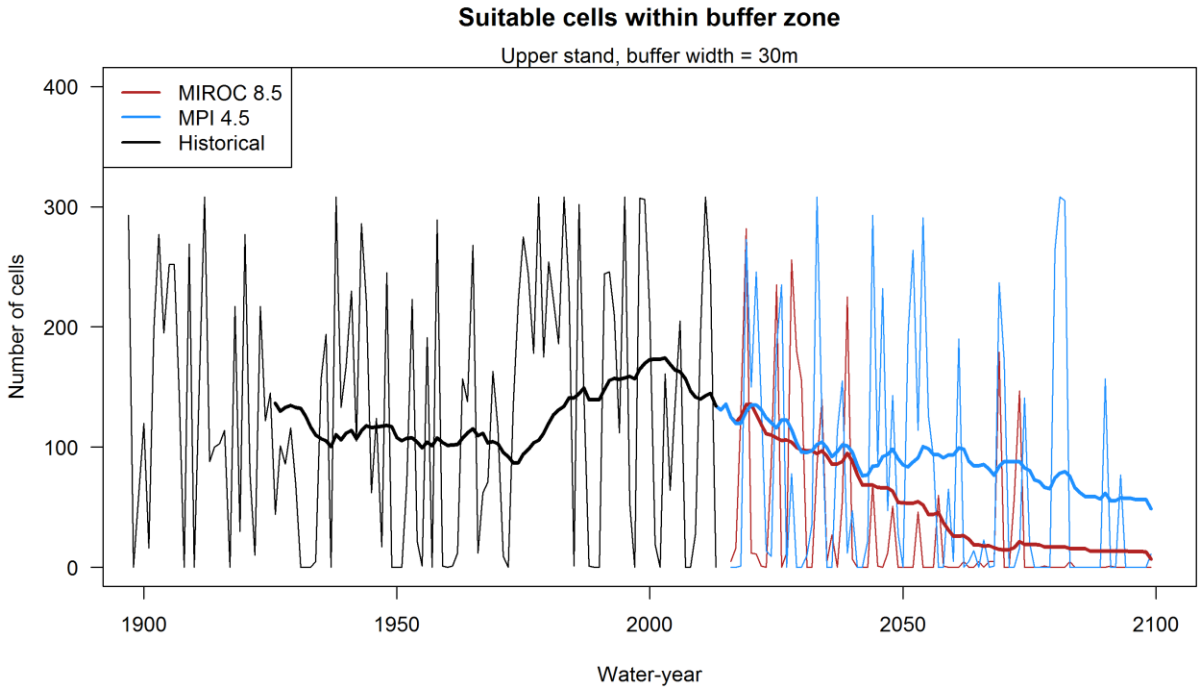

Fig. 6. Time series of the number of suitable cells within a 30 m buffer (average dispersal distance) for the upper ponderosa pine stand for the harshest (MIROC RCP 8.5) and mildest (MPI RCP 4.5) climate change projections. Suitable cells were defined as RWI ≥ 1. Thick lines represent right-aligned 30-year moving averages.

Table 4. Number of suitable cells within buffered areas (expressed as increasing buffer widths; m) around the upper and lower ponderosa pine stands for mid- (2040-2069; first number) and end-of-century (2070-2099; second number) average climate across CMIP5 projections. Suitable cells were defined as RWI ≥ 1.

GCM	30 m	60 m	90 m	120 m	150 m
Upper					
CCSM4 RCP 8.5	0, 0	1, 0	7, 6	14, 12	24, 21
MIROC RCP 8.5	0, 0	1, 0	6, 2	12, 4	21, 10
MIROC RCP 4.5	0, 0	3, 0	8, 1	14, 3	23, 8
MPI RCP 4.5	52, 0	66, 5	83, 11	103, 19	131, 35
Lower					
CCSM4 RCP 8.5	53, 35	58, 36	58, 36	58, 36	58, 36
MIROC RCP 8.5	40, 7	46, 7	46, 7	46, 7	47, 7
MIROC RCP 4.5	83, 15	93, 15	96, 15	96, 15	100, 15
MPI RCP 4.5	292, 108	332, 120	360, 123	387, 124	414, 128

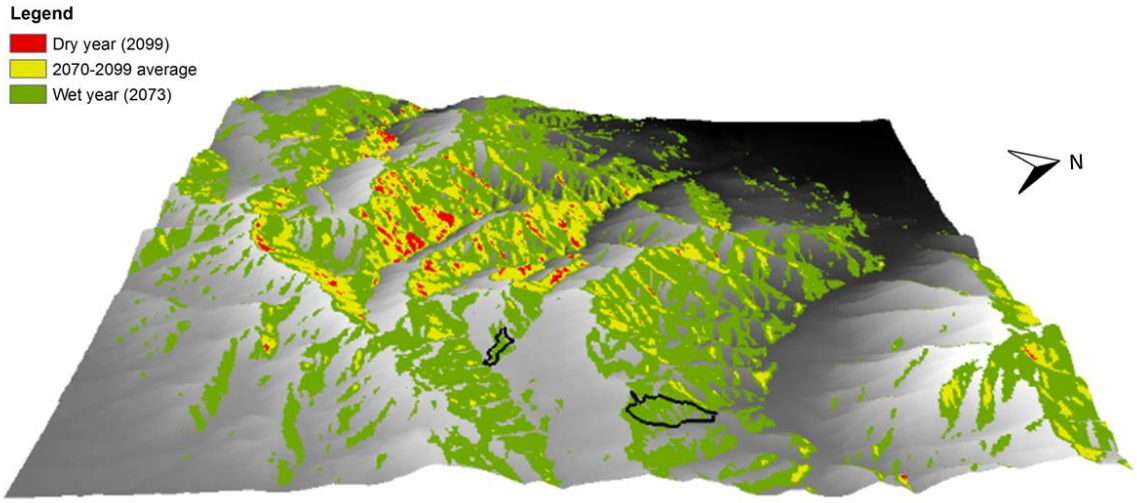

Fig. 7. Comparison of suitable growing habitat for ponderosa pine at Tejon Ranch for average 2070-2099 climate and the driest (2099) and wettest years (2073) of that 30-year period. Suitable growing habitat was defined as mapped RWI ≥ 1. Black outlines represent current ponderosa pine stands.

Discussion

Why is ponderosa pine not more common at Tejon Ranch?

Ponderosa pine is rare at Tejon Ranch, occupying less than 1% of the study landscape. Historically, ponderosa pine was marginally more common at Tejon Ranch according to Wieslander Vegetation Type Mapping (VTM) surveys from the 1920s and 1930s, occupying a few canyons at lower elevations where a few relict trees remain today (Kelly et al. 2005, 2008); however, the species still appears to inhabit a small portion of its available habitat across the landscape, but conspicuously not the high elevation, north-facing slopes where projected RWI is greatest. These areas are mostly occupied by dense stands of white fir (*Abies concolor*) (F. Davis unpublished data), which would prohibit shade-intolerant ponderosa pine establishment in the absence of gap-creating disturbance (Cooper 1961, Fulé et al. 1997). As a post hoc analysis, we compared the distributions in climate space (AET vs. CWD; sensu Stephenson 1998) of four dominant tree species that occupy relatively high elevations of the study landscape (*P. jeffreyi, Q. kelloggii, Q. chrysolepis* and *A. concolor*) in addition to ponderosa pine (Fig. 7). The climate space occupied by ponderosa pine overlaps with each of these other species, suggesting that competition and lack of disturbance may contribute to the rarity of ponderosa pine across other high-elevation areas. These phenomena reinforce the limitations of single-species distribution modeling that does not account for competition among species (Clark et al. 2014).

Utilization of potential habitat at higher elevations will depend on the remaining ponderosa trees, many of which are decades away from peak reproductive years. As such, mid-century climate projections may best reflect the conditions under which ponderosa pine would be attempting to colonize new areas. Our results show that spatiotemporal climate

variability may facilitate local range shifts or stepping-stone habitat connectivity within average dispersal distance; however, long-distance dispersal would be required for the majority of the 21st Century across all climate projections (71-88% of years). Although rare long-distance dispersal events have occurred for ponderosa pine as far as 290 km from source populations (Johansen and Latta 2003), repeated colonizations are needed to form self-sustaining populations (Lesser and Jackson 2013). The dramatically reduced adult population, however, will likely severely limit the potential for future recruitment in climatically more suitable locations at Tejon Ranch. Additionally, similar to other conifers, ponderosa pine has high rate of outcrossing (81-96%; Farris and Mitton 1984), which would limit establishment of new stands when the parent population is small.

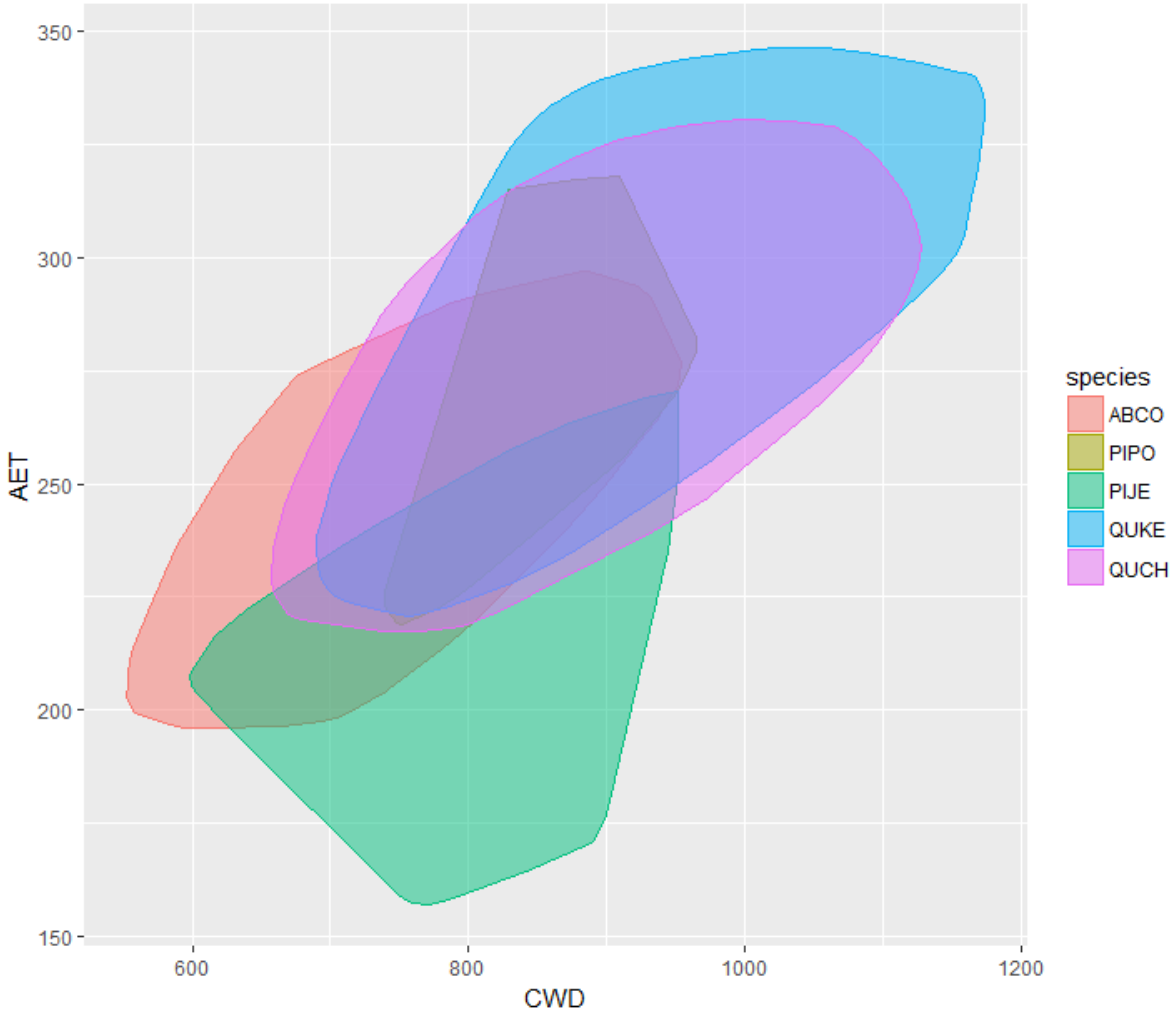

Fig. 7. Distribution of dominant high-elevation tree species at Tejon Ranch based on water-year actual evapotranspiration (AET; mm) and climatic water deficit (CWD; mm) based on 2014 Landsat 8 image classification (F. Davis unpublished data). ABCO = *Abies concolor*, PIPO = *Pinus ponderosa*, PIJE = *P. jeffreyi*, QUKE = *Quercus kelloggii*, QUCH = *Q. chrysolepis*.

Limitations and broader implications

Our mapped projections of ponderosa pine growth across the landscape should be interpreted qualitatively and with some caution; climate-growth relationships may be non-stationary through time due to a variety of factors including competition (inter- or intra-

specific), emergence of novel climates and carbon dioxide-enhanced intrinsic water-use efficiency. For example, the loss of most adult ponderosa pines may increase growth rates of remaining ponderosa trees (Oliver and Dolph 1992). Although climate-growth relationships are commonly assumed to be static in climate reconstructions, it is difficult to make quantitative growth estimates based on extrapolation to future climates without accounting for disturbance feedbacks and unknown responses to non-analogue climates (Keeling and Sala 2012). Not only may fires and insect outbreaks lead to non-linear climate-growth relationships, but disturbance influences on patch dynamics and canopy structure are important considerations for potential ponderosa pine redistribution at Tejon Ranch and require simulation modeling for future predictions (e.g., Serra Diaz et al. 2015). In addition, it is not clear how water-use efficiency may change across the range of ponderosa pine. Knapp and Soule (2011) observed increasing water-use efficiency during the 20th Century in the Northern Rockies, but these patterns were specific to mature trees. Further, genetic experiments have shown that populations from drier interior climates tend to be more water-use efficient than those from wetter Pacific climates (Monson and Grant 1989). Therefore, although general climate warming and increasing evaporative demand across western North America will likely have widespread negative effects on ponderosa pine and other tree species (Williams et al. 2013), ponderosa pine at Tejon Ranch and more broadly face somewhat uncertain future growth trajectories. Finally, soil properties (e.g., water holding capacity, depth) that influence subsurface redistribution of water and rooting depth mediate forest AET (Garcia and Tague 2015) and remain a potential source of uncertainty in predicting ponderosa growth and distribution across the landscape.

Our designation of suitable patches influenced predictions of future patch structure substantially. The decision to use mapped RWI ≥ 1 was somewhat arbitrary, but was considered an intermediate selection. Other research shows that conifers do not necessarily inhabit optimal locations owing to competition (Rehfeldt et al. 1999, Serra-Diaz et al. 2013), suggesting that ponderosa pine may ultimately inhabit locations with relatively low projected RWI at Tejon Ranch. Nonetheless, our approach was not intended as a definitive prediction of future ponderosa pine growth and distribution, but rather as a demonstration of the importance of spatiotemporal climate variability for determining future patch structure through the lens of a potentially dispersal-limited tree species. This unique coupling of tree rings with fine-resolution climate grids enables novel envisioning of future tree distributions as a function of topographically controlled and interannual climate variability and may be used to inform reforestation or assisted colonization efforts. Long-term average (e.g., 30-years) climates mask recruitment opportunities for tree species (Serra-Diaz et al. 2016) by overlooking interannual climate variability, but our study illustrates the spatial component of this temporal variability played out through shifting patch dynamics.

References

Ackerly DD, Cornwell WK, Weiss SB, Flint LE, Flint AL (2015) A geographic mosaic of climate change impacts on terrestrial vegetation: Which areas are most at risk? *PloS one*, **10**, e0130629.

Anderson EA (1976) A point energy and mass balance model of a snow cover. Technical report NWS 19. U.S National Oceanographic and Atmospheric Administration (NOAA). Silver Spring, MD

Barrett JW (1979) Silviculture of ponderosa pine in the Pacific Northwest: the state of our knowledge. USDA Forest Service, General Technical Report PNW-97. Pacific Northwest Forest and Range Experiment Station, Portland, OR. 106 p.

Bender DJ, Tischendorf L, Fahrig L (2003) Using patch isolation metrics to predict animal movement in binary landscapes. *Landscape Ecology*, **18**, 17-39.

Brown PM, Wu R (2005) Climate and disturbance forcing of episodic tree recruitment in a southwestern ponderosa pine landscape. *Ecology*, **86**, 3030-3038.

Bunn AG (2008) A dendrochronology program library in R (dplR). *Dendrochronologia*, *26*(2), 115-124.

Bunn AG, Korpela M, Biondi F *et al.* (2016) dplR: Dendrochonology Program Library in R. R package version 1.6.4. https://CRAN.R-project.org/package=dplR.

Carnwath GC, Peterson DW, Nelson CR (2012) Effect of crown class and habitat type on climate–growth relationships of ponderosa pine and Douglas-fir. *Forest Ecology and Management*, **285**, 44-52.

Clark JS, Silman M, Kern R, Macklin E, HilleRisLambers J (1999) Seed dispersal near and far: patterns across temperate and tropical forests. *Ecology*, **80**, 1475-1494.

Clark JS, Gelfand AE, Woodall CW, Zhu K (2014) More than the sum of the parts: forest climate response from joint species distribution models. *Ecological Applications*, **24**, 990-999.

Cooper, CF (1961) Pattern in ponderosa pine forests. *Ecology*, **42**, 493-499.

Daly C, Halbleib M, Smith JI *et al*. (2008) Physiographically sensitive mapping of climatological temperature and precipitation across the conterminous United States. *International Journal of Climatology*, **28**, 2031-2064.

Davis FW, Sweet LC, Serra-Diaz JM *et al*. (2016) Shrinking windows of opportunity for oak seedling establishment in southern California mountains. *Ecosphere*, **7**, e01573.

Dobrowski SZ (2011) A climatic basis for microrefugia: the influence of terrain on climate. *Global Change Biology*, **17**, 1022-1035.

Farris MA, Mitton JB (1984) Population density, outcrossing rate, and heterozygote superiority in ponderosa pine. *Evolution*, **38**, 1151-1154.

Flint AL, Flint LE, Hevesi JA, Blainey JB (2004) Fundamental Concepts of Recharge in the Desert Southwest: A Regional Modeling Perspective, in Groundwater Recharge in a Desert Environment: The Southwestern United States (eds J. F. Hogan, F. M. Phillips and B. R. Scanlon), American Geophysical Union, Washington, D. C.. doi: 10.1029/009WSA10.

Flint LE, Flint AL (2012) Downscaling future climate scenarios to fine scales for hydrologic and ecological modeling and analysis. *Ecological Processes*, **2**, 1-15.

Flint LE, Flint AL, Thorne JH, Boynton R (2013) Fine-scale hydrologic modeling for regional landscape applications: the California Basin Characterization Model development and performance. *Ecological Processes*, **2**, 1-21.

Franklin J, Davis FW, Ikegami M *et al*. (2013) Modeling plant species distributions under future climates: how fine scale do climate projections need to be?. *Global Change Biology*, **19**, 473-483.

Fritts HC (1976) Tree rings and climate, 567 pp. *Academic, San Diego, Calif*.

Fulé PZ, Covington WW, Moore MM (1997) Determining reference conditions for ecosystem management of southwestern ponderosa pine forests. *Ecological Applications*, **7**, 895-908.

Garcia ES, Tague CL (2015) Subsurface storage capacity influences climate-evapotranspiration interactions in three western United States catchments. *Hydrology and Earth System Sciences*, **19**, 4845.

Grissino-Mayer HD (2001) Evaluating crossdating accuracy: a manual and tutorial for the computer program COFECHA. *Tree-Ring Research*, **57**, 205-221.

Hessburg PF, Salter RB, James KM (2007) Re-examining fire severity relations in pre-management era mixed conifer forests: inferences from landscape patterns of forest structure. *Landscape Ecology*, **22**, 5-24.

Hijmans RJ (2016) raster: Geographic Data Analysis and Modeling. R package version 2.5-8. https://CRAN.R-project.org/package=raster

Holmes RL (1983) Computer-assisted quality control in tree-ring dating and measurement. *Tree-ring Bulletin*, **43**, 69-78.

Johansen AD, Latta RG (2003) Mitochondrial haplotype distribution, seed dispersal and patterns of postglacial expansion of ponderosa pine. *Molecular Ecology*, **12**, 293-298.

Keeling EG, Sala A (2012) Changing growth response to wildfire in old-growth ponderosa pine trees in montane forests of north central Idaho. *Global Change Biology*, **18**, 1117-1126.

Kroiss SJ, HilleRisLambers J (2015) Recruitment limitation of long-lived conifers: implications for climate change responses. *Ecology*, **96**, 1286-1297.

Lesser MR, Jackson ST (2013) Contributions of long-distance dispersal to population growth in colonising Pinus ponderosa populations. *Ecology Letters*, **16**, 380-389.

Little EL (1971) Atlas of United States trees. Vol. 1. Conifers and important hardwoods. Misc. pub. 1146. *US Department of Agriculture, Forest Service, Washington, DC*.

Kelly M, Allen-Diaz B, Kobzina N (2005) Digitization of a historic dataset: the Wieslander California vegetation type mapping project. *Madroño*, **52**, 191-201.

Kelly M, Ueda KI, Allen-Diaz B (2008) Considerations for ecological reconstruction of historic vegetation: Analysis of the spatial uncertainties in the California Vegetation Type Map dataset. *Plant Ecology*, **194**, 37-49.

Knapp PA, Soule PT (2011) Increasing water-use efficiency and age-specific growth responses of old-growth ponderosa pine trees in the Northern Rockies. *Global Change Biology*, **17**, 631-641.

League K, Veblen T (2006) Climatic variability and episodic Pinus ponderosa establishment along the forest-grassland ecotones of Colorado. *Forest Ecology and Management*, **228**, 98-107.

McCullough IM, Davis FW, Dingman, JR *et al*. (2016) High and dry: high elevations disproportionately exposed to regional climate change in Mediterranean-climate landscapes. *Landscape Ecology*, **31**, 1063-1075.

Monson RK, Grant MC (1989) Experimental studies of ponderosa pine. III. Differences in photosynthesis, stomatal conductance, and water-use efficiency between two genetic lines. *American Journal of Botany*, **76**, 1041-1047.

Moore JW, Heath ZR (2015*)* Forest health protection survey: Aerial detection survey—April 15th–17th, *USDA Forest Service, Davis, Calif.* Available at http://www.fs.usda.gov/detail/r5/forest-grasslandhealth/?cid=fsbdev3_046696.

Oliver WW, Dolph KL (1992) Mixed-conifer seedling growth varies in response to overstory release. *Forest Ecology and Management*, **48**, 179-183.

Priestley CHB, Taylor RJ (1972) On the assessment of surface heat flux and evaporation using large-scale parameters. *Monthly Weather Review*, **100**, 81–92.

Rehfeldt GE, Ying CC, Spittlehouse DL, Hamilton DA (1999) Genetic responses to climate in Pinus contorta: niche breadth, climate change, and reforestation. *Ecological Monographs*, **69**, 375-407.

Rull V (2009) Microrefugia. *Journal of Biogeography*, **36**, 481-484.

Sánchez Meador AJ, Moore MM, Bakker JD, Parysow PF (2009) 108 years of change in spatial pattern following selective harvest of a Pinus ponderosa stand in northern Arizona, USA. *Journal of Vegetation Science*, **20**, 79-90.

Sánchez Meador AJ, Parysow PF, Moore MM (2010) Historical Stem-Mapped Permanent Plots Increase Precision of Reconstructed Reference Data in Ponderosa Pine Forests of Northern Arizona. *Restoration Ecology*, **18**, 224-234.

Savage M, Brown PM, Feddema J (1996) The role of climate in a pine forest regeneration pulse in the southwestern United States. *Ecoscience*, **3**, 310-318.

Serra-Diaz JM, Keenan TF, Ninyerola M, Sabaté S, Gracia C, Lloret F (2013) Geographical patterns of congruence and incongruence between correlative species distribution models and a process-based ecophysiological growth model. *Journal of Biogeography*, **40**, 1928-1938.

Serra-Diaz JM, Franklin J, Ninyerola M *et al*. (2014) Bioclimatic velocity: the pace of species exposure to climate change. *Diversity and Distributions*, **20**, 169-180.

Serra-Diaz JM, Scheller RM, Syphard AD, Franklin J (2015) Disturbance and climate microrefugia mediate tree range shifts during climate change. *Landscape Ecology*, **30**, 1039-1053.

Serra-Diaz JM, Franklin J, Sweet LC *et al*. (2016) Averaged 30 year climate change projections mask opportunities for species establishment. *Ecography*, **39**, 844-845.

Speer JH (2010) *Fundamentals of tree-ring research*. University of Arizona Press.

Stephenson N (1998) Actual evapotranspiration and deficit: biologically meaningful correlates of vegetation distribution across spatial scales. *Journal of Biogeography*, **25**, 855-870.

Vander Wall SB (2002) Masting in animal-dispersed pines facilitates seed dispersal. *Ecology*, **83**, 3508-3516.

Vander Wall SB (2003) Effects of seed size of wind-dispersed pines (Pinus) on secondary seed dispersal and the caching behavior of rodents. *Oikos*, **100**, 25-34.

Vander Wall SB (2008) On the relative contributions of wind vs. animals to seed dispersal of four Sierra Nevada pines. *Ecology*, **89**, 1837-1849.

White AS (1985) Presettlement regeneration patterns in a southwestern ponderosa pine stand. *Ecology*, **66**, 589-594.

Williams AP, Allen CD, Macalady, AK (2013) Temperature as a potent driver of regional forest drought stress and tree mortality. *Nature Climate Change*, **3**, 292-297.

Young DJ, Stevens JT, Earles JM *et al*. (2017) Long-term climate and competition explain forest mortality patterns under extreme drought. *Ecology Letters*, **20**, 78-86.

Appendix

A1. *Tree ring sampling and preparation*

Tree cores were handled using standard procedures in dendrochronology (Speer 2010). Cores were stored in paper straws or ventilated plastic straws for transport from Tejon Ranch to the laboratory. We allowed samples to air dry for approximately one week before gluing to wooden mounts, after which we sanded cores with progressively finer sandpaper (220, 400 and 600 grit) to make annual rings visible. Several overly twisted or irreparably broken cores were discarded, but somewhat twisted cores were salvaged using boiled water and manual realignment. We used the open-source software Tellervo ® and a Velmex ® sliding platform connected to a microscope to measure annual ring widths to the nearest micrometer. Ring widths from the same tree were averaged. Rings were manually cross-dated using paper skeleton plots. We used COFECHA version 6.06P (Holmes 1983, Grissino-Mayer 2001) to validate cross-dating by analyzing correlations among trees in each stand, between both stands and between our the average of both stands and a neighboring, published tree-ring chronology (Crystal Cave, Sequoia National Park, CA (36°57’ N, 118°78’ W)), downloaded from the International Tree Ring Data Bank (ITRDB). ITRDB chronologies are rigorously verified and can be employed with high confidence of accuracy. We selected Crystal Cave because it provided a close comparison to Tejon Ranch in terms of geographic proximity and elevation (1640 m). Inter-series correlations for the upper and lower stands were 0.55 and 0.58, respectively, whereas correlation between the upper and lower stands was 0.58. The correlation between averaged lower and upper stand ring width and the Crystal Cave chronology was 0.62. All possible problems identified by COFECHA were manually investigated. Although COFECHA identified only one dating error, we

eliminated additional cores from several trees due to twisting and mechanical damage (rotten or irreparably broken wood) that caused anomalous ring measurements. In the end, we used 28 and 22 trees from the lower and upper stands, respectively, in our analyses. Fritts (1976) recommends samples of at least 20 trees for climate response analyses. To remove size-related growth trends and maximize climatic signal, we standardized ring widths into a unitless ring width index (RWI; where 1 = average growth across sampled years) using a negative exponential function in the R package dplR (Bunn et al. 2008, 2016).

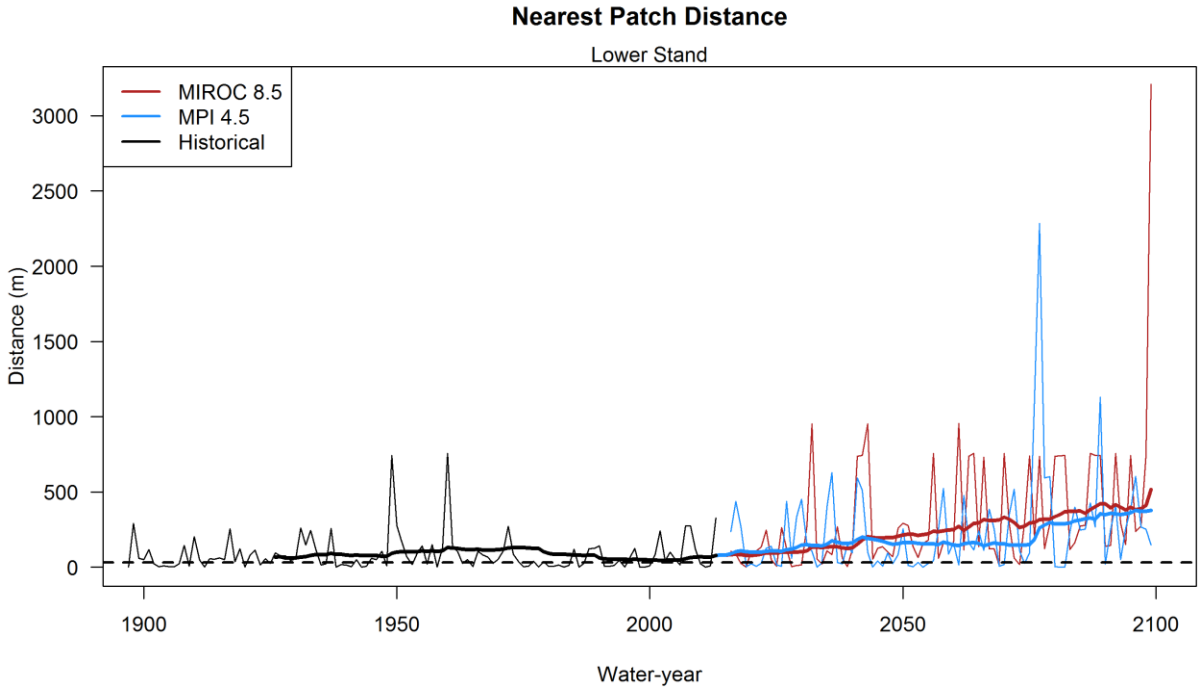

Fig. A1. Time series of distance to nearest suitable patch for the lower ponderosa pine stand for the harshest (MIROC RCP 8.5) and mildest (MPI RCP 4.5) climate change projections. Patches were defined as a minimum of 1 cell with RWI ≥ 1. Thick lines represent right-aligned 30-year moving averages. Dashed line represents average dispersal distance (30 m).

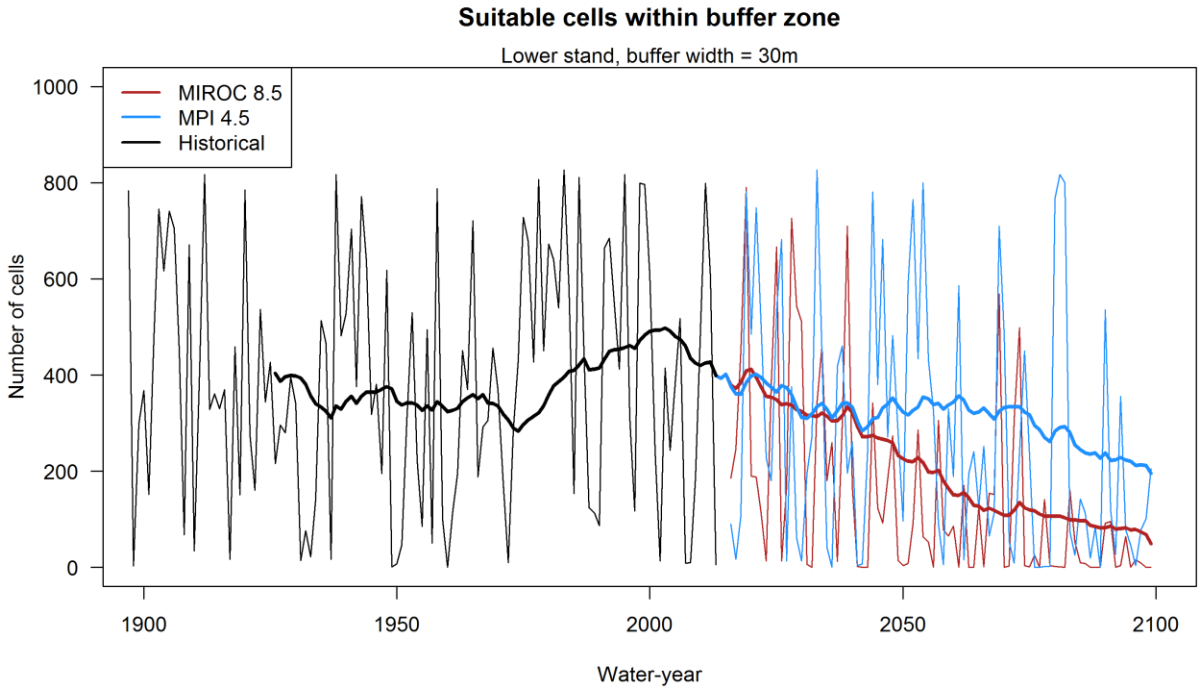

Fig. A2. Time series of the number of suitable cells within a 30 m buffer (average dispersal distance) for the lower ponderosa pine stand for the harshest (MIROC RCP 8.5) and mildest (MPI RCP 4.5) climate change projections. Suitable cells were defined as RWI ≥ 1. Thick lines represent right-aligned 30-year moving averages.

Table A1. Nearest patch distance (m) from lower and upper ponderosa pine stands at Tejon Ranch for mid- (2040-2069; first number) and end-of-century (2070-2099; second number) average climate as a function of varying patch size (four-neighbor rule) and ring width index (RWI) thresholds of favorable growing habitat.

	RWI ≥ 1.2		RWI ≥ 1.1		RWI ≥ 1		RWI ≥ 0.9		RWI ≥ 0.8	
GCM	**Lower**	**Upper**	**Lower**	**Upper**	**Lower**	**Upper**	**Lower**	**Upper**	**Lower**	**Upper**
patch ≥ 1 cell										
CCSM4 RCP 8.5	758, 947	630, 679	275, 275	507, 575	159, 173	397, 405	93, 115	148, 166	52, 58	45, 70
MIROC RCP 8.5	758, 973	712, 1131	293, 758	524, 676	176, 277	429, 517	108, 163	154, 278	57, 94	86, 153
MIROC RCP 4.5	758, 956	676, 1019	275, 743	507, 620	151, 241	254, 449	88, 124	112, 252	50, 77	39, 95
MPI RCP 4.5	256, 298	409, 600	124, 256	245, 437	76, 127	75, 247	21, 77	22, 79	6, 25	8, 25
patch ≥ 2 cells										
CCSM4 RCP 8.5	847, 947	632, 679	275, 275	573, 575	164, 211	397, 405	105, 115	148, 229	52, 58	46, 70
MIROC RCP 8.5	839, 973	712, 1131	293, 839	602, 676	182, 277	429, 590	108, 165	154, 426	57, 105	86, 153
MIROC RCP 4.5	839, 956	676, 1019	275, 743	507, 620	151, 241	254, 449	88, 124	127, 252	50, 77	39, 95
MPI RCP 4.5	256, 329	409, 600	135, 256	245, 437	76, 137	76, 247	23, 77	23, 79	6, 25	8, 26
patch ≥ 3 cells										
CCSM4 RCP 8.5	895, 947	679, 679	275, 275	573, 575	185, 219	397, 405	107, 118	148, 229	52, 58	52, 87
MIROC RCP 8.5	884, 2100	731, 1131	733, 883	602, 285	192, 277	429, 590	110, 173	154, 426	57, 105	86, 153
MIROC RCP 4.5	883, 971	676, 1107	275, 743	572, 620	164, 267	391, 503	102, 135	127, 252	50, 77	44, 95
MPI RCP 4.5	256, 883	473, 600	138, 256	275, 489	76, 147	93, 377	23, 77	23, 97	2, 27	8, 26
patch ≥ 4 cells										
CCSM4 RCP 8.5	895, 947	679, 679	275, 303	573, 575	185, 219	397, 405	107, 125	148, 229	52, 58	52, 87
MIROC RCP 8.5	884, 3390	1019, 1133	733, 883	602, 717	197, 277	429, 590	110, 182	154, 426	57, 107	86, 153
MIROC RCP 4.5	883, 971	676, 1107	275, 833	572, 620	174, 267	391, 503	103, 142	127, 380	50, 77	44, 95
MPI RCP 4.5	256, 883	473, 600	145, 256	375, 489	76, 152	93, 377	23, 77	23, 97	6, 38	8, 26

Table A2. Number of suitable cells within varying buffers around upper and lower ponderosa pine stands at Tejon Ranch for mid- (2040-2069; first number) and end-of-century (2070-2099; second number) average climate as a function of ring width index (RWI) thresholds of favorable growing habitat.

	Upper stand					Lower stand				
GCM	**30 m***	**60 m**	**90 m**	**120 m**	**150 m**	**30 m**	**60 m**	**90 m**	**120 m**	**150 m**
RWI ≥ 1.2										
CCSM4 RCP 8.5	0, 0	0, 0	0, 0	0, 0	2,2	0,0	0,0	0,0	0,0	0,0
MIROC RCP 8.5	0, 0	0, 0	0, 0	0, 0	1, 0	0,0	0,0	0,0	0,0	0,0
MIROC RCP 4.5	0, 0	0, 0	0, 0	0, 0	2, 0	0,0	0,0	0,0	0,0	0,0
MPI RCP 4.5	0, 0	0, 0	5, 0	11, 1	20, 3	17,3	18,3	18,3	18,3	18,3
RWI ≥ 1.1										
CCSM4 RCP 8.5	0, 0	0, 0	0, 0	1, 1	6,6	9,8	9,8	9,8	9,8	9,8
MIROC RCP 8.5	0, 0	0, 0	0, 0	0, 0	2,2	4,0	4,0	4,0	4,0	4,0
MIROC RCP 4.5	0, 0	0, 0	0, 0	1,0	5,2	9,1	9,1	9,1	9,1	9,1
MPI RCP 4.5	0, 0	6,0	12,2	20,4	36,11	116,17	129,18	133,18	135,18	139,18
RWI ≥ 1										
CCSM4 RCP 8.5	0, 0	1,0	7,6	14,12	24,21	53, 35	58, 36	58, 36	58, 36	58, 36
MIROC RCP 8.5	0, 0	1,0	6,2	12,4	21,10	40, 7	46, 7	46, 7	46, 7	47, 7
MIROC RCP 4.5	0, 0	3,0	8,1	14,3	23,8	83, 15	93, 15	96, 15	96, 15	100, 15
MPI RCP 4.5	52,0	66,5	83,11	103,19	131,35	292, 108	332, 120	360, 123	387, 124	414, 128
RWI ≥ 0.9										
CCSM4 RCP 8.5	12,2	24,10	34,19	46,27	66,43	210, 169	237, 190	254, 200	268, 210	282, 219
MIROC RCP 8.5	11,0	19,2	29,4	38,6	51,12	187, 57	211, 65	225, 65	235, 65	249, 67

	Upper stand					Lower stand				
GCM	**30 m***	**60 m**	**90 m**	**120 m**	**150 m**	**30 m**	**60 m**	**90 m**	**120 m**	**150 m**
MIROC RCP 4.5	25,1	37,1	49,11	61,19	81,30	232, 129	263, 144	284, 148	302, 156	321, 162
MPI RCP 4.5	144,44	184,58	223,73	269,89	317,114	476, 279	538, 315	590, 342	641, 368	690, 394
RWI ≥ 0.8										
CCSM4 RCP 8.5	83, 62	101,77	122,92	145,113	179,141	359, 317	406, 358	443, 389	480, 422	517, 453
MIROC RCP 8.5	65,12	78,21	92,31	111,42	136,56	329, 207	368, 231	400, 246	432, 262	465, 277
MIROC RCP 4.5	103,47	122,60	140,73	166,87	200,111	380, 279	432, 314	471, 340	509, 365	550, 390
MPI RCP 4.5	224,135	297,172	369,209	452,255	549,303	678, 460	762, 522	844, 568	917, 619	986, 666
RWI ≥ 0.7										
CCSM4 RCP 8.5	179,144	226,182	273,219	328,265	385,312	537, 489	606, 552	671, 604	732, 658	791, 709
MIROC RCP 8.5	144,68	177,81	203,95	233,114	270,139	478, 337	540, 379	590, 412	641, 447	696, 481
MIROC RCP 4.5	187,128	239,157	285,180	335,210	389,247	564, 434	636, 491	703, 534	770, 582	831, 629
MPI RCP 4.5	278,219	369,287	463,357	569,436	686,529	786, 665	894, 746	997, 825	1089, 898	1174, 967

*average dispersal distance (Vander Wall 2002)

References

Bunn AG (2008) A dendrochronology program library in R (dplR). *Dendrochronologia*, *26*(2), 115-124.

Bunn AG, Korpela M, Biondi F *et al.* (2016) dplR: Dendrochonology Program Library in R. R package version 1.6.4. https://CRAN.R-project.org/package=dplR.

Fritts HC (1976) Tree rings and climate, 567 pp. *Academic, San Diego, Calif*.

Grissino-Mayer HD (2001) Evaluating crossdating accuracy: a manual and tutorial for the computer program COFECHA. *Tree-Ring Research*, **57**, 205-221.

Holmes RL (1983) Computer-assisted quality control in tree-ring dating and measurement. *Tree-ring Bulletin*, **43**, 69-78.

Speer JH (2010) *Fundamentals of tree-ring research*. University of Arizona Press.

Vander Wall SB (2002) Masting in animal-dispersed pines facilitates seed dispersal. *Ecology*, **83**, 3508-3516.

CHAPTER 3

A RANGE OF POSSIBILITIES: ASSESSING GEOGRAPHIC VARIATION IN CLIMATE SENSITIVITY OF PONDEROSA PINE USING TREE RINGS

Ian M. McCullough[1], Frank W. Davis[1] and A. Park Williams[2]

[1]Bren School of Environmental Science & Management, University of California, Santa Barbara, CA, USA, 93106

[2] Lamont–Doherty Earth Observatory, Columbia University, Palisades, NY, USA 10964

Abstract

Climate change has emerged as a major threat to biodiversity, but we lack understanding of how sensitivity to climate variability differs across species' ranges. We examined the sensitivity of ponderosa pine (*Pinus ponderosa*), a common, commercially important tree species found throughout the western United States, to climate variability across the western United States using tree rings mostly from the International Tree Ring Data Bank (161 chronologies) and multiple climate products for 1930-1979. We compared interannual tree ring variation to water-year precipitation (wyppt), May-July vapor pressure deficit (MJJ VPD), April-July precipitation (AMJJ ppt) and average winter (Dec-Feb) minimum temperature (winter tmn). We mapped growth-climate correlations for each variable and applied hierarchical agglomerative cluster analysis to identify five main groups of climate sensitivities, one of which contained mostly climate-insensitive populations. Ponderosa pine growth was sensitive to wyppt, AMJJ ppt and MJJ VPD throughout its range, but sensitivities were greater in the Southern Rockies and Northern Great Plains than in Pacific and Southwestern populations. Sensitivities to winter tmn were weaker than responses to other climate variables, but Pacific and interior populations mostly demonstrated positive and negative tmn responses, respectively. In summary, our analyses revealed the general pattern that interior populations of ponderosa pine were more climate-sensitive than Pacific populations, but there is considerable heterogeneity in sensitivity throughout the species' range. Sensitivities to climate variables were related to position along corresponding climate gradients for all variables except MJJ VPD, but the unevenness of these relationships suggests a role of local adaptation. Our results illustrate the variation in climate response for

a uniquely wide-ranging species and suggest that “leading” and “trailing” range edge concepts can oversimplify patterns of species exposure to climate change.

Introduction

Assessments of species’ vulnerability to climate change are commonly performed using climate envelope models, which generally project population and range shifts based on climate change exposure (Dawson et al. 2011). Exposure-based vulnerability assessments generally rely on correlative occupancy-environment relationships (Pacifici et al. 2015) and do not take into account local or population-level variation in sensitivity to climate across species’ ranges that can be crucial for predicting overall vulnerability to climate change (Williams et al. 2008, Rehfeldt et al. 1999, Davis and Shaw 2001, Sork et al. 2010).

Tree rings offer a means to assess range-wide variation in climate sensitivity in tree species. Using published chronologies from the International Tree Ring Data Bank (ITRDB), Chen et al. (2010) found distinct responses of Douglas-fir (*Pseudotsuga menziesii*) between interior and coastal varieties in western North America, conforming to seasonal climate variability. Restiano et al. (2016) found that Douglas-fir populations throughout the species’ range were sensitive to vapor pressure deficit (VPD) and climatic water deficit, but that populations near the southern range limit were most sensitive. Conversely, Cavin and Jump (2016) found that range-core populations of European beech (*Fagus sylvatica*) were the most sensitive to drought, which they attributed to local adaptation of southern populations to seasonal, warm droughts. Similarly, Hacket-Pain et al. (2016) found widespread drought limitation in European beech across southern range limit and range-core populations. The

ultimate significance and determinants of geographic differentiation in tree species' growth responses to climate remains an open question.

Determining the importance of local adaptation is best approached by combining genetic and climate response data across entire ranges (Franks et al. 2014). Lacking genetic data for the study trees, there is still value in examining a species whose range spans wide climate gradients and has well-documented phylogeography and genetic history to support interpretation of climate responses. We selected ponderosa pine (*Pinus ponderosa*), an ecologically and commercially important tree species, as a case study for analyzing intra-specific variation in growth response to climate. Ponderosa pine generally inhabits dry, mountainous areas throughout western North America from British Columbia to the American Southwest (Little 1971). This extensive range provides an opportunity to examine intra-specific variation in climate sensitivity across widely varying climate regimes, including Mediterranean, monsoonal and continental climates.

Ponderosa pine phylogeography

Ponderosa pine has traditionally been divided into two varieties: Pacific (*P. ponderosa* var. *ponderosa*) and interior (*P. ponderosa* var. *scopulorum*), separated by the Continental Divide (Little 1979). Conkle and Critchfield (1988) and Callaham (2013a, b) suggested additional subdivision into several races and subspecies, but Potter et al. (2015) found little genetic basis for these distinctions. Although there is some (primarily west-east) gene flow between the two varieties in Montana (Latta and Mitton 1999), the varieties may have been separated well before the last glacial maximum (18,000 years ago) (Potter et al. 2015). Lascoux et al. (2004) estimated a much longer separation of 250,000 years. After

glacial retreat, both varieties expanded their ranges from likely multiple refugia of unknown location, which coupled with complex mountain terrain has resulted in a geographically heterogeneous genetic structure and numerous disjunct and genetically isolated populations (Latta and Mitton 1999, Johansen and Latta 2003, Potter et al. 2013, 2015). A few long-distance dispersal events contributed to overall range expansion (Johansen and Latta 2003, Lesser and Jackson 2013, Shinneman et al. 2016). Potter et al. (2015) demonstrated considerable gene flow within but not between varieties and evidence for as many as 9 distinct genetic clusters (5 interior, 4 Pacific). Shinneman et al. (2016) found 10 discrete haplotypes that while generally conforming to interior and Pacific varietal bounds, also inhabited distinct climatic niches. Overall, these various genetic studies revealed a complex phylogeography and heterogeneous genetic structure of ponderosa pine that may mediate current and future climate sensitivities.

Genetic basis for climate adaptation in P. ponderosa

Provenance trials of ponderosa pine revealed abrupt genetic variation along local elevational gradients, variation which manifested in tradeoffs between growth potential and cold hardiness (Rehfeldt 1986a, 1986b, 1990, 1991). These findings suggest climate sensitivities may be relatively localized as the result of the combined influence of regional climate, local topoclimatic variation and genetically based local adaptation. Studies of other conifers at regional scales have shown variable climate sensitivities over relatively short geographic distances according to local climate gradients (e.g., Griesbauer and Green 2010, Ashiq and Anand 2016). Previous local and regional research has demonstrated that ponderosa pine growth is primarily sensitive to precipitation and secondarily to temperature

(with seasonal variations) (Fritts et al. 1965, 1976, Veblen et al. 2000, Yeh and Wensel 2000, Kusnierczyk and Ettl 2002, Watson and Luckman 2002, Knutson and Pyke 2008, Williams et al. 2010a, Carnwath et al. 2012, Adams et al. 2014, Dannenberg and Wise 2016).

The aforementioned studies were conducted over different time periods using a variety of climate metrics and sampling methods. Our analysis considered ponderosa climate sensitivity across its entire range using consistent climate and tree-ring data. We also examined the relationships between climate sensitivity and rangewide climate gradients. We expected that precipitation variables would be positively correlated with ponderosa pine growth throughout its range and that these correlations would generally decrease in wetter locations. Additionally, we expected interior populations, which experience more extreme temperature fluctuations, to be relatively more sensitive to cold temperatures in winter and heat-driven in summer than populations closer to the Pacific coast.

Methods

Tree-ring chronologies

We obtained 159 ponderosa pine tree-ring chronologies from the ITRDB and developed two additional chronologies from Tejon Ranch, CA, bringing the total to 161 chronologies (Fig. 1, A1-2). All chronologies were downloaded as raw ring widths and converted to a unitless ring width index (RWI) using a negative exponential function in the dplR package in R (Bunn 2008, Bunn et al. 2016) to ensure all chronologies were standardized with a common approach. This relatively conservative method removes the age-related ring-width trend in tree-ring chronologies attributed to tree geometry and potentially rapid growth of young trees (Cook 1985). Although the negative exponential function has

received some criticism and several alternatives have been offered (e.g., Biondi and Qaedan 2008), this method was developed for the kind of chronologies we used (i.e., shade-intolerant pines in open canopy stands) (Cook 1985). We limited our analyses to the time period 1930-1979, balancing the benefit of long growth records across a large number of sites, our desire to analyze a common set of years across all chronologies and the reliability of corresponding downscaled climate grids (see downscaled climate data methods below).

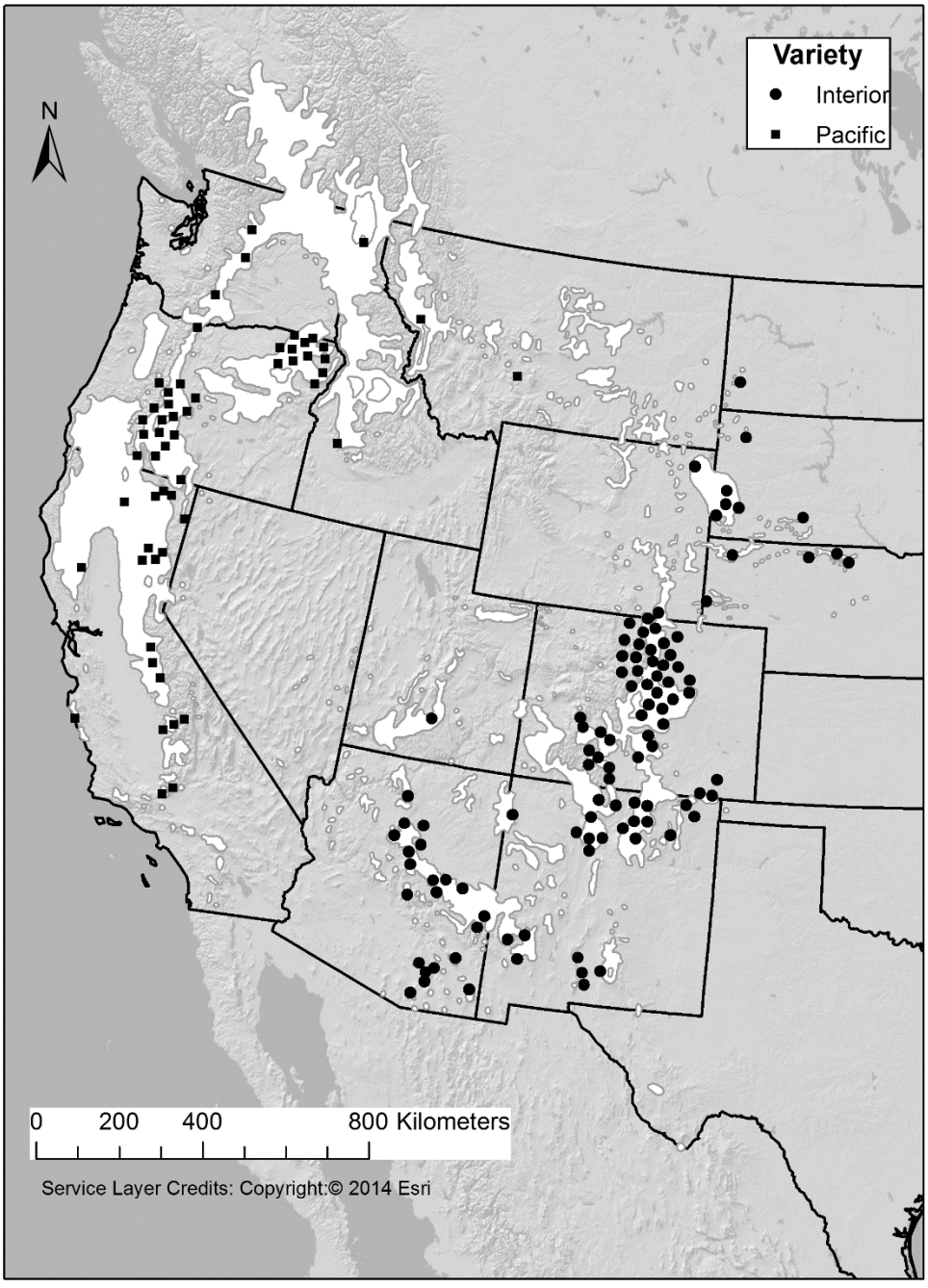

Fig. 1. Locations of ponderosa pine tree-ring chronologies (n = 161) laid atop a range map (Little 1971) and symbolized by variety (Little 1979). All but two chronologies were taken from the International Tree Ring Data Bank (ITRDB). We sampled two chronologies from Tejon Ranch, the southernmost sites in California. Dots were jittered for display only.

Downscaled climate data and variable selection

Climate data included the 1/24° ClimGrid (Vose et al. 2014) and PRISM (Daly et al. 2008) grids. We used monthly precipitation, minimum and maximum air temperature and saturation vapor pressure from ClimGrid and actual vapor pressure from PRISM (used to compute vapor pressure deficit; VPD). Although these grids are relatively coarse with respect to climatic heterogeneity in mountain landscapes, the relatively imprecise location records of tree-ring chronologies (often tenths of degrees latitude and longitude) limited the usefulness of finer resolution grids. Furthermore, we were primarily interested in inter-annual climate variability, for which high spatial resolution is not necessary given the relatively sparse distribution of weather stations used to generate the climate grids. For assessment of growth response to climate, we explored numerous potential derived climate indices, but intercorrelations among these variables made statistical results difficult to interpret (Fritts et al. 1971, Cropper 1984). We ultimately selected a subset of variables that were not highly correlated and based on current understanding of the species' ecology and physiology (Fritts 1976, Zang and Biondi 2013).

We used exploratory correlation matrices and principal component analysis (PCA) to narrow the set of potential climate variables from 128 to four: water-year (previous Oct 1 – current Sep 30) and Apr-Jul precipitation (wyppt and AMJJ ppt, respectively), MJJ VPD and winter (Dec-Feb) minimum temperatures (winter tmn). Although previous research has shown that seasonal precipitation controls vary across the range of ponderosa pine, wyppt was highly correlated ($r = 0.95$) with Oct-Mar precipitation across our study sites so we included AMJJ as the only seasonal precipitation variable ($r = -0.02$ with wyppt). We included MJJ VPD rather than maximum temperature because VPD integrates humidity and

air temperature to describe atmospheric aridity conditions that may induce stomatal closure and reduced growth (McDowell et al. 2008, Adams et al. 2009, Williams et al. 2013). We included winter tmn based on Bigelow et al. (2014), who found positive correlations between warming winters and growth in the northern Sierra Nevada, CA, and the notion that adaptations for cold tolerance are associated with tradeoffs in growth potential (Rehfeldt 1986a, 1986b, 1990, 1991).

Climate sensitivity mapping and cluster analysis

We mapped Pearson correlation coefficients (r) between RWI and the four climate variables at each of the 161 sites to visualize geographic patterns of climate sensitivity. We used hierarchical agglomerative cluster analysis of the correlation values to group sites based on multivariate climate sensitivities. We used a Euclidean distance matrix and Ward's method to minimize within-cluster sum of squares. Here we show the results based on five clusters. We inspected a sum of squares scree plot to identify a range of potential numbers of clusters. We iteratively experimented with 2-7 clusters, visually inspecting differences among clusters after each successive split. We ultimately settled on 5 clusters given that minimal additional information was revealed beyond this number. We performed pairwise comparisons of cluster means for each climate variable. We also performed pairwise comparisons on 1930-1979 averages for the four climate variables across the five clusters to assess whether differences in climate sensitivities corresponded to differences in mean climatology.

Results

Climate sensitivity mapping

Water-year precipitation (wyppt) was significantly correlated ($p < 0.05$) with RWI at 120 of 161 (74.5%) sites (Table 1). In general, wyppt was positively correlated with RWI throughout ponderosa pine's range, but correlations were overall weaker and more variable in the Pacific Northwest (Fig. 2a). MJJ VPD was significantly correlated with RWI at 112 sites (69.6%) (Table 1). Correlation with MJJ VPD were almost entirely negative, and more negative at interior sites (Fig. 2b). AMJJ ppt was significantly correlated with RWI at 96 sites (59.6%) (Table 1) and the relationship was mostly positive, except for a few Pacific sites where relationships were weakly negative (Fig. 2c). Particularly in California, where Mediterranean climates dominate, weak relationships with AMJJ ppt (i.e., absolute $r < 0.30$) coincided with low AMJJ ppt. Winter tmn was significantly correlated with growth at the fewest sites (20; 12.4%) and the median correlation was close to zero (Table 1). There was a clear geographic pattern to the winter tmn correlations, which ranged from weakly negative in the Rocky Mountains to weakly positive in the Sierra Nevada, Cascade and southwestern US Sky Island mountains (Fig. 2d).

Table 1. Significant climate-growth correlations (r) across 161 sites (1930-1979)

Variable	p = 0.05	p = 0.1	Median r	5% r	95% r
wyppt	120	128	0.40	0.02	0.60
MJJ VPD	112	124	-0.39	-0.58	-0.04
AMJJ ppt	96	109	0.31	-0.02	0.57
winter tmn	20	29	0.04	-0.21	0.36

wyppt = water-year (Oct 1-Sep 30) precipitation (mm), MJJ VPD = May-Jul vapor pressure deficit (kPa), AMJJ ppt = Apr-Jul precipitation (mm) and winter tmn = Dec-Feb minimum temperature (°C).

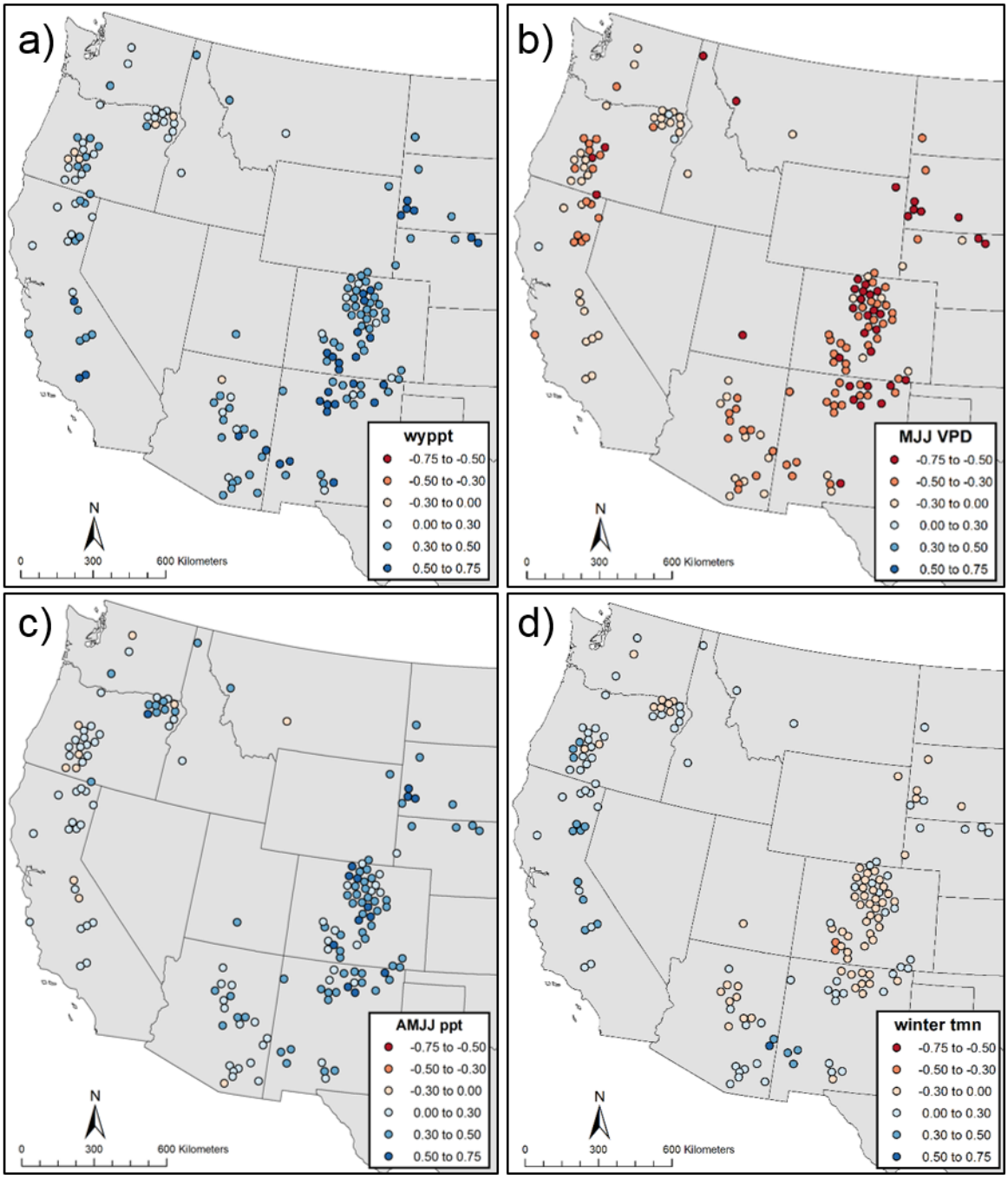

Fig. 2. Pearson correlation coefficients (r) between ponderosa pine standardized ring width index (RWI) and individual climate variables (1930-1979). Sites were jittered for display only. a) wyppt = water-year (Oct 1-Sep 30) precipitation (mm), b) MJJ VPD = May-Jul vapor pressure deficit (kPa), c) AMJJ ppt = Apr-Jul precipitation (mm) and d) winter tmn = Dec-Feb minimum temperature (°C).

Cluster analysis

The cluster analysis revealed geographically heterogeneous patterns of climate sensitivities. Cluster 1 (n = 21) mostly represented low-latitude sites in New Mexico and Arizona (Fig. 3). On average, cluster 1 was positively correlated with wyppt, AMJJ ppt and winter tmn and negatively correlated with MJJ VPD (Table 2). Cluster 1 was also the most sensitive to wyppt compared to other clusters (Fig. 4a). Cluster 2 (n = 47) represented mostly interior sites, particularly in Colorado, northern New Mexico and South Dakota (Fig. 3). On average, cluster 2 was less sensitive to wyppt than cluster 1, but was more strongly positively and negatively correlated with AMJJ ppt and MJJ VPD, respectively. Cluster 2 was the only cluster negatively correlated with winter tmn (Table 2, Fig. 4). Cluster 3 (n = 16) was the least representative of the populations sampled, containing sites in the Sierra Nevada and southern Arizona and New Mexico. Cluster 3 was the least sensitive to AMJJ ppt and the most positively correlated with winter tmn (Table 2). Cluster 4 (n=53) was the most widespread cluster, containing groups of sites in Arizona, Colorado and Oregon (Fig. 3). Overall, the sign relationships were similar to clusters 1-3, but sensitivity to winter tmn was closest to zero among all clusters (Table 2, Fig. 4). Cluster 5 (n = 24) contained mostly northern Pacific sites (Fig. 3) and was the least climate sensitive (average absolute $r \leq 0.13$) among clusters (Table 2, Fig. 4).

Differences in climate sensitivities across clusters generally corresponded to differences in climate, except for MJJ VPD (Figs. 4-5). Clusters with greater wyppt were decreasingly sensitive to wyppt whereas clusters with greater AMJJ ppt were more sensitive to AMJJ ppt Clusters with warmer winter tmn were more positively correlated with winter tmn. Conversely, sensitivity to MJJ VPD was not strongest at sites with high mean MJJ VPD.

For example, although cluster 2 populations displayed the most negative response to MJJ VPD, mean MJJ VPD levels among cluster 2 populations were considerably lower than those of clusters 1 and 3. Similarly, the analysis of climate sensitivities along climate gradients revealed similar patterns. We found linear relationships (absolute $r \geq 0.40$) between wyppt, AMJJ ppt and winter tmn sensitivities and each corresponding climate gradient, but not for MJJ VPD ($r = 0.14$) (Fig. 6). In other words, sensitivities to wyppt, AMJJ ppt and winter tmn were generally predictable across the range of ponderosa pine based on position along corresponding gradients, but sensitivities to MJJ VPD were consistently negative regardless of range position, potentially contributing to the finding of Williams et al. (2013) that a regionally averaged southwestern US tree-ring records (including ponderosa pine) correlates more strongly with warm-season VPD than with cold-season precipitation. Results of pairwise comparisons for climate sensitivities and climate across clusters were included in supporting information (Table A3).

Table 2. Mean climate sensitivities and climate across clusters (1930-1979)

Cluster	wyppt (mm)	AMJJ ppt (mm)	MJJ VPD (kPa)	winter tmn (°C)	n
Mean climate sensitivities (r)					
1	0.54	0.38	-0.39	0.16	21
2	0.46	0.44	-0.50	-0.13	47
3	0.38	0.17	-0.27	0.38	16
4	0.32	0.29	-0.37	0.03	53
5	0.08	0.11	-0.13	0.11	24
Mean climate					
1	210.77	163.56	15.49	-6.99	
2	219.23	203.42	11.35	-10.39	
3	364.58	138.69	14.54	-3.63	
4	262.43	163.28	13.16	-6.78	
5	362.09	145.30	12.00	-5.54	

wyppt = water-year (Oct 1-Sep 30) precipitation (mm), MJJ VPD = May-Jul vapor pressure deficit (kPa), AMJJ ppt = Apr-Jul precipitation (mm) and winter tmn = Dec-Feb minimum temperature (°C).

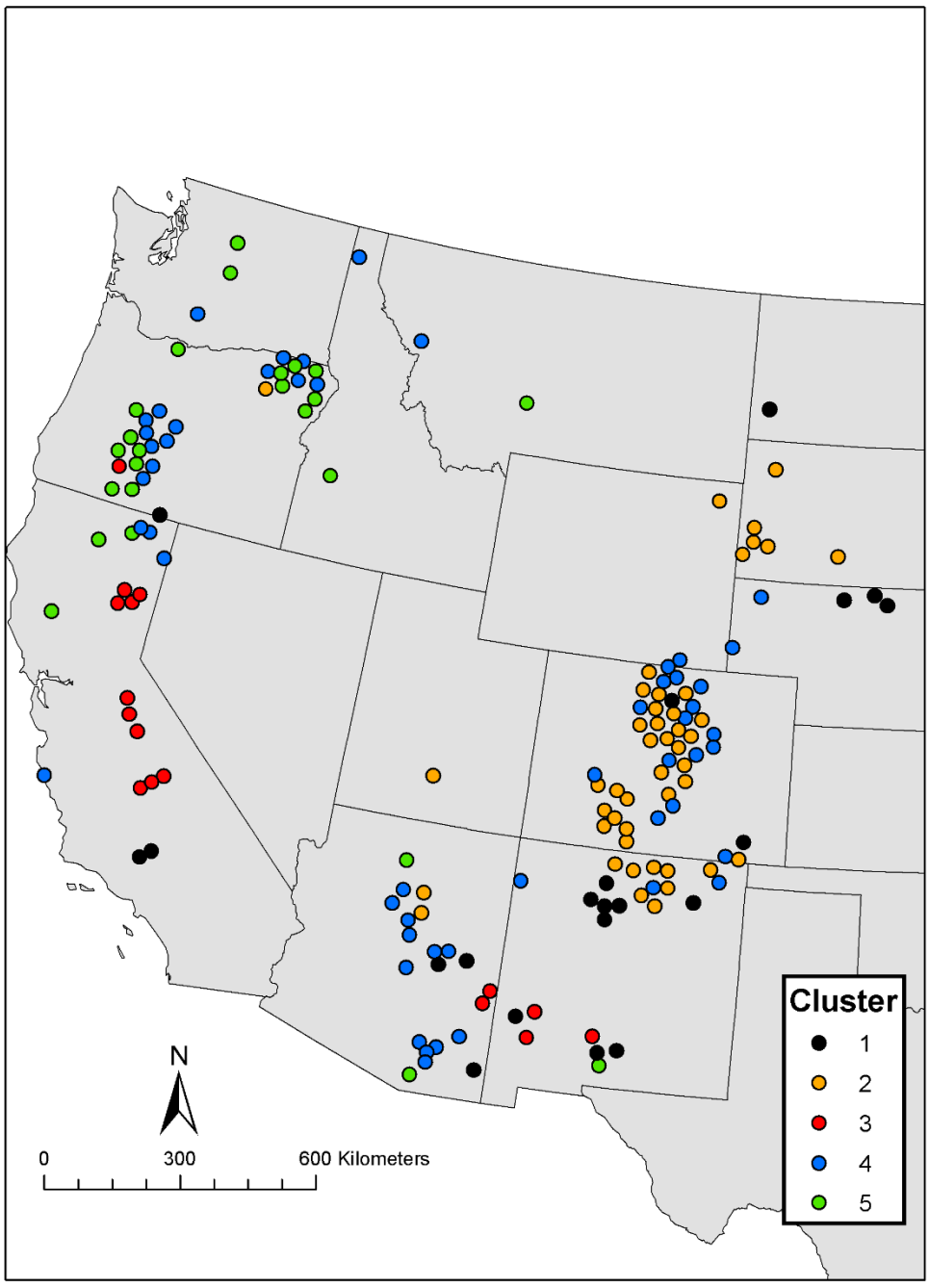

Fig. 3. Clusters from the hierarchical agglomerative cluster analysis based on ponderosa pine climate sensitivities (relationships between standardized ring width index (RWI) and climate variables over 1930-1979). Sites were jittered for display only.

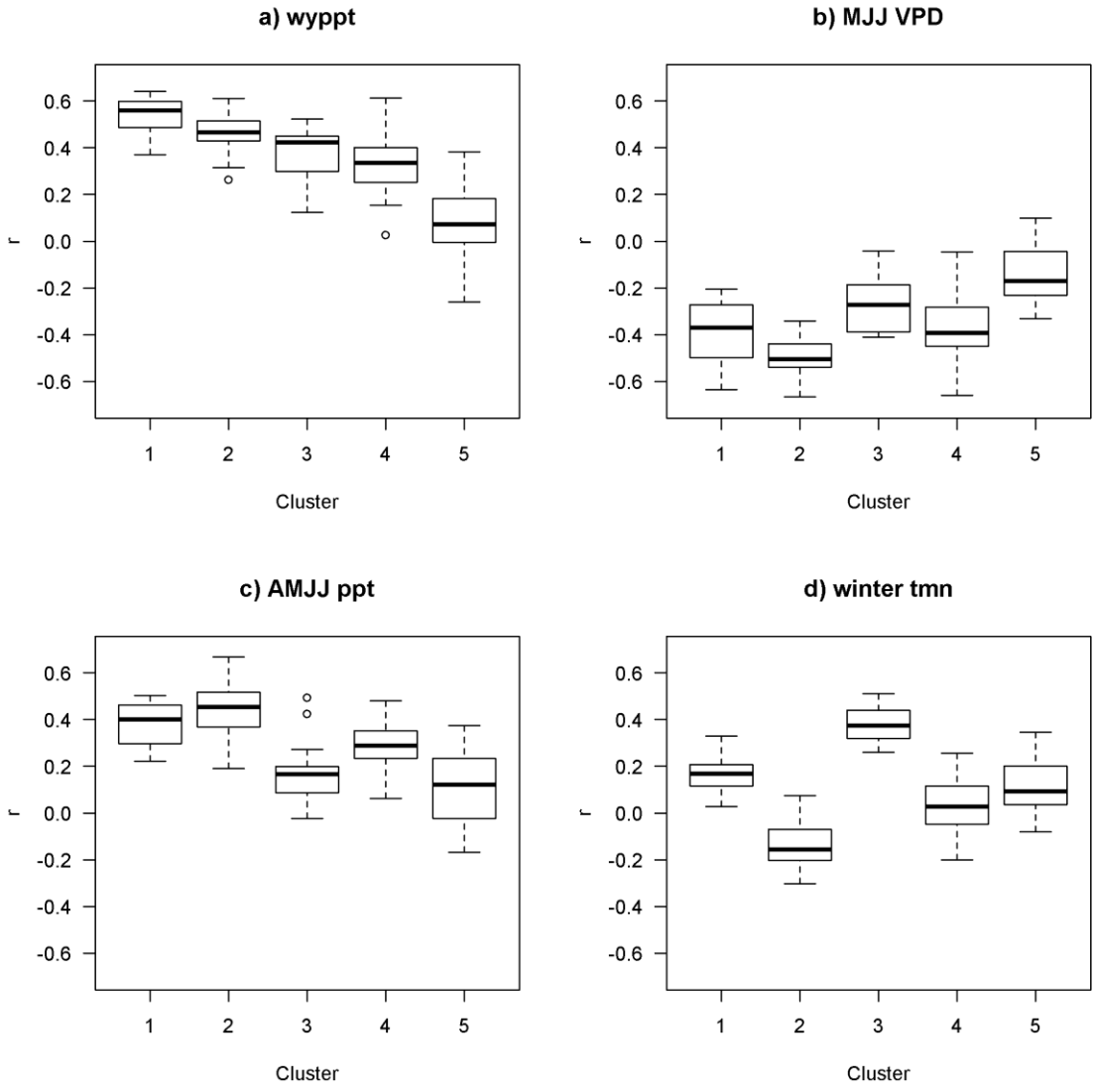

Fig. 4. Pearson correlation coefficients (r) between ponderosa pine standardized ring width index (RWI) and individual climate variables (1930-1979) by cluster. Number of sites in clusters: 1) 21, 2) 47, 3) 16, 4) 53, 5) 24. a) wyppt = water-year (Oct 1-Sep 30) precipitation (mm), b) MJJ VPD = May-Jul vapor pressure deficit (kPa), c) AMJJ ppt = Apr-Jul precipitation (mm) and d) winter tmn = Dec-Feb minimum temperature (°C). Bold lines represent medians, upper and lower box limits represent interquartile ranges (IQR), whiskers represent IQR +/- 1.5 * IQR and dots represent outliers.

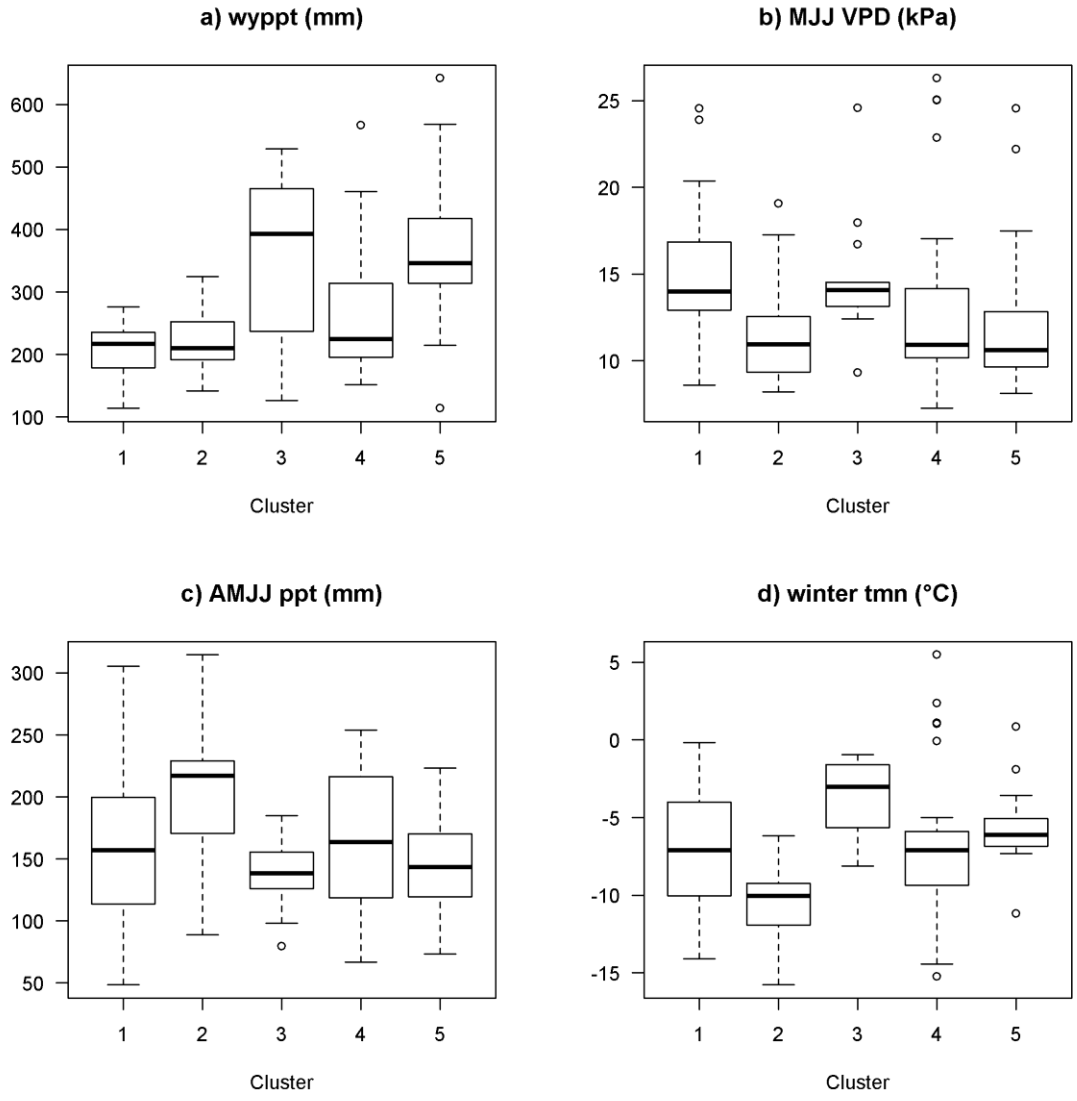

Fig. 5. Mean climate distributions (1930-1979 means) by cluster. Number of sites in clusters: 1) 21, 2) 47, 3) 16, 4) 53, 5) 24. a) wyppt = water-year (Oct 1-Sep 30) precipitation (mm), b) MJJ VPD = May-Jul vapor pressure deficit (kPa), c) AMJJ ppt = Apr-Jul precipitation (mm) and d) winter tmn = Dec-Feb minimum temperature (°C). Bold lines represent medians, upper and lower box limits represent interquartile ranges (IQR), whiskers represent IQR +/- 1.5 * IQR and dots represent outliers.

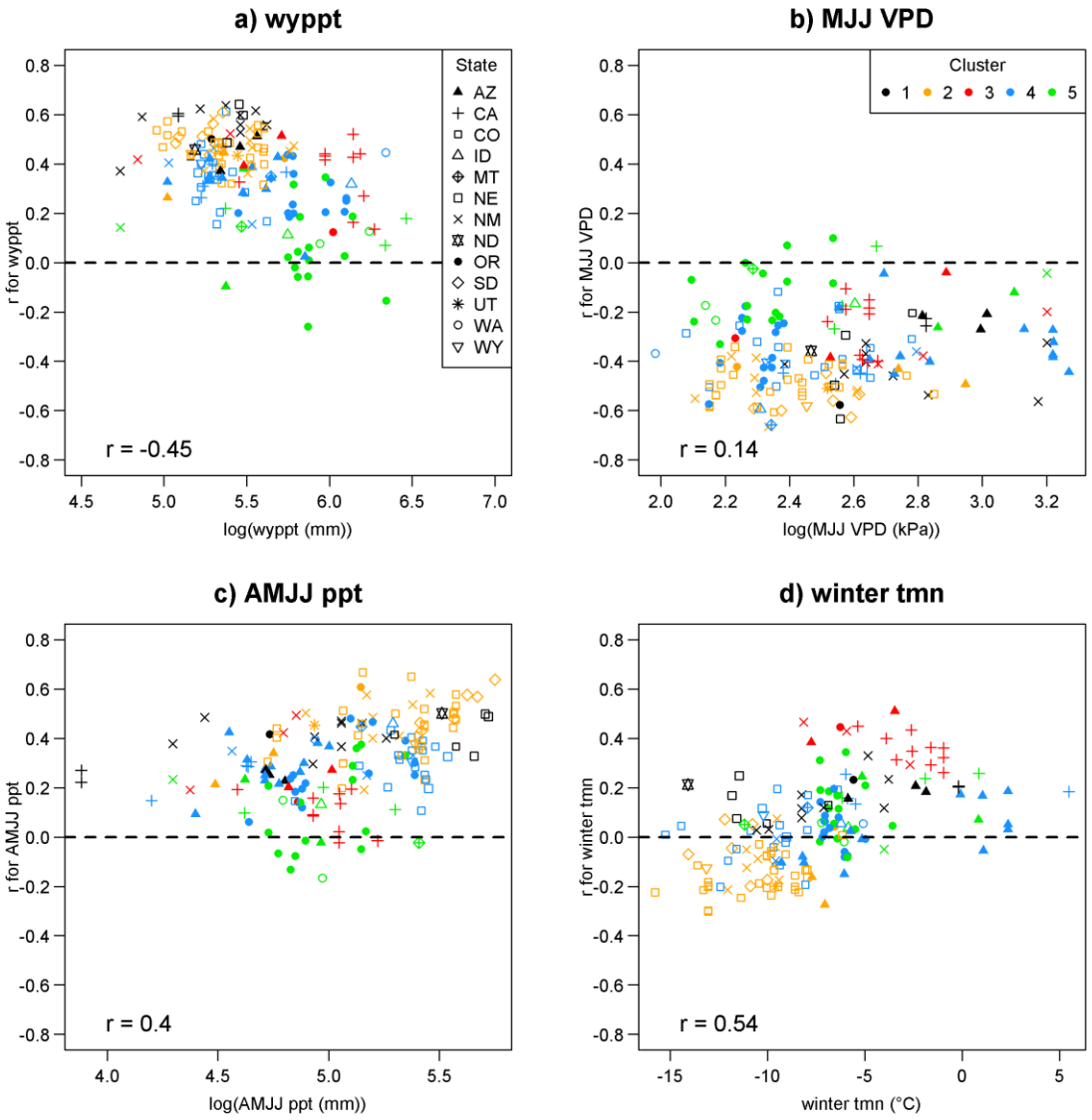

Fig 6. Relationship (Pearson correlation coefficient) between climate sensitivity (r) and the mean conditions for the corresponding climate variable during 1930-1979. a) wyppt = water-year (Oct 1-Sep 30) precipitation (mm), b) MJJ VPD = May-Jul vapor pressure deficit (kPa), c) AMJJ ppt = Apr-Jul precipitation (mm) and d) winter tmn = Dec-Feb minimum temperature (°C). Log scales are base 10.

Discussion

Range position and local adaptation

Linear relationships between climate sensitivities and mean climate for the corresponding climate variables suggest general relationships that apply across ponderosa pine populations; e.g., drier sites are generally more sensitive to wyppt. At the same time, divergent climate sensitivities at similar positions along climate gradients suggest that local adaptation contributes to climate sensitivities. For example, we encountered a few relatively dry sites in Arizona and New Mexico with weak sensitivity to wyppt (absolute $r < 0.2$), whereas correlations at similar wyppt levels were commonly two to three times greater in other regions. These findings support the notion that southern range edge populations of tree species are not necessarily the most sensitive to climate; we found precipitation limitation throughout the range of ponderosa pine and correlations were generally strongest in the range center. Cavin and Jump's (2016) European beech study offered that local adaptation buffered southern range edge populations and our study suggests the same may be true for ponderosa pine. Populations from drier climates are more water-use efficient, which is evidence for greater adaptation to drought for southern interior populations (Monson and Grant 1989). Potter et al. (2015) identified the Southwest as an area of particularly high genetic diversity, consistent with genetic patterns observed in tree species (Hampe and Petit 2005). Other areas of relatively high genetic diversity generally corresponded to areas where we found heterogeneous climate sensitivities (northeastern Oregon, northern California and southwestern Oregon) (Potter et al. 2015). Therefore, geographic patterns of genetic structure likely contribute to geographic patterns of climate sensitivities by promoting local adaptation and increasing heterogeneity in climate responses.

Although we found evidence of local adaptation, there are potentially confounding effects of non-linear growth-climate relationships and/or noise in downscaled climate data. Precipitation timing and form mediate available water; monthly precipitation totals cannot account for moisture lost as runoff during large storms. Furthermore, monthly precipitation and VPD do not account for uncertainties in rooting depth and soil water holding capacity that combine to influence moisture availability for trees. Therefore, unknown differences among sites may have contributed to observed differences in climate sensitivities; however, relatively large differences in sensitivities to similar climate (i.e., $r \sim 0.6$ for MJJ VPD) nonetheless suggest a role of adaptation.

On the use of ITRDB chronologies

Although ITRDB chronologies were often sampled for climate reconstruction (e.g., Graumlich 1987) or hydrological reconstruction (e.g., Malevich et al. 2013) and require that our results be interpreted with some caution, a recent study demonstrated that this "classic" sampling design has only minor influences on climate-growth correlations compared to other sampling methods at multi-decadal time scales (Nehrbass-Ahles et al. 2014). Furthermore, ITRDB chronologies represent the most spatially extensive set of inherently long-term data available for ponderosa pine and their use ensures some consistency in our data in terms of potentially confounding effects of vegetation structure (i.e., competition) or soils, given that exposed sites probably contained relatively well-drained soils. There is not likely to be a systematic geographical bias in selection for exposed sites in ITRDB chronologies (Chen et al. 2010), so we did not expect differences in site exposure in our study.

Climate change vulnerability

Climate envelope models project range shifts for both ponderosa pine varieties (Rehfeldt et al. 2014b). Interior populations, which generally inhabit higher elevations than Pacific populations, are more threatened due to the reduced potential for local shifts to higher elevations. Without a considerable redistribution of genotypes, most populations currently inhabit locations that will be unsuitable in the 2060s, except for some Pacific populations, and historical rates of gene dispersal are incompatible with the pace of modern climate change (Rehfeldt et al. 2014c). Recruitment lags have already been observed in tree species (Zhu et al. 2012). Areas of greater genetic diversity, however, may contain greater adaptive capacity and should be prioritized in conservation plans for ponderosa pine (Potter et al. 2015).

The overwhelmingly negative responses to MJJ VPD reflect the isohydric ecophysiology of ponderosa pine. Isohydric plants tightly regulate stomata to maintain relatively stable water potentials under drought conditions, but at the cost of reduced carbon assimilation (McDowell et al. 2008). The lack of a linear relationship between MJJ VPD sensitivity and mean MJJ VPD is consistent with an isohydric strategy. Ponderosa pine is adapted to withstand seasonal droughts and can shift biomass allocation from leaves to sapwood under warmer and drier conditions (Callaway et al. 1994, Delucia et al. 2000). Long-term exposure to droughts, however, may increase mortality vulnerability due to carbon starvation and bark beetle attacks and ultimately kill trees (McDowell et al. 2011, Tague et al. 2013). Carbon starvation was implicated in dieback of pinyon pine (*P. edulis*), an isohydric conifer, in the Southwest under warm drought (Adams et al. 2009, 2013), but synergies between bark beetles and carbon metabolism are unclear (Meddens et al. 2015).

Resin production is energetically expensive and drought-induced declines in carbon assimilation reduce the ability of trees to produce and transport resin for bark beetle defense (McDowell et al. 2011). In ponderosa pine, increased carbon allocation to resin production reduces risk of mortality from bark beetles (Kane and Kolb 2010). Seedling experiments have shown declines in carbon assimilation in response to soil moisture depletion, warming temperatures and VPD increases (Panek and Goldstein 2001). Therefore, future climate warming-induced increases in VPD are mechanistically associated with declines in forest vigor, including productivity and beetle defense capability (Williams et al. 2013).

Although future precipitation projections are variable and uncertain, warming temperatures will increase evaporative demand significantly and may deplete soil moisture earlier during growing seasons regardless of total precipitation and thus expose trees to greater moisture stress in dry years (Williams et al. 2013, Allen et al. 2015). Whereas increasing atmospheric carbon dioxide (CO_2) concentrations are expected to enhance plant water-use efficiency, which may enhance drought resilience and reduce aridity-driven soil moisture losses to some degree (e.g., Keenan et al. 2013, Roderick et al. 2015, Milly and Dunne 2016), model representation of physiological response to drought and enhanced CO_2 is known to be overly simple (Mankin et al. in review) and the effects of enhanced CO_2 thus far appear complex (e.g., Holmes et al. 2014, Chen et al. 2016, Levesque et al. 2017), geographically variable (De Kauwe et al. 2013, Zhu et al. 2016), and dependent on factors such as nutrient availability that are not well represented in models (Lee et al. 2013, Mankin et al. in review). Furthermore, warming temperatures increase the fraction of total precipitation that falls as rain versus snow, which increases runoff and evaporation and reduces water storage in snowpack. The shift in the relationship between winter tmn

sensitivity and winter tmn from positive to negative among the warmest sites in our study (Fig. 6d) may be evidence of these phenomena; at the warmest sites, the proportion of winter precipitation that falls as snow is smallest. As winter temperatures warm, tree growth generally increases, except near the freezing threshold at which point more precipitation falls as rain instead of snow. Therefore, locations on the cusp of transitioning from snow- to rain-dominated precipitation regimes may be particularly exposed to future climate change (McCullough et al. 2016).

In conclusion, although ponderosa pine populations with tightly coupled historical growth-climate relationships may be particularly sensitive to growth declines under climate change, the species' wide range of climate sensitivities suggests that the species as a whole may be able to withstand greater changes in mean climate than other species more uniformly sensitive to a single variable. Even as all populations will likely become exposed to locally novel climate conditions during the 21st Century, including more frequent and severe global change-type droughts (Adams et al. 2009, Overpeck and Udall 2010, Allen et al. 2015), local adaptation may buffer some populations from growth declines. Future work on ponderosa pine and other tree species should target relationships between climate responses and geographic patterns of genetic variability. Our results suggest these relationships exist, but we were unable to couple climate responses and genetic structure directly. More broadly, our study uses long-term data to demonstrate how climate sensitivity may vary among populations of wide-ranging species and how this variability is determined by a combination of position along environmental gradients and local adaptation.

References

Adams HD, Guardiola-Claramonte M, Barron-Gafford GA *et al*. (2009) Temperature sensitivity of drought-induced tree mortality portends increased regional die-off under global-change-type drought. *PNAS*, **106**, 7063-7066.

Adams HD, Germino MJ, Breshears DD *et al*. (2013) Nonstructural leaf carbohydrate dynamics of Pinus edulis during drought-induced tree mortality reveal role for carbon metabolism in mortality mechanism. *New Phytologist*, **197**, 1142-1151.

Adams HR, Barnard HR, Loomis AK (2014) Topography alters tree growth–climate relationships in a semi-arid forested catchment. *Ecosphere*, **5**, 1-16.

Allen CD, Breshears DD, McDowell NG (2015) On underestimation of global vulnerability to tree mortality and forest die-off from hotter drought in the Anthropocene. *Ecosphere*, **6**, 1-55.

Ashiq MW, Anand M (2016) Spatial and temporal variability in dendroclimatic growth response of red pine (Pinus resinosa Ait.) to climate in northern Ontario, Canada. *Forest Ecology and Management*, **372**, 109-119.

Bigelow SW, Papaik MJ, Caum C, North MP (2014) Faster growth in warmer winters for large trees in a Mediterranean-climate ecosystem. *Climatic Change*, **123**, 215-224.

Biondi F, Qeadan F (2008) A theory-driven approach to tree-ring standardization: defining the biological trend from expected basal area increment. *Tree-Ring Research*, **64**, 81-96.

Breshears DD, Cobb NS, Rich PM *et al*. (2005) Regional vegetation die-off in response to global-change-type drought. *PNAS*, **102**, 15144-15148.

Bunn AG (2008) A dendrochronology program library in R (dplR). *Dendrochronologia*, *26*(2), 115-124.

Bunn AG, Korpela M, Biondi F *et al.* (2016) dplR: Dendrochonology Program Library in R. R package version 1.6.4. https://CRAN.R-project.org/package=dplR.

Callaham RZ (2013a) Pinus ponderosa: a taxonomic review with five subspecies in the United States. *Research Paper PSW-RP-264. Albany, CA: USDA Forest Service, Pacific Southwest Research Station*.

Callaham RZ (2013b) Pinus ponderosa: geographic races and subspecies based on morphological variation. *Research Paper PSW-RP-265. Albany, CA: USDA Forest Service, Pacific Southwest Research Station*.

Callaway RM, DeLucia EH, Schlesinger WH (1994) Biomass allocation of montane and desert ponderosa pine: an analog for response to climate change. *Ecology*, **75**, 1474-1481.

Carnwath GC, Peterson DW, Nelson CR (2012) Effect of crown class and habitat type on climate–growth relationships of ponderosa pine and Douglas-fir. *Forest Ecology and Management*, **285**, 44-52.

Cavin L, Jump A (2016) Highest drought sensitivity and lowest resistance to growth suppression is found in the range core of the tree Fagus sylvatica L. not the equatorial range edge (Forthcoming). *Global Change Biology*, **23**, 362-379.

Chen PY, Welsh C, Hamann A (2010) Geographic variation in growth response of Douglas-fir to interannual climate variability and projected climate change. *Global Change Biology*, **16**, 3374-3385.

Chen HYH, Luo Y, Reich PB, Searle EB, Biswas SR (2016), Climate change-associated trends in net biomass change are age dependent in western boreal forests of Canada, *Ecology Letters*, **19**, 1150-1158,

Clark JS, Iverson L, Woodall CW *et al*. (2016) The impacts of increasing drought on forest dynamics, structure, and biodiversity in the United States. *Global Change Biology*, **22**, 2329-2352.

Conkle MT, Critchfield WB (1988) Genetic variation and hybridization of ponderosa pine. In: Ponderosa Pine: the species and its management, Washington State University Cooperative Extension, p. 27-43.

Cook ER (1985) A time series analysis approach to tree ring standardization. Dissertation, University of Arizona, Tucson, Arizona, USA.

Copenhaver-Parry PE, Cannon E (2016) The relative influences of climate and competition on tree growth along montane ecotones in the Rocky Mountains. *Oecologia*, **182**, 13-25.

Cropper JP (1984) Multicollinearity within selected western North American temperature and precipitation data sets. *Tree-Ring Bulletin*, **44**, 29-37.

Daly C, Halbleib M, Smith JI *et al*. (2008) Physiographically sensitive mapping of climatological temperature and precipitation across the conterminous United States. *International Journal of Climatology*, **28**, 2031-2064.

Dannenberg MP, Wise EK (2016) Seasonal climate signals from multiple tree ring metrics: A case study of Pinus ponderosa in the upper Columbia River Basin. *Journal of Geophysical Research: Biogeosciences*, **121**, 1178-1189.

Davis MB, Shaw RG (2001) Range shifts and adaptive responses to Quaternary climate change. *Science*, **292**, 673-679.

Dawson TP, Jackson ST, House JI *et al*. (2011) Beyond predictions: biodiversity conservation in a changing climate. *Science*, **332**, 53-58.

De Kauwe MG, Medlyn BE, Zaehle S *et al*. (2013) Forest water use and water use efficiency at
elevated CO2: a model-data intercomparison at two contrasting temperate forest FACE sites, *Global Change Biology*, **19**, 1759-1779.

Delucia EH, Maherali H, Carey EV (2000) Climate-driven changes in biomass allocation in pines. *Global Change Biology*, **6**, 587-593.

Franks SJ, Weber JJ, Aitken SN (2014) Evolutionary and plastic responses to climate change in terrestrial plant populations. *Evolutionary Applications*, **7**, 123-139.

Fritts HC, Smith DG, Cardis JW, Budelsky CA (1965) Tree-Ring Characteristics Along a Vegetation Gradient in Northern Arizona. *Ecology*, **46**, 393-401.

Fritts HC, Blasing TJ, Hayden BP, Kutzbach JE (1971) Multivariate techniques for specifying tree-growth and climate relationships and for reconstructing anomalies in paleoclimate. *Journal of Applied Meteorology*, **10**, 845-864.

Fritts HC (1976) Tree rings and climate, 567 pp. *Academic, San Diego, Calif*.

Fulé PZ, Covington WW, Moore MM (1997) Determining reference conditions for ecosystem management of southwestern ponderosa pine forests. *Ecological Applications*, **7**, 895-908.

Graumlich LJ (1987) Precipitation variation in the Pacific Northwest (1675–1975) as reconstructed from tree rings. *Annals of the Association of American Geographers*, **77**, 19-29.

Griesbauer HP, Green DS (2010) Regional and ecological patterns in interior Douglas-fir climate-growth relationships in British Columbia, Canada. *Canadian Journal of Forest Research*, **40**, 308-321.

Hacket-Pain AJ, Cavin L, Friend AD, Jump AS (2016) Consistent limitation of growth by high temperature and low precipitation from range core to southern edge of European beech indicates widespread vulnerability to changing climate. *European Journal of Forest Research*, **135**, 897-909.

Hampe A, Petit RJ (2005) Conserving biodiversity under climate change: the rear edge matters. *Ecology Letters*, **8**, 461-467.

Holmes CD (2014) Air pollution and forest water use. *Nature*, **507**, E1-E2.

Johansen AD, Latta RG (2003) Mitochondrial haplotype distribution, seed dispersal and patterns of postglacial expansion of ponderosa pine. *Molecular Ecology*, **12**, 293-298.

Kane JM, Kolb TE (2010) Importance of resin ducts in reducing ponderosa pine mortality from bark beetle attack. *Oecologia*, **164**, 601-609.

Keenan TF, Hollinger DY, Bohrer D *et al*. (2013) Increase in forest water-use efficiency as atmospheric carbon dioxide concentrations rise. Nature, **499**, 324-327.

Knutson KC, Pyke DA (2008) Western juniper and ponderosa pine ecotonal climate-growth relationships across landscape gradients in southern Oregon. *Canadian Journal of Forest Research*, **38**, 3021-3032.

Kusnierczyk E, Ettl GJ (2002) Growth response of ponderosa pine (Pinus ponderosa) to climate in the eastern Cascade Mountains, Washington, USA: Implications for climatic change. *Ecoscience*, **9**, 544-551.

Lascoux M, Palmé AE, Cheddadi R, Latta RG (2004) Impact of Ice Ages on the genetic structure of trees and shrubs. *Philosophical Transactions of the Royal Society of London B: Biological Sciences*, **359**, 197-207.

Latta RG, Mitton JB (1999) Historical separation and present gene flow through a zone of secondary contact in ponderosa pine. *Evolution*, **53**, 769-776.

Lee E, Felzer BS, Kothavala Z (2013) Effects of nitrogen limitation on hydrological processes in CLM4-CN, *Journal of Advances in Modeling Earth Systems*, **5**, 741-754.

Lesser MR, Jackson ST (2013) Contributions of long-distance dispersal to population growth in colonising Pinus ponderosa populations. *Ecology Letters*, **16**, 380-389.

Levesque M, Andreu-Hayles L, Pederson N (2017) Water availability drives gas exchange and growth of trees in northeastern US, not elevated CO2 and reduced acid deposition, *Scientific Reports*, **7**, 46158.

Little EL (1971) Atlas of United States trees. Vol. 1. Conifers and important hardwoods. Misc. pub. 1146. *US Department of Agriculture, Forest Service, Washington, DC*.

Little EL (1979) Checklist of United States Trees (Native and Naturalized). *US Department of Agriculture, Forest Service, Washington, DC*.

Malevich SB, Woodhouse CA, Meko DM (2013) Tree-ring reconstructed hydroclimate of the Upper Klamath basin. *Journal of Hydrology*, **495**, 13-22.

Mankin JS, Smerdon JE, Cook BI, Williams AP, Seager R (In review) The curious case of projected 21st-century drying but greening in the American West. *Journal of Climate*.

McCullough IM, Davis FW, Dingman, JR *et al*. (2016) High and dry: high elevations disproportionately exposed to regional climate change in Mediterranean-climate landscapes. *Landscape Ecology*, **31**, 1063-1075.

McDowell N, Pockman WT, Allen CD *et al*. (2008) Mechanisms of plant survival and mortality during drought: why do some plants survive while others succumb to drought? *New Phytologist*, **178**, 719-739.

McDowell NG, Beerling DJ, Breshears DD (2011) The interdependence of mechanisms underlying climate-driven vegetation mortality. *Trends in Ecology & Evolution*, **26**, 523-532.

McKenzie D, Hessl AE, Peterson DL (2001) Recent growth of conifer species of western North America: assessing spatial patterns of radial growth trends. *Canadian Journal of Forest Research*, **31**, 526-538.

Meddens AJ, Hicke JA, Macalady AK, Buotte PC, Cowles TR, Allen CD (2015) Patterns and causes of observed piñon pine mortality in the southwestern United States. *New Phytologist*, **206**, 91-97.

Milly PCD, Dunne KA (2016) Potential evapotranspiration and continental drying, *Nature Climate Change*, **6**, 946-949.

Monson RK, Grant MC (1989) Experimental studies of ponderosa pine. III. Differences in photosynthesis, stomatal conductance, and water-use efficiency between two genetic lines. *American Journal of Botany*, **76**, 1041-1047.

Nehrbass-Ahles C, Babst F, Klesse S *et al*. (2014) The influence of sampling design on tree-ring-based quantification of forest growth. *Global Change Biology*, **20**, 2867-2885.

Overpeck J, Udall B (2010) Dry times ahead. *Science*, **328**, 1642-1643.

Pacifici M, Foden WB, Visconti P *et al*. (2015) Assessing species vulnerability to climate change. *Nature Climate Change*, **5**, 215-224.

Panek JA, Goldstein AH (2001) Response of stomatal conductance to drought in ponderosa pine: implications for carbon and ozone uptake. *Tree Physiology*, **21**, 337-344.

Potter KM, Hipkins VD, Mahalovich MF, Means RE (2013) Mitochondrial DNA haplotype distribution patterns in Pinus ponderosa (Pinaceae): range-wide evolutionary history and implications for conservation. *American Journal of Botany*, **100**, 1562-1579.

Potter KM, Hipkins VD, Mahalovich MF, Means RE (2015) Nuclear genetic variation across the range of ponderosa pine (Pinus ponderosa): Phylogeographic, taxonomic and conservation implications. *Tree Genetics & Genomes*, **11**, 1-23.

Rehfeldt GE (1986a) Adaptive Variation in Pinus ponderosa from Intermountain Regions. I Snake and Salmon River Basins. *Forest Science*, **32**, 79-92.

Rehfeldt GE (1986b) Adaptive Variation in Pinus ponderosa from Intermountain Regions. II. Middle Columbia. In: US Department of Agriculture Forest Service. Res. Pap. INT-373, p. 9.

Rehfeldt GE (1990) Genetic differentiation among populations of Pinus ponderosa from the upper Colorado River Basin. *Botanical Gazette*, **151**, 125-137.

Rehfeldt GE (1991) A model of genetic variation for Pinus ponderosa in the Inland Northwest (USA): applications in gene resource management. *Canadian Journal of Forest Research*, **21**, 1491-1500.

Rehfeldt GE, Ying CC, Spittlehouse DL, Hamilton DA (1999) Genetic responses to climate in Pinus contorta: niche breadth, climate change, and reforestation. *Ecological Monographs*, **69**, 375-407.

Rehfeldt GE, Leites, LP, St Clair JB *et al*. (2014a) Comparative genetic responses to climate in the varieties of Pinus ponderosa and Pseudotsuga menziesii: Clines in growth potential. *Forest Ecology and Management*, **324**, 138-146.

Rehfeldt GE, Jaquish BC, López-Upton J *et al*. (2014b) Comparative genetic responses to climate for the varieties of Pinus ponderosa and Pseudotsuga menziesii: Realized climate niches. *Forest Ecology and Management*, **324**, 126-137.

Rehfeldt GE, Jaquish BC, Sáenz-Romero C *et al*. (2014c) Comparative genetic responses to climate in the varieties of Pinus ponderosa and Pseudotsuga menziesii: reforestation. *Forest Ecology and Management*, **324**, 147-157.

Restaino CM, Peterson DL, Littell J (2016) Increased water deficit decreases Douglas fir growth throughout western US forests. *PNAS*, **113**, 9557-9562.

Roderick ML, Greve P, Farquhar GD (2015) On the assessment of aridity with changes in atmospheric CO2. *Water Resources Research*, **51**, 5450-5463.

Shinneman DJ, Means RE, Potter KM, Hipkins VD (2016) Exploring climate niches of ponderosa pine (Pinus ponderosa Douglas ex Lawson) haplotypes in the Western United States: Implications for evolutionary history and conservation. *PloS one*, **11**, e0151811.

Sork VL, Davis FW, Westfall R *et al*. (2010) Gene movement and genetic association with

regional climate gradients in California valley oak (Quercus lobata Née) in the face of climate change. *Molecular Ecology*, **19**, 3806-3823.

Tague CL, McDowell NG, Allen CD (2013) An integrated model of environmental effects on growth, carbohydrate balance, and mortality of Pinus ponderosa forests in the southern Rocky Mountains. *PloS one*, **8**, e80286.

Veblen TT, Kitzberger T, Donnegan J (2000) Climatic and human influences on fire regimes in ponderosa pine forests in the Colorado Front Range. *Ecological Applications*, **10**, 1178-1195.

Vose RS, Applequist S, Squires M *et al*. (2014) Gridded 5km GHCN-Daily Temperature and Precipitation Dataset (nCLIMGRID), Version 1. Maximum temperature, minimum temperature and precipitation. NOAA National Centers for Environmental Information. DOI:10.7289/V5SX6B56. Accessed February 11, 2017.

Watson E, Luckman BH (2002) The dendroclimatic signal in Douglas-fir and ponderosa pine tree-ring chronologies from the southern Canadian Cordillera. *Canadian Journal of Forest Research*, **32**, 1858-1874.

Williams AP, Allen CD, Millar CI *et al*. (2010a) Forest responses to increasing aridity and warmth in the southwestern United States. *PNAS*, **107**, 21289-21294.

Williams AP, Michaelsen J, Leavitt SW, Still CJ (2010b) Using tree rings to predict the response of tree growth to climate change in the continental United States during the twenty-first century. *Earth Interactions*, **14**, 1-20.

Williams AP, Xu C, McDowell NG (2011) Who is the new sheriff in town regulating boreal forest growth? *Environmental Research Letters*, **6**, 041004.

Williams AP, Allen CD, Macalady, AK (2013) Temperature as a potent driver of regional forest drought stress and tree mortality. *Nature Climate Change*, **3**, 292-297.

Williams SE, Shoo LP, Isaac JL, Hoffmann AA, Langham G (2008) Towards an integrated framework for assessing the vulnerability of species to climate change. *PLoS Biol*, **6**, e325.

Yeh HY, Wensel LC (2000) The relationship between tree diameter growth and climate for coniferous species in northern California. *Canadian Journal of Forest Research*, **30**, 1463-1471.

Zang C, Biondi F (2013) Dendroclimatic calibration in R: the bootRes package for response and correlation function analysis. *Dendrochronologia*, **31**, 68-74.

Zhu K, Woodall CW, Clark JS (2012) Failure to migrate: lack of tree range expansion in response to climate change. *Global Change Biology*, **18**, 1042-1052.

Zhu Z, Piao, S, Myneni RB *et al*. (2016) Greening of the Earth and its drivers, *Nature Climate Change*, **6**, 791-795.

Appendix

Table A1. Ponderosa pine tree-ring chronologies from the International Tree Ring Data Bank (ITRDB) (except Tejon Ranch, CA)

Name	State	Lat (°N)	Long (°W)	Elevation (m)	n trees
Basin Area, Grand Canyon NP	AZ	36.13	-111.88	2800	14
Beaver Creek	AZ	33.70	-109.23	2392	32
Beaver Creek Watershed	AZ	34.88	-111.57	2050	19
Girl's Ranch	AZ	34.38	-110.42	1969	28
Grasshopper Recollection	AZ	34.07	-110.62	1798	26
Green Mountain	AZ	32.38	-110.68	2194	29
Gus Pearson	AZ	35.27	-111.75	2255	65
Helen's Dome	AZ	32.22	-110.55	2535	15
Mount Hopkin's	AZ	31.70	-110.87	2133	20
Muletank	AZ	34.32	-110.77	2362	12
Noon Creek	AZ	32.65	-109.82	2346	20
North Slope	AZ	32.22	-110.55	2441	14
Ord Mountain	AZ	33.90	-111.40	2133	18
Rhyolite Canyon	AZ	32.00	-109.33	1828	16
Robinson Mountain Recollection	AZ	35.38	-111.53	2225	26
Rocky Gulch	AZ	34.72	-111.50	1965	20
Rose Peak Recollection	AZ	33.42	-109.37	2316	22
Sit. Gravel Pit	AZ	34.25	-109.93	2072	24
Slate Mountain Recollection	AZ	35.50	-111.83	2194	35
Tucson Side	AZ	32.20	-110.55	2362	28
Walnut Canyon	AZ	35.17	-111.52	2057	21
Antelope Lake Recollection	CA	40.15	-120.60	1480	51
Antelope Lake Update	CA	40.10	-120.63	1385	69
Black Cone	CA	41.18	-120.12	2195	18
Crystal Cave Sequoia NP	CA	36.57	-118.78	1640	38
Dalton Reservoir	CA	41.62	-120.70	1531	38
Dalton Reservoir Update	CA	41.67	-120.98	1513	55
Damon's Butte	CA	41.50	-121.17	1448	26
Greenville Saddle	CA	40.22	-120.92	1768	34
Grizzly Peak	CA	41.17	-122.03	1463	38
Hodgdon Yosemite NP	CA	37.80	-119.87	1722	35

Name	State	Lat (°N)	Long (°W)	Elevation (m)	n trees
Oak Flat Road Yosemite NP	CA	37.75	-119.77	1803	35
Panorama Point Sequoia NP	CA	36.55	-118.82	1570	28
Plumas County	CA	40.00	-121.00	1254	30
Ranger Station Peak Sequoia NP	CA	36.55	-118.82	1772	39
Santa Lucia Mountains	CA	36.07	-121.57	625	26
Snow White Ridge	CA	38.13	-120.05	1731	26
St. John Mountain	CA	39.43	-122.68	1555	45
Tejon Ranch Lower	CA	35.00	-118.57	1453	28
Tejon Ranch Upper	CA	34.97	-118.59	1676	22
Alto Picnic Ground	CO	40.05	-105.43	2560	23
Bennett Creek	CO	40.67	-105.52	2301	30
Big Elk Meadows	CO	40.22	-105.42	2438	57
Black Forest East	CO	39.50	-104.22	1800	33
Boulder Ridge Road	CO	40.98	-105.67	2650	35
Cochetopa Dome	CO	38.25	-106.67	2835	49
Crags Hotel	CO	39.93	-105.30	2002	25
Deer Mountain	CO	40.37	-105.58	2605	21
Deer Mountain Recollection	CO	40.37	-105.58	2605	23
Devil's Gulch	CO	40.42	-105.47	2400	22
Eagle Rock	CO	39.38	-105.17	2103	32
Eldora	CO	39.95	-105.55	2650	21
Eldorado Canyon	CO	39.93	-105.27	1889	32
Elevenmile Reservoir	CO	38.87	-105.43	2743	19
Great Sand Dunes Lower	CO	37.78	-105.50	2530	61
Happy Meadows	CO	39.02	-105.37	2440	24
Horsetooth Reservoir A	CO	40.53	-105.13	1706	20
Indian Creek	CO	39.37	-105.13	2400	48
Jamestown	CO	40.13	-105.42	2469	21
Jefferson County	CO	39.68	-105.20	1965	24
Jefferson County Recollection	CO	39.68	-105.20	1965	20
Kassler Recollect	CO	39.45	-105.13	1828	20
Kim	CO	37.23	-103.25	1650	18
Lykins Gulch	CO	40.17	-105.28	1798	22
Mesa de Maya	CO	37.10	-103.62	2060	12
Meyer Ranch	CO	39.55	-105.27	2530	24
Monarch Lake	CO	40.10	-105.73	2621	19

Name	State	Lat (°N)	Long (°W)	Elevation (m)	n trees
Oak Creek	CO	38.30	-105.28	2408	12
Ophir Creek	CO	38.07	-105.13	2438	31
Ormes Peak	CO	38.95	-104.95	2895	23
Platt Bradbury	CO	37.47	-106.30	2835	20
Pool Table Pines	CO	37.78	-106.82	2877	23
Ridge Road	CO	39.38	-104.20	1850	13
Roadsite	CO	38.10	-106.37	2621	28
Rustic	CO	40.72	-105.58	2499	33
Sapinero Mesa	CO	38.32	-107.20	2700	18
Sheep Pen Canyon	CO	37.07	-103.27	1580	30
Soap Creek	CO	38.53	-107.32	2417	41
South Fork	CO	37.67	-106.65	2591	35
Terrace Lake Pines	CO	37.38	-106.28	2658	21
Turkey Creek Bluff	CO	38.60	-104.87	1938	21
Van Bibber Creek	CO	40.37	-105.25	1920	26
Van Bibber Update	CO	39.80	-105.25	1920	19
Wheelman	CO	40.00	-105.37	1950	19
Wilson Ranch	CO	37.63	-106.68	2560	23
East Side Trail	ID	43.75	-116.10	1825	34
Wellner Cliffs RNA	ID	48.37	-116.79	903	41
Paine Gulch	MT	46.08	-110.82	1650	36
Rock Creek West	MT	46.95	-114.33	1555	47
Burning Coal Vein	ND	46.60	-103.47	792	51
Ash Canyon	NE	42.63	-103.25	1280	45
Canyon Road	NE	41.52	-103.93	1530	15
Long Pine Creek	NE	42.67	-99.72	670	31
Niobara Valley Preserve	NE	42.82	-100.00	720	47
Snake River	NE	42.70	-100.87	810	37
Abouselman Spring	NM	35.80	-106.62	2438	32
Baca	NM	35.82	-106.57	2515	32
Black Mountain	NM	33.38	-108.23	2651	23
Burned Mountain	NM	36.67	-106.20	2755	24
Cabresto Canyon	NM	36.73	-105.47	2835	33
Canyon del Potrero, Mesa Alta	NM	36.28	-106.65	2525	70
Capulin Volcano	NM	36.77	-103.95	2380	10
Cat Mesa	NM	35.78	-106.62	2515	15

Name	State	Lat (°N)	Long (°W)	Elevation (m)	n trees
Cornay Ranch	NM	36.80	-103.98	2020	24
Elephant Rock	NM	36.70	-105.43	2743	35
Elk Canyon	NM	33.05	-106.53	2499	30
Fenton Lake	NM	35.88	-106.67	2560	16
Garcia Park	NM	36.33	-105.37	2743	20
Gila Cliff Dwellings	NM	33.22	-108.27	1767	12
Hoosier Canyon	NM	32.70	-106.35	1204	22
McKenna Park	NM	33.25	-108.50	2500	10
Mill Canyon	NM	36.07	-104.35	1710	19
Mouth of La Junta	NM	36.12	-105.52	2713	17
Narbona Pass, Chuska Mountains	NM	36.09	-108.87	2650	21
Osha Mountain	NM	36.30	-105.42	2896	37
Rio Pueblo	NM	36.15	-105.60	2469	29
Spring Canyon	NM	32.72	-106.37	1054	20
Tres Piedras	NM	36.62	-105.98	2500	36
West Side Roa	NM	32.80	-105.90	2250	19
Bally Mountain	OR	45.28	-118.57	1453	18
Big Sink	OR	45.78	-117.92	1206	42
Blue Jay Spring	OR	42.92	-121.53	1490	26
Calimus Butte	OR	42.63	-121.53	2020	20
Crater Lake	OR	42.78	-122.07	1370	21
Cross Canyon Oregon	OR	45.97	-117.68	1317	28
Deschutes	OR	43.47	-121.40	1420	21
Diamond Lake	OR	43.08	-121.95	1510	20
Drumhill Ridge	OR	45.47	-118.20	885	10
Emigrant Springs	OR	45.55	-118.48	1169	19
Experimental Forest	OR	43.72	-121.60	1530	24
Fish Lake	OR	45.00	-117.07	1600	43
Grizzly Bear	OR	45.97	-117.72	1231	33
Indian Crossing	OR	45.12	-117.02	1448	27
Junction of HWYS 51 and 97	OR	43.32	-121.75	1420	25
Lakeview Update	OR	42.03	-120.57	1645	36
Lava Cast Forest	OR	43.68	-121.25	1500	34
Little Aspen Butte	OR	42.27	-122.08	1650	24
Lookout Mountain	OR	45.83	-117.80	1372	18
Lookout Mountain Lower	OR	43.75	-121.65	1320	19

Name	State	Lat (°N)	Long (°W)	Elevation (m)	n trees
Lugar Springs	OR	45.77	-117.97	1200	20
Mill Creek RNA	OR	45.50	-121.42	1002	43
Pringle Falls Prescribed Fire	OR	43.73	-121.65	1320	18
Pringle Falls RNA	OR	43.70	-121.62	1460	29
Skookum Butte	OR	43.23	-121.65	1670	19
Summit Springs	OR	45.68	-117.47	1354	24
Surveyor Flow	OR	43.62	-121.30	1550	10
Telephone Draw	OR	42.93	-121.62	1550	20
Telephone Draw South	OR	42.75	-121.52	1550	14
Wenaha 1 and 2	OR	45.82	-117.67	738	8
Buckhorn Mountain	SD	43.78	-103.60	1768	33
Cedar Butte	SD	43.60	-101.12	785	16
Eagle Nest Canyon	SD	45.35	-103.13	1090	38
Grace Coolidge	SD	43.75	-103.35	1234	25
Pilger Mountain	SD	43.50	-103.88	1392	12
Reno Gulch	SD	43.90	-103.60	1658	32
Upper Sand Creek RNA	UT	37.98	-111.60	2690	36
Blewett Pass	WA	47.35	-120.55	1240	39
North Fork Campground	WA	48.00	-120.60	915	40
Rimrock Slope White Pass	WA	46.33	-121.17	820	5
Devils Tower NM	WY	44.58	-104.70	1319	5
Vedauwoo	WY	41.15	-105.37	2500	26

A2. Tree-ring sampling at Tejon Ranch, CA

Study area

Of the 161 total tree-ring chronologies used in this study, 159 originated from the International Tree Ring Data Bank (ITRDB). We sampled the remaining two chronologies from Tejon Ranch, CA in 2013 and 2014. A full list of all chronologies used in this study is included in Table A1.

Tejon Ranch is located in the western Tehachapi Mountains, California, USA (34°58´N, 118°35´W). The site is private land owned and managed by the Tejon Ranch Company and is used for ranching, resource extraction, agriculture, residential and commercial development and biodiversity conservation. The topographically varied landscape spans an elevational gradient of 370-2,364 m and supports numerous vegetation communities including grasslands, desert, chaparral, deciduous and evergreen oak woodlands and montane conifer forests. The climate is Mediterranean, with hot, dry summers and cool, wet winters. Between 1896 and 2010, average annual maximum and minimum temperatures were 19.61°C (SD = 0.65) and 7.31°C (SD = 0.64), respectively. Average annual precipitation over the same period was 388.12 mm (SD = 134.26) (Flint and Flint 2012). In portions of the landscape roughly above 1500-1600 m, precipitation regimes are historically snow-dominated (Western Regional Climate Center 2015). At low elevations, soils are granite-derived, coarse-loamy thermic typic Haploxerolls with maximum depths of approximately 61-122 cm (USDA 2015). High elevation sites include coarse-sandy loams derived from schist and classified as mesic Pachic Haploxerolls, as well as granite-derived medium- and coarse-sandy loams classified as mesic Haploxerolls. Maximum soil depths at high elevations are approximately 127-229 cm (USDA 2015).

Ponderosa pine is locally uncommon at Tejon Ranch and occurs in two main stands on north-facing slopes at approximately 1450 and 1650 m, hereinafter referred to as "lower" and "upper" stands, respectively. A few scattered trees exist at higher elevations in white fir (*Abies concolor*)-dominated stands, as well as within deep canyons at lower elevations and near the margins of the main stands. Survey data from the 1930s Wieslander Vegetation Type Mapping (VTM) project suggest that ponderosa pine was historically more common at Tejon Ranch, having more extensively inhabited riparian areas at lower elevations and some of the same canyons where only relict trees remain today (Kelly et al. 2005, 2008). This evidence suggests a gradual, upward range contraction of the species. We found no visual fire evidence in either pine stand, nor scars in any of our cores. Signs of pine beetles (*Dendroctonus* spp.) were encountered in both stands, particularly in the lower stand. The recent multi-year drought likely crippled the ability of adult trees to repel insect attacks, contributing to dieback of > 90% of adult trees in the lower stand during 2013-2016. Dieback began more modestly in the upper stand in late 2013, but increased substantially in the following years. As of late 2016, approximately 75% of adult trees were dead in the upper stand. We inferred dieback timing from field observation and interpretation of recent aerial photographs (National Agriculture Imagery Program; NAIP).

Tree-ring sampling and preparation

We collected increment cores from the upper stand in August 2013 and from the lower stand in August and September 2014. We sampled 22 and 28 trees in each respective stand, with each tree sampled twice (once on the uphill side of the tree and once on the cross-slope 90° from the first core). We generally selected adult, overstory trees to represent

general stand characteristics and exclude light competition effects. Trees in unusual microsites were avoided. We did not intentionally target tree piths. Samples were transported in paper or ventilated plastic straws. After approximately a week of air drying, cores were glued to wooden mounts and sanded successively with 220, 400 and 600 grit sandpaper. A few twisted cores were salvaged using boiled water and manual realignment. We used the open-source software Tellervo ® and a Velmex ® sliding platform connected to a microscope to measure ring widths to the nearest micrometer. Ring widths from the same tree were averaged. Rings were manually cross-dated using paper skeleton plots. We used COFECHA version 6.06P (Holmes 1983, Grissino-Mayer 2001) to validate cross-dating by analyzing correlations among trees within our study site and between our study site and a neighboring, published tree-ring chronology (Crystal Cave, Sequoia National Park, CA (36°57’ N, 118°78’ W), downloaded from ITRDB). We selected Crystal Cave because it provided a close comparison to Tejon Ranch in terms of geographic proximity and elevation (1640 m).

Table A3. Significant differences between cluster pairs based on pairwise comparisons (p = 0.05)

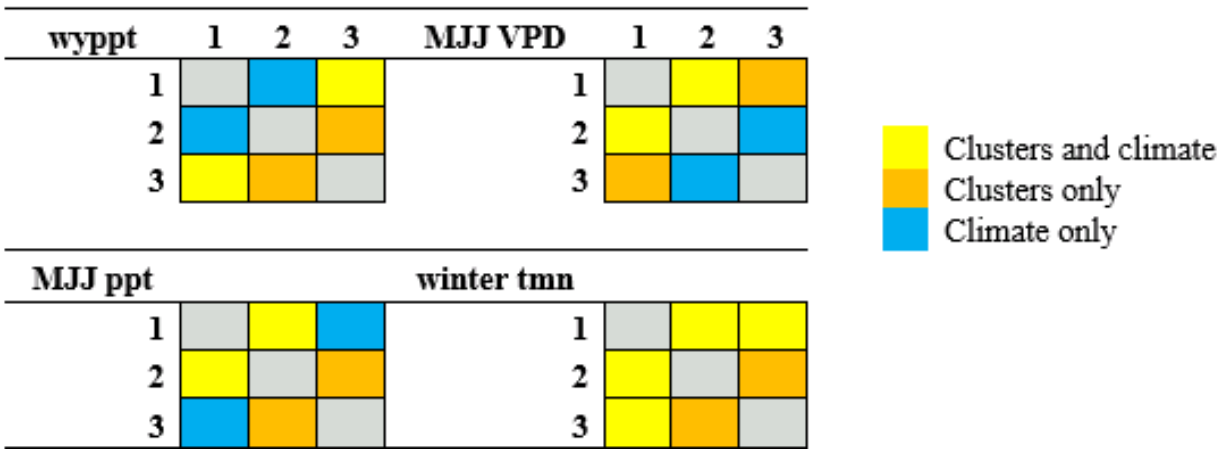

wyppt = water-year (Oct 1-Sep 30) precipitation (mm), MJJ VPD = May-Jul vapor pressure deficit (kPa), AMJJ ppt = Apr-Jul precipitation (mm), winter tmn = Dec-Feb minimum temperature (°C)

References

Grissino-Mayer HD (2001) Evaluating crossdating accuracy: a manual and tutorial for the computer program COFECHA. *Tree-Ring Research*, **57**, 205-221.

Holmes RL (1983) Computer-assisted quality control in tree-ring dating and measurement. *Tree-ring Bulletin*, **43**, 69-78.

Kelly M, Allen-Diaz B, Kobzina N (2005) Digitization of a historic dataset: the Wieslander California vegetation type mapping project. *Madroño*, **52**, 191-201.

Kelly M, Ueda KI, Allen-Diaz B (2008) Considerations for ecological reconstruction of historic vegetation: Analysis of the spatial uncertainties in the California Vegetation Type Map dataset. *Plant Ecology*, **194**, 37-49.

McCullough IM, Davis FW, Dingman, JR *et al*. (2016) High and dry: high elevations disproportionately exposed to regional climate change in Mediterranean-climate landscapes. *Landscape Ecology*, **31**, 1063-1075.